UNIVERSITÀ DEGLI STUDI DI MILANO

GRADUATE SCHOOL IN PHARMACOLOGICAL SCIENCES

Department of Pharmacological and Biomolecular Sciences

PhD. in Pharmacological Sciences,

XXVI° cycle

"Pathogenic role of microglia-derived microvesicles in Neurodegeneration"

BIO/14

TUTOR: Prof.ssa Michela Metteoli

CO-TUTOR: Dott.ssa Claudia Verderio

COORDINATORE: Prof. Alberto Panerai

POOJA JOSHI

Matr. R09345

Academic Year 2012-2013

INDEX

1. SUMMARY

The characteristic feature of Alzheimer's disease (AD) is the presence of extracellular amyloid-beta (Abeta) plaques, which are surrounded by activated microglial cells. Microglial cells during the long course of the disease can induce neuroinflammation and drive neurodegeneration. Recent evidence indicates that neuroinflammation negatively co-relates with cognitive state in AD. Furthermore it's well accepted now that soluble pre-fibrillar Abeta species, rather than insoluble fibrils, are the most toxic forms of Abeta. This hypothesis is supported by the fact that plaque load reaches plateau before the clinical onset of AD.

We investigated whether membrane microvesicles (MVs) released extracellularly by reactive microglia may contribute to AD degeneration. We found that production of myeloid MVs is strikingly high in AD patients and in subjects with mild cognitive impairment, and that AD MVs are toxic for cultured neurons. We demonstrated the mechanism responsible for MV neurotoxicity *in vitro*, using MVs produced by primary microglia. We found that MV lipids can promote formation of soluble Aβ species from extracellular insoluble aggregates. Moreover we showed that MVs can be carriers of neurotoxic Aβ forms that are trafficked to MVs after internalization into microglia. Neurotoxicity of MVs was neutralized by the Aβ interacting protein PrP and anti- Aβ antibodies, which prevented binding to neurons of neurotoxic soluble Aβ species. Finally, administration of the MV shedding inhibitor FTY720 for a period of 6 weeks significantly improved memory performance and reduced brain inflammation in APP/PS1 mice. This study identifies microglial MVs as a novel mechanism by which reactive microglia contribute to AD degeneration and suggests that FTY720, by inhibiting MV shedding can ameliorate the pathophisiology and cognitive defects in a mouse AD model.

2. INTRODUCTION

2.1 Alzheimer's disease and its pathology.

Alzheimer's disease (AD) is the leading cause for dementia in the world. It is an age-related neurodegenerative disorder that affects 7% of people older than 65 years and about 40% of people older than 80 years (Glass CK, et al., 2010). In 2010, 36 million people suffered from AD and it has been estimated that every year this number increases by 7.7 million patients (Werner P, et al., 2012). The neuropathological changes of AD has both positive and negative features. Classical positive lesions consist of abundant amyloid plaques and neurofibrillary tangles, neuropil threads, and dystrophic neurites containing hyperphosphorylated tau (Terry RD, et al., 1991; Mandelkow and Mandelkow, 1998; Trojanowski and Lee, 2000; Iqbal and Grundke-Iqbal, 2002; Crews and Masliah, 2010), that are accompanied by astrogliosis (Beach et al., 1989; Itagaki et al., 1989) and microglial cell activation (Rogers et al., 1988; Itagaki et al., 1989;Masliah et al., 1991). Sometimes Congophilic amyloid angiopathy (CAA) is also observed. In the hippocampus are also found unique plaque, which include Hirano bodies and granulovacuolar degeneration. Hirano bodies are eosinophilic rod-like cytoplasmic inclusion, relatively common in the stratum lacunosum of the hippocampal CA1 region in the elderly. In the AD patients the number of Hirano bodies is abnormally high (Gibson and Tomlison, 1977). Neuronal loss and synapse loss largely parallel tangle formation, although whether tangles are causative of neuronal loss or synaptic loss remains uncertain (Gómez Isla, et al., 1997; Iqbal and Grundke Iqbal, 2002; Bussière et al. 2003; Hof et al., 2003; Yoshiyama et al., 2007; Spires Jones, et al., 2008; de Calignon, et al., 2009, 2010; Kimura et al., 2010).

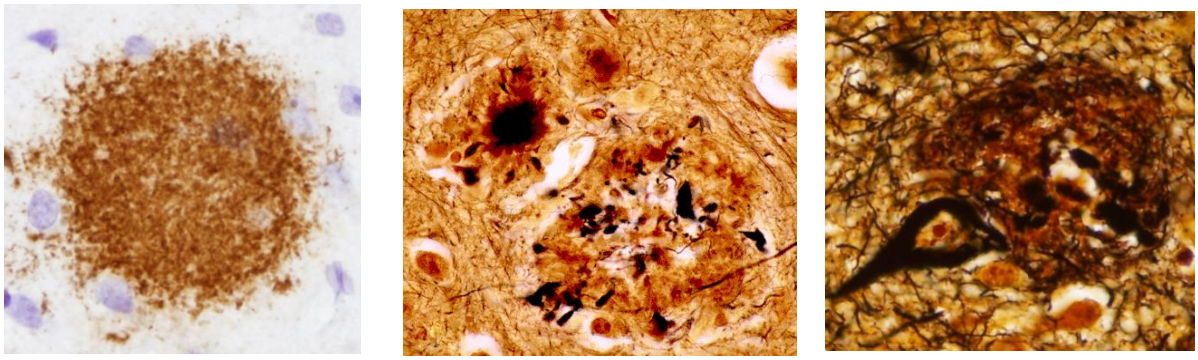

Diffused Plaque | Neurite Plaque | Neurofibrillary Tangles

Figure 2.1 Two main lesions in AD, senile plaques (**SPs**) and neurofibrillary tangles (**NFTs**). Two types of SP **diffuse plaques with** exracellular amyloid deposits **and neuritic plaques** consist of degenerating neuronal processes with tau paired helical filaments along with reactive astrocytes and microglia. **(Alberto Serrano-Pozo, et al., 2011)**

2.2 Cellular metabolism of Amyloid precursor protein (APP).

APP is a type I membrane protein and follows the conventional secretory pathway from the endoplasmic reticulum (ER) to the plasma membrane. During this process, APP undergoes several co-and post-translational modifications, including N-and O-glycosylation, tyrosine sulphation, and phosphorylation. Already on the way to the cell surface, APP can undergo endoproteolytic processing by secretases and soluble variants of APP are generated which are secreted extracellularly. The Aβ domain is located within APP at the junction between the intraluminal and transmembrane domains. Two enzymatic steps liberate Aβ from APP. In the first "β-cleavage" step, β-site APP-cleaving enzyme (BACE-1) (Vassar et al., 1999) cleaves APP at or near the N-terminus of the Aβ peptide; then, in the second, or "γ-cleavage" step, the membrane-bound C-terminal APP fragment (CTF) generated by BACE-1 is cleaved by the γ-secretase, a multimeric complex thought to be made up of an essential quartet of transmembrane proteins—presenilin 1 (or 2), nicastrin, anterior pharynx-defective phenotype 1 (APH-1) and PS-enhancer 2 (PEN-2) (Edbauer et al., 2003). Alternatively, APP can be subjected to the proteolytic cleavage by α-secretase, which occurs within the sequence of Aβ, thus precluding the formation of the amyloidogenic fragments. α-Secretase gives rise to the secretion of the neuroprotective sAPPα fragment and to a C-terminal stub that is then cleaved by γ-secretase. Thus APP is processed in two different catabolic pathways: a minor amyloidogenic pathway, in which APP is cleaved by β- and γ-secretases releasing Aβ peptide and a predominant (> 90%) non-amyloidogenic pathway in which the protein is successively cleaved by α- and γ-secretases precluding production of Aβ. APP after its synthesis in the endoplasmic reticulum is then transported through the golgi apparatus to the trans golgi network, where the highest concentrations of APP are found in neurons (Xu H, et al., 1997; Hartmann T, et al., 1997; Greenfield JP, et a.,1999). From there, APP can be transported in secretory vesicles to the cell surface where α-secretases are located.

The functions of the APP and its various metabolites is not yet clear, but there is a lot of literature that indicates its role in neurite outgrowth, synaptogenesis, neuronal trafficking along the axon, transmembrane signal transduction, cell adhesion, as well as in the control of gene expression and calcium metabolism, which is essential for synaptic transmission (Berridge, et al., 1998). Disruption of calcium homeostasis is considered the common pathway for aging and AD (Khachaturian, et al., 1989). Amyloidogenic Aβ has been suggested to function as ion channel regulator and as a transcriptional activator (Ohyagi, et al., 2005; Pearson and Peers, 2006; Hardy, 2007;

Bailey et al., 2011). Indeed APP intracellular domain (AICD) is able to regulate transcription of several genes, including APP itself, the β-secretase BACE-1 and the Aβ-degrading enzyme neprilysin (Cao and Sudhof, 2001; Pardossi Piquard, et al., 2005; Müller et al., 2007; Belyaev et al., 2009, 2010).

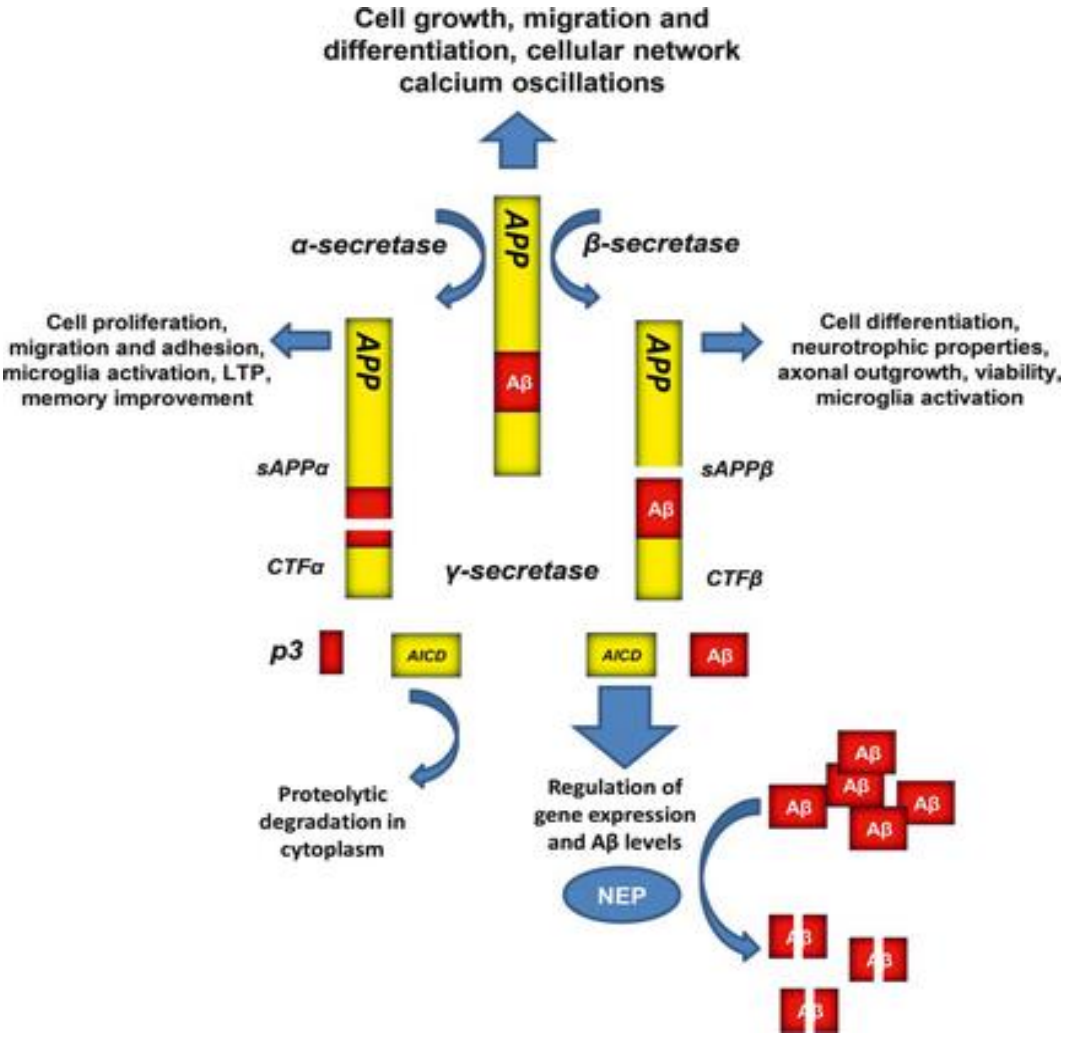

Figure2.2 The amyloidogenicand non-amyloidogenic pathways of amyloid precursor protein (APP) processing and its metabolites. Ab, amyloid b-peptide; sAPPa and sAPPb, N-terminal shed ectodomains of APP; CTFa and CTFb, C-terminal fragments of APP produced by the actions of a- or b-secretases, respectively; AICD, APP intracellular domain; p3, fragment of APP after cleavage by a- and c-secretases; NEP, neprilysin. **(J.-N. Octave et al. 2013)**

2.3 Amyloidgenic pathway of Abeta .

Generally, amyloid refers to misfolded peptides or proteins that demonstrate a stable, cross-beta super-secondary structure that renders the proteins insoluble, fibrous-like, and resistant to proteolysis. Each type of amyloidosis is classified according to clinical signs and the main peptide or protein that constitutes the amyloid fibrils. Amyloidosis deposits contain not only fibrils but also

nonfibrillar components such as glycosaminoglycans (GAGs), apolipoprotein E (apoE), and serum amyloid P (SAP) components.

Aβ is an aggregated protein deposited within plaque cores found in AD brain. The Aβ monomers are generated in most of the body's cells, including vascular endothelial cells (Kitazume S, et al., 2010) thyroid epithelial cells (Schmitt TL, et al., 1995) and neuronal and nonneuronal cultured cells. However, neuronal cells seem to generate greater amounts of Aβ than other cell types (Fukumoto H, et al., 1999). In its monomeric form, this protein is harmless (Giuffrida ML, et al., 2010). Aβ monomers form a random coil or α helix conformation transmitted to a β hairpin. This structure facilitates polymerisation reaction which triggers monomer polimerization to short, soluble, metastable intermediates called oligomers. Oligomers self can be rapidly extended by monomer addition to form curvilinear protofibrils. Finally, protofibrils are bundled together to form the large, insoluble, cross β-sheet fibrils which accumulate in plaques. Steps within the Aβ aggregation pathway are reversible, such that deposited fibrils could give rise to soluble oligomers and intermediates. Among A*β* peptides, A*β* 1-42 and pyroglutamate-modified A*β* very rapidly aggregate and initiate the complex multistep process that leads to mature fibrils and plaque (Schilling S, et al., 2006; Bieschke J, et al., 2012).

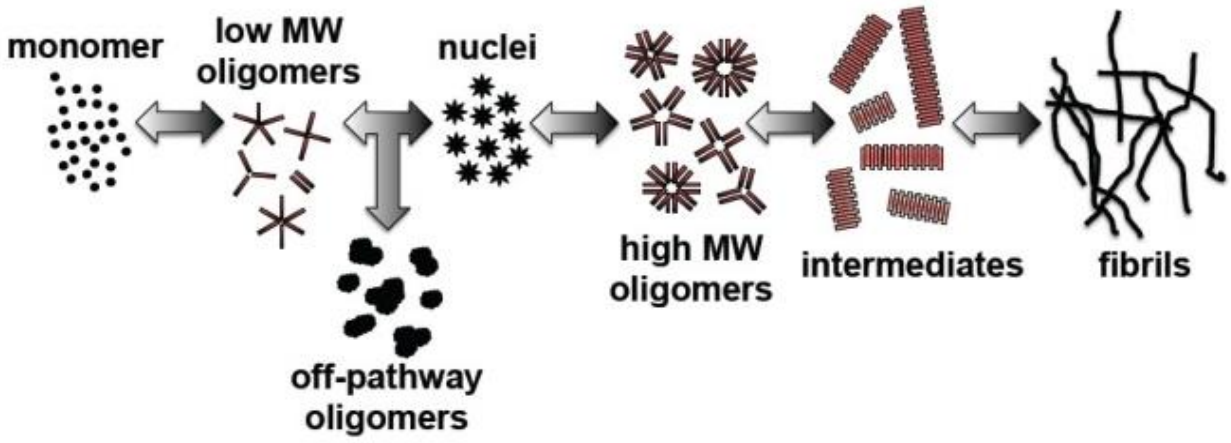

Figure2.3 The Aβaggregation process. **N. Elizabeth Pryor, et al., 2011**

2.4 Oligomeric abeta and neurotoxicity.

Recent evidence suggests that soluble aggregates of Aβ, rather than monomers or insoluble fibrils, are responsible for the cellular pathology associated with AD (Caughey B, et al., 2003; Glabe CG,

2006; Roychaudhuri R, et al., 2009). A lot of in vitro studies, done independently by different groups, showes that soluble aggregates, formed by synthetic $A\beta_{1-40}$ and $A\beta_{1-42,}$ induce cellular dysfunction and toxicity in cultured cells (Lambert MP, et al., 1998; Gonzalez-Velasquez F.J., et al. 2008; Hartley DM, et al., 1999) whereas in vivo, Aβ dodecamers (Aβ-56) isolated from the brains of transgenic AD mice were shown to induce memory deficits (Lesne S, et al., 2006). Furthermore, soluble Aβ aggregates generated in cell culture drastically inhibit hippocampal long term potentiation in rats (Walsh DM, et al., 2002) while there is a poor correlation between the levels of insoluble Aβ fibrils and AD severity, in mouse models (Westerman M, et al.,2002). Thus, it is widely accepted that soluble Aβ oligomers rather than insoluble fibrils impair cognitive function. The toxicity of small soluble Aβ species has been proposed to depend on their interaction with specific neuronal proteins, such as the NMDA receptor (Snyder EM, et al.,2005) or the prion protein PrP^C (Lauren J, et al.,2009), which modulates NMDA receptors through Fyn kinase (Um JW, et al.,2012). Alternatively, soluble Aβ oligomers may damage neurons by binding to multiple membrane components, including lipids, thereby changing membrane permeability and causing calcium ion leakage into the cell (Benilova, et al., 2012; Verdier Y, et al., 2004).

2.5 Alzheimer's Disease and genetics

In less than 5% of the cases, AD is inherited as an autosomal dominant trait, and results from mutations in the APP gene or in the presenilin (PS) genes (Tanzi, *et al*., 1996; Hardy, 1997; Tanzi and Bertram, 2005) encoding PS1 or PS2, the catalytic subunits of the γ-secretase multiprotein complex (De Strooper,2003; Edbauer, *et al*., 2003). In these inherited AD cases, Aβ production is substantially enhanced and plays a key role in the etiology of the disease. Following the amyloid cascade hypothesis (Hardy and Selkoe, 2002; Goate and Hardy, 2012), accumulations of Aβ, especially an increased ratio of $A\beta_{42}$: $A\beta_{40}$, are the initial triggers for the disease process.

ApoE is a major lipoprotein in the brain and mediates transport of cholesterol and other lipids between neurons and glial cells. Importantly, ApoE is also linked to the metabolism of Aβ by affecting its aggregation in and clearance from the brain. Inheritance of the apolipoprotein E (ApoE4) allele is the major genetic risk factor that is associated with late onset AD (Potter and Wisniewski, 2012). Several environmental factors are known as risk factors for Late onset AD including, aging, head trauma, type 2 diabetes, hypertension, hypercholesterolemia, and vascular pathology.

2.6 Inflammation and Neurodegeneration.

Microglial cells, which are the resident macrophages of the CNS, play a crucial role in the process of neuroinflammation. Microglia have three different morphologies: resting, activated, and amoeboid/phagocytic. The healthy, non-inflamed brain contains almost entirely "resting" microglia which are highly ramified, with a small, static cell body, but with dynamic and branched processes actively surveying the brain parenchyma. In response to any brain alteration (cytokines and many signalling molecules produced during acute inflammation) microglia transform from a ramified to an activated phagocytic morphology, and start releasing pro-inflammatory mediators. During chronic neuroinflammation, these cells can remain activated for extended periods, releasing large quantities of cytokines and neurotoxic molecules, which contribute to long-term neuro-degeneration (Liu and Hong, 2003).However recently it has become apparent that the microglial activation is a more dynamic and diverse process than it was considered previously. Indeed, depending on the type and duration of the stimulus that microglial cells receive from the brain microenvironment, microglia can acquire different functional state and change their phenotype during the disease progression. The two opposite phenotypes that microglia can acquire among different activation states are usually called M1 proinflammatory phenotype, and M2 phenotype. M1 (or classically activated) microglia are effector cells which produce an aggressive first-line immune response. M1 phenotype can be induced in vitro by exposure of microglia to interferon (IFN)-gamma and tumour necrosis factor α. M2 (or alternatively activated) microglia have instead roles in wound healing and in promoting tissue repair. M2 phenotype can be induced in vitro by exposure to anti-inflammatory cytokines, such as IL-4 and IL13. Microglia express the two classes of major histocompatibility complex, MHC class 1 and MHC class 2, and although these antigen presenters are mainly involved in the reaction to infectious disease, they are thought to play a role in the development of neuroinflammation (Al Nimer, et al., 2011). Depending on the pathology, different pathways contribute to inflammation processes activated in neurodegenerative diseases. Factors released from damaged neurons such as α-synuclein in PD, deposits of amyloid aggregates in AD, and SOD1 in ASL trigger activation of microglia which, in turn, release pro-inflammatory molecules. Furthermore, inflammation leads to enhanced levels of oxidative stress; astrocytes, release ROS and NO that, together with NADPH oxidase stimulation, provoke microglia activation. Subsequently, activated microglia secrete signals to recruit $CD4^+$ $CD25^+$ T cells, which directly affect

neurons via Fas/Fas–ligand interaction. However, other events, such as mitochondrial dysfunction, protein aggregation, glutamate excitotoxicity, and loss of trophic factor support, may promote neuronal cell death. For instance, tumor necrosis factor-α (TNF-α), a major pro-inflammatory cytokine, activates microglia and cause neurotoxicity in motor neurons. The inflammatory mediators such as TNF-α, IL-1β, and IL6 derived from non-neuronal cells including microglia modulate the progression of neuronal cell death in neurodegenerative disease. Apoptosis and necrosis of neurons result in the release of ATP, which further activates microglia through the purinergic P2X7 receptor.

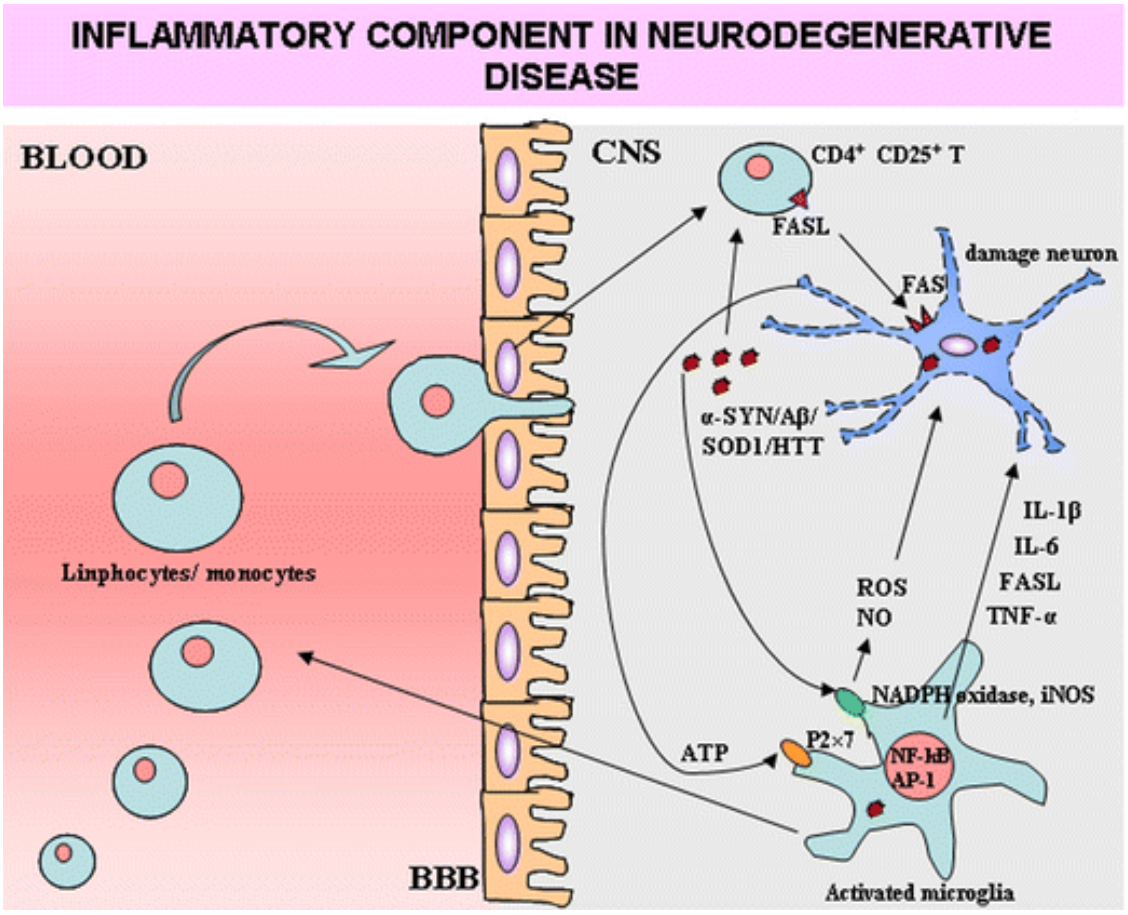

Figure2.4 Different inflammatory pathway involved in neurodegenerative diseases. **(Nuzzo D, et al 2013)**

2.7 Neuroinflammation promotes neurotoxicity in AD.

Alois Alzheimer himself originally identified inflammation of the brain's glial supporting cells as one of the hallmark of AD pathology (Alzheimer et al., 1995). In AD, the inflammatory response involves

microglial cells and astrocytes, which surround the amyloid plaques (Wyss-Coray, et al., 2003). Aβ inducing local inflammation and amplify neuronal death (Nikolaev et al., 2009). The main pathway of glial cell activation by Aβ is through toll-like receptors. Toll-like receptor activation gives rise to an inflammatory response that is beneficial at early stages of disease, decreasing Aβ burden, but very detrimental at later stages by increasing inflammation and neurotoxicity (Carrero, et al., 2012).

Indeed ramified, resting microglia exert a protective influence over synaptic excitotoxicity (Vinet, et al., 2012) by increasing neuronal adenosine A1 receptors through CXC3CL1 expression (Lauro, et al., 2010). Conversely A beta-activated microglia contribute to excitotoxic synaptic damage (Medeiros et al., 2010). Consistent with the original observation made by Alois Alzheimer Aβ plaques also induce astrocytic reactivity (Smits, et al., 2002) and there is strong evidence for the involvement of the cytokines IL-1β and TNF-α in astrocyte activation by Aβ oligomers.

In addition it has been clearly established that Aβ plaques facilitate the movement of components of the peripheral immune system such as T cells and macrophages into the brain (Stalder, et al., 2005) and increased peripheral inflammation is capable of propagating sustained and damaging neuroinflammation in a positive feedback loop.

In human patients the role played by inflammation in neuron degeneration is suggested by several lines of evidence:

i) Subjects with high plaque burden without dementia show virtually no evidence of neuroinflammation (Lue LF, et al., 1996).

ii) Recent PET studies (Edison P, et al., 2008; Okello A, et al., 2009) show an inverse correlation between the cognitive status and activation of microglia.

iii) Activation of microglia increases linearly throughout the disease course and correlates with AD neurodegeneration (Serrabo-Pozo A, et al., 2011).

Moreover, recent studies demonstrating that variants of TREM2 and CD33, two receptors expressed in microglial cells, increase the risk for late onset AD (Okello A, et al., 2009; Hollingworth P, et al., 2011) have refocused the spotlight on microglia as major contributing factor in AD.

Although multiple preclinical evidence indicates that microglia activation promotes neuronal dysfunction and neuron elimination (Giulian D, et al., 1996; Fuhrmann M, et al., 2010) and accelerates AD progression (Bealnilova I, et al., 2012; Tan B, et al., 2012; Weitz TM, et al., 2012) the molecular mechanisms by which microglia exert neurotoxicity remain largely unknown.

2.8 Exosomes and Shed Microvesicles (MVs)

Exosomes are a population of small extracellular membrane vesicles (50-90 nm) released by an endocytic pathway. Generation of exosomes occurs inside the lumen of multivesicular bodies (MVBs) through budding, fission ad segregation of their membrane. Depending upon their biological characteristics, intracellular MVBs either traffic to lysosomes, where they are subjected to proteosomal degradation (degradative MVBs), or to the plasma membrane, where they release exosomes in the extracellular space (exocytic MVBs) upon fusion with the plasma membrane (Mathivanan, et al., 2010). The ESCRT (endosomal sorting complex required for transport) machinery, is involved in sorting of vesicles inside MVBs. Fission of exosome membrane is facilitated by components of the ESCRT-III complex, called charged multivesicular body proteins (CHMPs); (Hanson, et al., 2009; Wollert and Hurley, 2010; Wollert, et al., 2009) and by the AAA-ATPase vacuolar protein sorting associated 4, VPS4 (Babst, 2005). There are various other factors that promote exosome biogenesis, including the sphingolipid ceramide produced by neutral sphingomyelinase (Kosaka, et al., 2010; Trajkovic, et al., 2008). Exosomes are enriched in several proteins and lipids of the MVB membrane, and, exosome biogenesis serves as a mechanism of regulated assembly of MVB components. Exosomes are enriched in numerous protein involved in membrane transport and fusion (i.e. annexin, flotillin, Rab GTPases), in MVB biogenesis (Alix), besides other typical molecules such as integrins and tetraspanins (CD63, CD9, CD81, CD82). They are also characterized by the presence of high levels of cholesterol, sphingolipids, ceramide and glycerophospolipids in their membrane (Simons and Raposo, 2009).

Microvesicles (MVs), sometimes refereed as shed vesicles or ectosomes (Sadallah, et al., 2011), are quite large membrane vesicles, more heterogeneous in size (100nm-1µm) and shape as compared to exosomes. They bud directly from the plasma membrane, upon cell activation and are released into the extracellular environment. A sorting process is involved in shedding of MVs, in which surface blebs selectively accumulates cellular constituents that are then packaged into MVs. Depending upon the cell of origin, MVs contain a variety of cell surface receptors, intracellular signalling proteins and genetic materials. An interesting feature of MVs is that they reflect the differential expression of proteins of donor cells and therefore MVs shed from distinct cells are molecularly different from each other. Composition and biological activity of MVs also vary depending on the state (e.g. resting, stimulated) of donor cells and depending on the agent employed for stimulation

(Bernimoulin, et al., 2008). However, in general shed vesicles are characterized by the presence of high levels of phosphatidylserine (PS) on their surface.

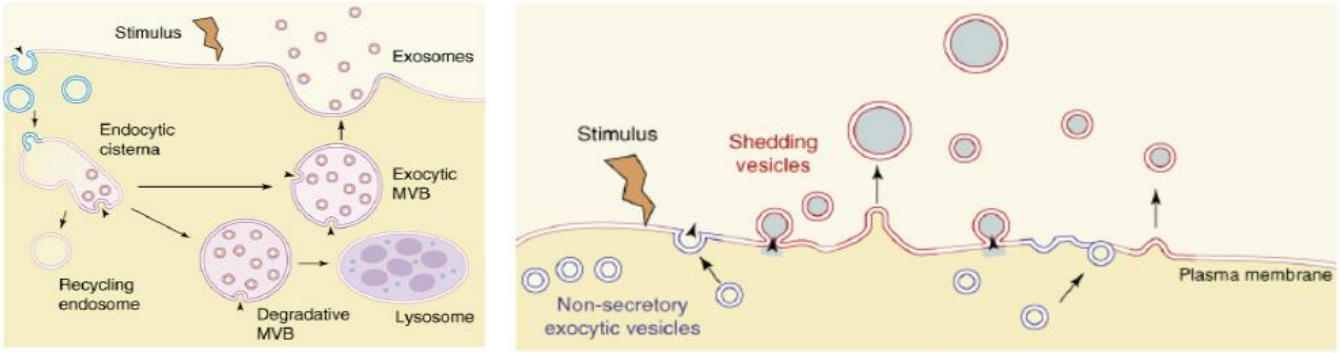

Figure2.5 Differences pathway of generation of Exosomes and Shed Vesicles**. (Cocucci et al, 2009)**

2.9 Pathological and physiological role of MVs.

MV shedding from the plasma membrane is now recognized as a widespread mode of intercellular communication. In addition it is widely accepted that MVs play a role in several physiological and pathological process such as cell proliferation, coagulation, vascular function, apoptosis, and inflammation and tumour progression. In physiological conditions platelet-derived MVs, by acting on macrophages, neutrophils and other platelets work as trigger of coagulation. However, vesicles are also present in the lipid core of atherosclerotic plaque where promote thrombotic signals (Cocucci et al, 2009). Moreover, vesicles secreted from different cells can influence the immune response, for example MVs can present antigen to T cells, or transfer the antigen-MHCII complex to dendritic cells, or directly activate natural killer cells and macrophages (Thery, et al., 2009). During inflammation MVs can act both as anti-inflammatory or pro-inflammatory mediators. Neutrophil derived microvescicles stimulate the production of anti-inflammatory cytokines and MVs released from fibroblasts promote the synthesis of pro-inflammatory cytokines, such as inteleukin-6 (IL-6), the monocyte chemotactic protein 1 and metalloproteinase. The most well characterized membrane vesicles are those released from blood cells, i.e. platelets, leukocytes, erythrocytes, and endothelial cells. However, accumulating evidence demonstrate that MVs and exosomes can also be released by brain cells and that these particles play an important function in the central nervous system (CNS) both in pathologic or healthy conditions. The exosomes derived from

oligodendrocytes control myelination, and those produced from Schwann cells support local axonal protein synthesis by delivering ribosomes to injured neuron. Moreover exosomes released by neuron may contribute to the spreading of pathogenic agents or degenerative proteins like beta-amyloid and alpha-synuclein (Emmanouilidou, et al., 2010).

2.10 Activated Microglia secrete shed microvesicles (MVs) in the extracellular matrix.

MV shedding from microglial cells has been the main research interest of our lab during the past years. The size of microglial MVs ranges from 0.1 μm –1 μm. As ectosomes produced by most cell types microglial MVs are characterized by high levels of externalized phosphatidylserine in their membrane. MV shedding increases upon microglial stimulation with ATP, a typical danger signal, and activation of the $P2X_7$ receptors, which are highly expressed in microglia. MVs produced by reactive microglia carry the pro-inflammatory cytokine interleukin-1β (IL-1β), together with the IL-1β-processing enzyme caspase-1, and the $P2X_7$ receptor (Bianco, et al., 2005), suggesting that they contain the main components of the inflammation. The budding of MVs is facilitated by externalization of acid sphingomyelinase, which by locally increasing ceramide levels in the inner leaflet of the plasma membrane modifies the membrane curvature (Bianco, et al., 2009). We recently showed that reactive microglia through the release of extracellular ectosomes propagate an inflammatory signal. Microglia-derived MVs can transmit inflammatory signals to recipient microglia, which indeed upregulate the co-stimulatory molecule CD86 and express pro-inflammatory genes like IL-1β, IL-6, inducible nitric oxide synthase, and cyclooxygenase-2 upon exposure to MVs produced by reactive microglia (Verderio, et al., 2012)

Intriguingly, microglia-derived MVs can also interact with neurons and stimulate spontaneous and evoked excitatory transmission both *in vitro* and after injection *in vivo*. Hippocampal neurons exposed to MVs show an increase in miniature excitatory post-synaptic current (mEPSC) frequency without changes in mEPSC amplitude. MVs affect the pre-synaptic site of the excitatory synapse by increasing the release probability of synaptic vesicles through induction of ceramide and sphingosine synthesis. Thus, microglial MVs appear to modulate synaptic activity and enhance neurotransmission (Antonucci, et al., 2012; Turola, et al., 2012).

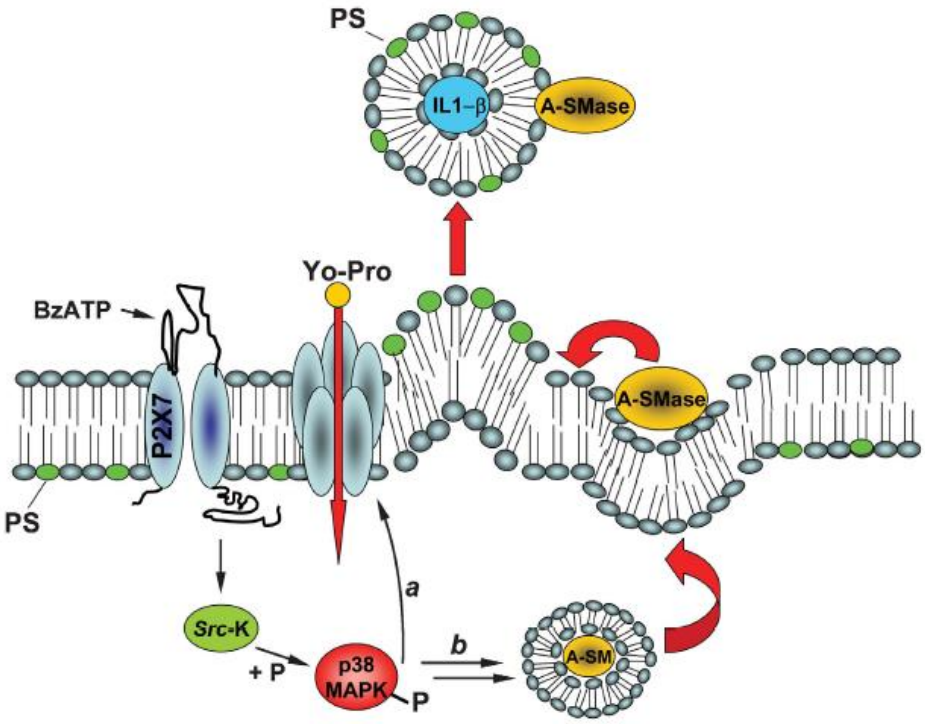

Figure 2.6 P2X7R---induced MVs shedding in glial cells (**Bianco, et al., 2009**).

2.11 Clinical Diagnosis in AD and prospective of MVs as biomarker.

In 1984, a working group established by the National Institute of Neurological and Communicative disorders and Stroke and the Alzheimer's Disease and Related Disorders Association created clinical diagnostic guidelines of probable AD (McKhann, et al.,1984), which were validated against neuropathological diagnosis with a sensitivity and specificity of around 80 and 70%, respectively (Knopman DS, et al., 2001). However, the criteria only allowed diagnosis when the patients were so severely affected by the disease process that they could not manage daily functioning in respect to intellectual and social abilities. In 2011 there was a revision of these guidelines by a new working group from the National Institute of Aging (Jack CR Jr, et al., 2011). Because of these new imaging techniques and the analysis of cerebrospinal fluid (CSF) biomarkers it is also possible to make a pre-dementia diagnosis of AD. The CSF biomarkers included in diagnostic criteria include the total amount of tau (T-tau), which reflects the intensity of neuroaxonal degeneration, P-tau, which may correlate with tangle pathology, and the 42 amino acid amiloidogenic peptide Aβ42, which correlates inversely with plaque pathology (Blennow K, et al.,2010). It is well known that the pathological processes in the brains of AD patients start more than a decade before the first symptoms are noticed (Price JL, et al., 1999). The temporal dynamics of biomarker levels in relation to changes in cognition have been described in a hypothetical model on the continuum of AD (Jack

CR Jr, et al., 2010). In line with this, the revised diagnostic guidelines identify three different stages of AD: preclinical AD, mild cognitive impairment (MCI) or prodromal AD and AD with dementia.
MVs are emerging as important diagnostic tool and therapeutic target (Cocucci, et al., 2009). Because of their small size, released MVs can move from the site of discharge and enter into biological fluids. MVs have been detected in almost all body fluids, including plasma, urine, milk, and the CSF (Camussi, et al., 2010). The presence of MVs in body fluid make them easy accessible and it has been suggested that the analysis of their concentration and molecular composition can open a window on the damaged tissue (Camussi, et al., 2010). Notably, recent findings of our laboratory identified microglia-derived MVs in the CSF as a novel biomarker of brain inflammation (Verderio C, et al., 2012; Colombo E, et al., 2012), which reflect the extent of microglial activation in patients with neuroinflammatory diseases .

Remarkably, typical proteins of EMVs, like flotilin, have been detected in the plaques of AD brain (Rajendran L, et al., 2006). Altogether these observations suggested that MVs may be involved in the spatiotemporal propagation of AD pathology throughout the brain, this possibility is recently demonstrated where misfolded tau and Aβ have been shown to propagate through the extracellular space and disrupt neuronal systems (de Calignon Alix, et al., 2012; Harris et al., 2010). Intrastatial injection of synthetic misfolded α- Syn led to the cell-to-cell transmission of pathologic α-Syn and Parkinson's-like Lewy pathology in wild type mice with progressive loss of dopamine neurons in the substantia nigra (Luk KC, et al., 2012).

2.12 Cross-talk of membrane lipids and Alzheimer-associated proteins.

In the last years, several molecular mechanisms have been identified that connect membrane lipids to the metabolism of AD related proteins, in particular Aβ generation and aggregation. Indeed, researchers have found that Aβ is produced in cholesterol-rich and detergent-resistant membrane microdomains of the plasma membrane, which are known as lipid rafts. So far studies have mainly focused on the role of cholesterol and sphingolipids on abeta processing. It has been clarified that alterations in the membrane lipid composition affect secretase activities, thereby modulating APP processing and generation of Aβ. In addition, it has been reported that membrane lipids impair the metabolism of tau. However, evidence was also provided that membrane lipids can directly interact with Aβ and modulate its aggregation. Thus, the two neuropathological hallmarks of AD, abeta plaques and neufibrillary tangles, could be both triggered by age-dependent changes in lipid metabolism. Conversely, membrane lipid composition is affected by APP and its derivatives Aβ and

CTFβ, which were shown to modulate lipid metabolic enzymes and directly bind membrane lipids including cholesterol and gangliosides. Tau also affects membrane lipid composition, likely via regulation of vesicular transport. Finally, ApoE as a major lipoprotein in the brain, also affect lipid composition, but also Aβ clearance and aggregation. These findings suggest a close interaction of metabolic pathways related to APP and membrane lipids. Hence, accumulating evidence indicate that alterations in secretase activities as well as dysregulation of lipid metabolic enzymes might underlie the initiation and progression of AD pathogenesis.

2.13 Membrane lipids: as Platform for Amyloid aggregation and/or destabilization

Recent biochemical studies indicated that natural sphingolipids and gangliosides, whose metabolism has been shown to be altered in AD patients (Mielke MM, et al., 2011), destabilize and rapidly resolubilize long Aβ fibrils to neurotoxic species (Martins IC, et al., 2008). These studies also showed that phospholipids stabilize toxic oligomers from monomeric peptides (Johansson AS, et al., 2007). The interaction between Aβ and the cholesterol is inversely correlated with the extent of the peptide-peptide interactions (Zhao LN, et al., 2011). The depletion of cholesterol or gangliosides has been shown to significantly reduce the amount of Aβ and its accumulation (Wakabayashi M, et al., 2009, 2005). In fact, the aggregation of Aβ to fibrills is mediated by the gangliosides on the lipid rafts, where a transition from the alpha-helix-rich conformation to the β-sheet-rich conformation is observed. Thus, the constituents of the raft-like membrane strictly control the amyloid formation. MVs which are derived from microglia cells, as a matter of fact should have similar membrane composition as its donor cells, therefore the membrane lipids of these MVs can serve as a platform to influence amyloid conformations and possibly play a defined role in AD pathology.

Figure 2.7 Model to describe MVs sphingolipids/ ganglioside induced alterations in the equilibrium of abeta aggregation pathway towards soluble non filrillar Aβ species.

2.14 FTY720: a MV shedding inhibitor

Fingolimod, FTY720, trade name **Gilenya**, is a pharmacological drug from Novartis. Fingolimod was synthesized by modifying myriocin, which is derived from *Isaria sinclairi,* an entomopathogenic fungus. The drug is a structural analogue of the natural sphingolipid sphingosine. After oral administration, fingolimod crosses the blood–brain barrier (BBB), because of its lipophilic nature and gets phosphorylated by sphingosine kinase producing P-fingolimod, which then binds to the S1P receptors ($S1P_{1,3-5}$) and exerts its biological action. Levels of fingolimod and active P-fingolymod have been shown to be higher in the brain compared to blood (Miron V, et al., 2008). The S1P receptors play key roles in the immune system including regulating lymphocyte migration from lymphoid tissue into circulation. By binding the S1P receptors, fingolimod prevents lymphocyte egress from lymphoids, thereby reducing lymphocyte infiltration into the CNS (Miron V, et al., 2008). Therefore, fingolimod phosphate (FTY720-P) prevents autoreactive lymphocytes from infiltrating the central nervous system (CNS) and suppresses subsequent neuroinflammation. Because of this property, fingolimod is a new oral drug for multiple sclerosis (Cohen JA, et al., 2011). Recent reports suggest that FTY70 is an inhibitor of A-SMase (Dawson G, et al., 2011), the enzyme that controls MV production. Consistently, work from our lab demonstrated that FTY720 completely abolished ATP-induced MV shedding from primary mouse microglia and strongly reduced production of myeloid MVs in the CSF of mice affected by EAE, the mouse model of human multiple sclerosis (Verderio C, et al., 2012).

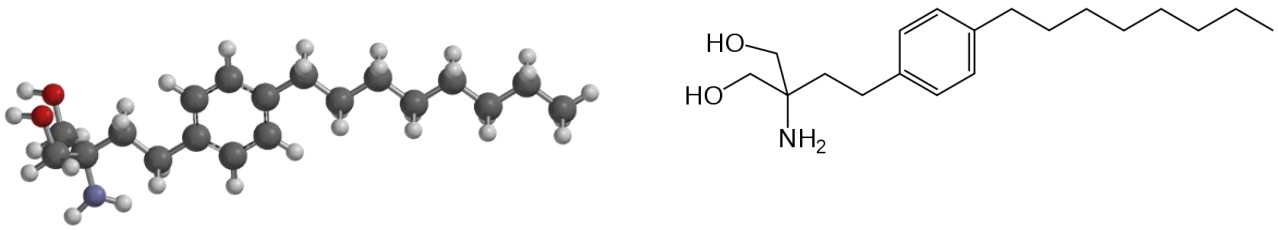

Figure2.8 Structure of FTY720

2.15 FTY720 and neuroprotection in AD

Reduced levels of S1P have been reported in AD patients as compared with the age-matched normal controls. In addition, it has been demonstrated in an ex vivo study, that S1P possesses neuroprotective effects against cell death induced by soluble Aβ oligomer by inhibiting the activation of acid sphingomyelinase (Gómez-Muñoz, et al., *2003*). Accordingly, SPK1 (S1P producing

enzyme) overexpression, has been described to promote neuronal survival upon Aβ exposure (Gomez A -Brouchet, et al., 2007).

It has recently been described that FTY720 protects from Aβ neurotoxicity both in vitro and in vivo (Doi Y, et al. 2013; Fatemeh Hemmati, et al. 2013; Asle-Rousta M, et al 2013). Chronic treatment for 5 days with FTY in rats which received single intra-hippocampus injection of Aβ 1-42 peptide, was observed to prevent hippocampus neuronal death along with p-38 over transcription. (Fatemeh Hemmati, et al. 2013). There was reduced neuroinflammation as determined by the diminished IL-1β and TNF-α mRNA levels (Fatemeh Hemmati, et al. 2013). Consistently, FTY720 administration in rats subjected to bilateral intra-hippocampal injection of Aβ 1-42 peptide, for 15 days, significantly decreased activity of caspase-3, in hippocampus and decreased neuronal loss in the CA1 area, induced by Aβ 1-42 (Asle-Rousta M, et al 2013). The protective actions of FTY720 also improved spatial learning and memory formation in these rat models (Fatemeh Hemmati, et al. 2013; Asle-Rousta M, et al 2013).This protective action of FTY720 may be ascribed to the capability of FTY720 to recapitulate the function of S1P and regulate the ceramide/S1P balance, as FTY720 decreases the levels of ceramides (S. Lahiri, et al.2009). However, recent reports also suggest that FTY720 may act directly on neural and non-neural CNS cells to reduce neurodegeneration and to promote reparative mechanisms by upregulating BDNF, a neurotrophin which is known to attenuate oligomeric Aβ-induced neurotoxicity (Doi Y, et al. 2013).

2.16 APPswe/PS1dE9 as AD mice model to study neuroinflammation and behavioural defects

APPswe/PS1dE9 mice, described by Jankowsky et al. in 2004, have overexpression of the Swedish mutation of APP, together with deletion of exon 9 in PS1 (Jankowsky J L, et al., 2004) Overexpression of the transgene construct leads to increase in parenchymal Aβ load. APPswe/PS1dE9 mice develop first Aβ plaques at the age of 4 months. As the plaque grows activated microglia and astrocytes surround them. By 12 months of age, the mice develop cognitive defects, as indicated by behavioral test measuring spatial navigation and reference learning, the Morris water maze (MWM) task, but memory deficits can be seen in radial arm water maze even at 6 months of age (Xiong H, et al.,2011). These mice do not exhibit neuronal loss, but display a variety of other clinically relevant AD-like symptoms. These include mild abnormalities in neuritis (Garcia M-Alloza, et al.,2010) loss in neuronal activity associated to plaque (Meyer M –Luehmann ,et al., 2009), increased mortality, high prevalence to unprovoked seizures (Minkeviciene R, et al., 2009), age-dependent deficits in the pre- and postsynaptic cholinergic transmission (Machová E, et al., 2010), and co-relation of the soluble

Aβ levels with behavioural deficits at 12 months of age which are comparable to some clinical AD cases (W Zhang, et al.,2011). Therefore, these mice represent a valuable tool to study new therapeutic approaches targeted specifically against the plaques and plaque related neuroinflammation. (Xiong H, et al., 2011).

3. MATERIAL & METHODS

3.1 Primary Culture and Animal Model

Mixed culture of primary cortical and hippocampal astrocytes were isolated from rat microglial cells which were established from E21 rat embryos and were maintained as described by Bianco F, et al., 2005. The transgenic mice model APPswe/PS1dE9 used, have overexpression of the Swedish mutation of APP, together with deletion of exon 9 in PS1 (Jankowsky J L, et al., 2004). The animal colony was provided by Dr. Annalisa Buffo, University of Turin Neuroscience Institute of Turin, Italy. The number of animal used and their suffering was minimized as much as possible, in accordance to the European Communities Council Directive of September 20, 2010 (2010/63/UE). All animal handling procedures were performed in accordance to the guidelines of the Institutional Animal Care and Use Committee of the University of Milan.

3.2 Vesicle Isolation by Differential Centrifugation

Microglial cells were deeply washed with PBS at 37°C. For MV shedding, microglia was stimulated with ATP (1mM) for 30mins in Krebs-Ringer solution (KRH, 125mM NaCl, 5mM KCl, 1.2mM $MgSO_4$, 1.2mM KH_2PO, 2mM $CaCl_2$, 6mM D-glucose, and 25mM HEPES/NaOH, pH 7.4) at 37°C and 5% CO_2.. The supernatant was then withdrawn and subjected to differential centrifugation at 4 C° as follows (all steps at 4°C): 2 times for 10 min at 300*g* to discard cells and debris (P1 pellet); supernatant, 20 min at 1,200*g* to obtain P2 vesicle fraction; supernatant, 30 min at 10,000*g* to obtain P3 vesicle population; supernatant, 1h at 110,000*g* to obtain P4 vesicles. For biochemical fractionation of MVs, total lipids were extracted through the method previously described (Riboni, *et al.*, 2000) with 2:1 (by volume) of chloroform and methanol. The lipid fraction was evaporated under a nitrogen stream, dried for 1 h at 50°C and resuspended in PBS at 40°C in order to obtain multilamellar vesicles. Small unilamellar vesicles were obtained by sonicating multilamellar vesicles, following the procedure of Barenholz, *et a.,* 1977.

3.3 Aβ-1 42 Preparations

Aβ (Anaspec, Fremont, CA) was prepared at a concentration of 2 mM in dimethyl sulfoxide (DMSO) that was maintained at 4°C.The lyophilised protein was properly suspended till there was a clean solution and was aliquoted. The aliquot stocked at -80°C was directly diluted to 4µM in neuronal

medium and kept overnight at 37°C. This Aβ 1-42 preparation was used as aggregated Aβ 1-42 in the experiments, and was different from fibrillar Aβ 1-42 preparation, consisting of more mature and stable fibrils.

The soluble and fibrillar Aβ1-42 were prepared by initially dissolving it in 100% hexafluoroisopropanol (HFP) (Sigma, St Louis, MO, USA) to obtain a 1 mM solution to deseed any aggregated protein and obtain a monomeric Aβ 1-42 . It was aliquoted in a sterile microcentrifuge tubes. The HFP was allowed to dry overnight in chemical hood and finally the remains of HFP was removed under vacuum using a SpeedVac and the peptide film was stored (desiccated) at −80 °C. Soluble Aβ 1-42 was prepared as described by Klein et al. Briefly the peptide film was freshly resuspended in 100% DMSO to 5mM, it was further diluted to 100μM in F-12 medium (Invitrogen, Paisley PA4 9RF, UK) and incubated for 24 h at 5°C. Following the incubation it was further centrifuged at 14,0000g for 10 min at 4°C to obtain only the soluble forms in the supernatant. For fibrillar Aβ1-42 preparation, Aβ or Hylite-488- Aβ peptide film freshly resuspended in DMSO was further diluted to 100μM in 10mM HCl (De Felice FG, et al., 2008). It was vortexed for 15sec and incubated for 24 h at 37°C. After incubation, it was diluted to 4μM in neuronal medium to be used for the experiment. By transmission electron microscopy the aggregation state of Aβ1-42 preparation was assessed with a Tecnai G2 T20 Twin microscope (FEI, Eindhoven, The Netherlands).

3.4 Thioflavin T Assay

Aβ preparations (peptide or fibrillar) were incubated with or without MVs, were diluted to 4μM in KRH and incubated overnight at 37 °C. In case of artificial liposomes and microglial MVs lipids Aβ preparations 4μM (peptide or fibrillar) where incubated overnight in incubator. For Thioflavin-T (ThT) assays, ThT (Fisher Scientific, Waltham, MA) powder was re-suspended in distilled water to 10mM stock. It was then filtered and diluted to 10μM and was added to the Aβ preparations and monitored in a Perkin-Elmer LS50 spectrofluorometer. ThT fluorescence emission spectra were recorded between 465 and 565 nm with 5 nm slits, using an excitation wavelength of 450 nm. For the time-course experiments, the samples were kept at 37°C and aliquots of 100μl were removed from the sample at each time point.

3.5 Measurement of fluorescent fibrils by confocal microscopy

Aβ 1–42 tagged with Hylite-488 (Anaspec, Fremont, CA) was used to prepare fibrils, as described previously. The fibrils incubated or not incubated overnight with MVs were exposed for 1h to 2 weeks old hippocampal neuronal culture plated on glass coverslips. Neurons were then fixed and stained in blue for MAP-2. Leica SP5 confocal microscope was used to acquire fluorescence images of Aβ 1–42 fibrils by an operator blinded to the study and analyzed using Image J 1.46r software. We then set a fixed threshold on Hylite-488-Aβ 1–42 positive images and, having selected the area parameter, in μm, at 0.1μm -infinite in "set measurements", area of single fibrils was automatically measured using "analyse particle" function. The percentage of fibrils charaterized by increasing area values - at intervals of $5\mu m^2$- was calculated and the cumulative distribution plot was constructed using OriginPro 8 software.

3.6 Neuronal Cultures and In Vitro Stimulation

E18 rat pups were used to isolate primary cultures of hippocampal neurons, which where plated onto poly-L-lysine-treated coverslips at 520 cells/mm^2 cell density and maintained in neurobasal with 2% B27 supplement and 2mM glutamine (neuronal medium). Hippocampal neurons DIV 9-15 were exposed to Aβ 1-42 (4 μM), or MVs (1μg/100μl) isolated from 1million microglial cells and to a combination of Aβ 1-42 and MVs for 1h. The combinations of Aβ 1-42, MVs were kept overnight at 37C° in incubator incubated in neuronal medium before being exposed to neurons. $1{,}7X10^5$ neurons were exposed to MVs produced by $1X10^6$ microglia (microglia: neuron ratio 6:1).

In a set of neutralizing experiments the mix of Aβ 1-42/MVs were added with anti-TNF-α plus anti-IL-1β antibodies (R&D Minneapolis, MN) or with the anti-Aβ antibodies 6E10 1:100 (Covance, Emerville, CA, USA) plus A11 1:200 (Invitrogen, Life Technologies Ltd., Paisley, UK) or with the prion protein PrP^C (4μM) for 30 minutes before being exposed to cultured neurons.

3.7 Viability of Cell

PI/calcein staining. Neuron were stained with calcein-AM (0.5 mg/ml, Invitrogen, Life Technologies Ltd., Paisley, UK), propidium iodide (PI) (1μg/ml, Molecular Probes, Life Technologies Ltd., Paisley, UK) and Hoechst (8.1 μM, Molecular Probes, Life Technologies Ltd., Paisley, UK) to look for live and dead cells in the neuronal cultures. Incubation was performed for 20 min in neuronal medium at

37° C and 5% $C0_2$. The cells were washed twice with KRH and then were maintained in KRH during acquisition of images. Viable cells were positive for Calcein-AM which emits green fluorescence signal. Conversely, PI emitted red fluorescence, and was found positive for dead cells as PI could reach their nuclei. Fluorescence images were acquired by Leica DMI 4000B microscope, equipped with DIC microscopy. We then calculated the ratio of dead cells (PI+ calcein–) to the total number of Hoechst stained neurons in and represented it as percentage of neuronal death.

Annexin-V assay. Incubation with annexin-V-FITC (1:100, BD Pharmingenor, Franklin Lakes, NJ) of live neurons was done for 5 min, which were later fixed with 4% paraformaldehyde and in non permeabilizing condition were counterstained for the neuronal marker SNAP-25 (mouse anti-SNAP-25, Sternberger Monoclonals, Baltimora, MD), to preserve annexin-V staining. Fluorescence images were acquired by a SPE Leica confocal microscope, equipped with an ACS APO 40x/1.15 oil objective. For the analysis of index of neurite density we quantified area of annexin-V+ apoptotic processes by Image J 1.46r software and further normalized to SNAP-25 immunoreactive area.

Cytoplasmic calcium levels. DIV 8-9 old hippocampal neuronal cultures in coverslip were loaded with 400μl 2μM Fura-2/AM (Invitrogen, Life Technologies Ltd., Paisley, UK) in neuronal medium for 45 min at 37° C. The neurons were washed in KRH and the coverslips were placed in the recording chamber of an inverted microscope (Axiovert 100, Zeiss) equipped with a calcium imaging unit. The light source used was a Polychrome V (TILL Photonics). Images were collected with a CCD Imago-QE camera (TILL Photonics) and analyzed with TILLvisION 4.01 software. The emission of the light was acquired at 505 nm at 1Hz, after excitation at 340 and 380 nm wavelengths. The fluorescence ratio of F340/380 was expressed as calcium concentration. The ratio values in selected region of interest (ROI) corresponding to neuronal somata were calculated from sequences of images to obtain temporal analysis. Basal calcium concentration was recorded from at least 100 neurons/condition in each experiment.

3.8 Immunocytochemical Staining

Neurons were fixed with 4% paraformaldehyde and were washed twice with PBS. They were further washed three times with low and high phosphate salt buffers. The cells were permeablized with 1XGSDB. Primary antibodies in 1XGSDB was incubated for 3hrs for the following markers: rabbit anti-beta tubulin 1:50(Sigma, St Louis, MO, USA) guinea pig anti-vGLUT-1 1:1000(Synaptic System,

Gottingen, Germany), mouse anti-PSD-95 (UC Davis/NIH NeuroMab Facility, CA, USA), mouse anti-MAP-2 1:1000 (Synaptic System, Goettingen, Germany). The coverslips were washed 3 times with high salt buffer. Secondary antibodies in 1XGSDB were conjugated with either Alexa-488, Alexa-555 or Alexa-633(Invitrogen, Life Technologies Ltd., Paisley, UK) fluorophores in concentration 1:200 and incubated for 1hrs. After incubation the cells were washed three times with high salt phosphate buffer, and three times with low salt phosphate buffer. The last wash was made in temporal phosphate 5mM and the coverslips were mounted and sealed with nail paint, and stored at -20° C till they were acquired. For quantification of V-glut-1 puncta per length unit, the length of single neuritis was measured using Image J 1.46r software and the number of positive puncta whose dimension was greater than 0.01 μm was quantified.

Quantification of Binding of Hylite-488 labeled Aβ $1\text{–}42$ (Anaspec, Fremont, CA, USA) to neurons was quantified using Image J 1.46r software. A fixed threshold was selected in the separate channels for Hylite-488-Aβ $1\text{–}42$ and β tubulin staining. Double positive punta were revealed by generating double-positive images of Hylite-488-Aβ $1\text{–}42$/β tubulin using "and" option of "image calculator" function, The resultant image was then subtracted from Hylite-488-Aβ $1\text{–}42$ using "subtract" option of image calculator and the final image thus obtained represents all the Hylite-488-Aβ $1\text{–}42$ positive binding co-localizing with β tubulin. For the analysis the area parameter was selected, in pixels, at 3-infinite in "set measurements", total co-localizing area was quantified using "analyse particle" function. Total β tubulin fluorescence area was directly measured in β tubulin fluorescence images, after setting a fixed threshold using "analyse particle" function, as described above. Finally, total Hylite-488-Aβ $1\text{–}42$/β tubulin co-localizing area was normalized to total β tubulin area in each field. β tubulin was revealed by Alexa-633 fluorophore, to avoid significant interference of Hylite-488 in the red channel. Quantification of binding was normalized to β tubulin due to the decrease in MAP2 immunofluorescence staining upon Aβ $1\text{–}42$ binding. Maximum projection of confocal stacks in the x-y plane and z-axis scans were generated using Image J 1.46r software.

3.9 Western Blotting.

The lysates of shed MVs and exosomes obtained from Microglial cells, either by ATP induced stimulus or through constitutive shedding, were separated by electrophoresis revealed using streptavidin (1: 1500, Sigma, St Louis, MO, USA), rabbit anti-alix (1:1000, Covalab, Billerica, MA, USA), mouse anti-Tsg101 (1:1000, Abcam, Cambridge, UK). For western blot analysis of brain cortical

samples of transgenic and wild type animals, 50 µg of cortical lysates was resolved on 15% Tri-Glycine SDS PAGE. The resolved proteins were transferred to nitrocellulose membrane (Millipore, San Diego, CA, USA) and then were incubated for 1 h at room temperature with a blocking buffer (5% dry milk dissolved in the tris buffered saline with tween-20 (TBST) buffer). The membranes were incubated overnight with the primary antibodies for markers GFAP (1:500) and MHCII (1:500) incubated for 3 hrs and were washed 3 times with TBST buffer. Secondary antibody for anti- mouse HRP was incubated for 1 hr and the membrane was further washed 3 times with TBST (0.1%) and 3 times with TBST (0.3%). The immunoreactive bands were detected using SuperSignal West Femto Pierce ECL (Thermo Fisher Scientific Inc., Rockford, IL) and ECL film (Amersham, GE Healthcare limited, UK).

3.10 Endogenous Glutamate Determination

High performance liquid chromatography was used to measure endogenous glutamate content. The analysis was done following pre-column derivatization with o-phthalaldehyde and then on a C18 reverse-phase chromatographic column (10 x 4.6 mm, 3 µm; at 30°C; Chrompack, Middleburg, The Netherlands) coupled with fluorometric detection (excitation wavelength 350 nm; emission wavelength 450 nm) discontinuous triphase gradient separation was done. The internal standard was Homoserine (Klein WL, et al., 2002).

3.11 SELDI TOF Mass Spectrometry

The Aβ isoforms were detected through immune-proteomic assay, and was performed as reported previously (De Felice FG, et al., 2008). In short, three microliters of the specific monoclonal antibodies (6E10+4G8) (Covance, Emerville, CA, USA) were incubated in a humidity chamber at total mAbs concentration of 0.125 mg/mL (concentration of each mAb 0.0625 mg/mL), for 2 h at RT to allow covalent binding to the PS20 ProteinChip Array (Bio-Rad, Hercules, CA, USA). Tris–HCl 0.5 M pH 8 was used to block unreacted sites, in a humid chamber at RT for 30 min. Spots were washed three times with PBS containing 0.5% (v/v) TritonX-100 and then twice with PBS. 5µl of sample was used to coat these spots and incubated in a humid chamber overnight. The spots weret washed three times with PBS containing 0.1% (v/v) TritonX-100, twice with PBS, and finally with deionized water. To the coated spots was added one microliter of α-cyano-4-hydroxy cinnamic acid (CHCA)

(Bio-Rad). Using the ProteinChip SELDI System, Enterprise Edition (Bio-Rad) mass identification was made.

3.12 ELISA Quantification

Quantitative determination of Aβ 1-42 and total Tau protein was performed using innotest ELISA kit (Innogenetics, Gent, Belgium), according to the manufacturer's procedures. Absorbance was detected at 450nm by 1420 Multilabel Counter Victor 2- Wallac, Finland.

3.13 Human Subjects

CSF from human samples with mild cognitive impairment (n=53), definitive AD (n=89) were obtained for diagnostic purposes from subjects according to Dubois criteria, and from age- and sex-matched cognitively preserved and neurologically healthy subjects, undergoing spinal anesthesia for orthopedic surgery, serving as controls (n=20). The ethical committee of the San Raffaele Scientific Institute approved this research project, and all subjects signed written informed consent.

3.14 Quantification and Isolation of MVs from human CSF

CSF samples were collected by lumbar puncture (200-300μl) and flow cytrometric analysis was done as described previously (Verderio C, et al., 2012). In brief, CSF from human subjects was stained with the myeloid marker IB4-FITC (Sigma, St Louis, MO, USA). The quantification of labeled MVs within a fixed time interval on a Canto II HTS flow cytometer and analyzed using FCS 3 software. A vesicle gate was determined using side-scatter (SSc) and FSc over the instrument noise (set by running PBS filtered through a 100 nm filter). IB4 positive events were evaluated within this gate, (number of events/ml) as a parameter of MV concentration. Human MVs were pelletted at 10,000 g from the volume of CSF after flow cytometry quantification in experiments, yielding 400 MVs, which is the amount produced in vitro by $1X10^6$ microglia. Re-suspension of MVs was done in neuronal medium and exposed to $1,7X10^5$ neurons. Alternatively, MVs (10,000 g pellet) were processed and analyzed by SELDI-TOF mass spectrometry.

3.15 Quantitative real time PCR

RNA was extracted from cortex of transgenic and wild type mice. cDNA synthesis from total RNA was performed using ThermoScriptTM RT-PCR system (Invitrogen) and Random Hexamers as primer. IL1-β, iNOS, COX-2, TGFβ and IL-6 mRNA levels were measured by real time PCR using Taqman® Gene Expression Assays on the ABI-Prism7000 sequence detection system (Applied Biosystems). 50 ng of starting RNA were used as template. The mRNA expression was normalized to the levels of GAPDH mRNA.

3.16 Passive Avoidance Test

In this performance task, there are two compartments in an apparatus, one light and one dark, connected via a sliding door. Each mouse was placed in the light compartment and allowed to enter the dark compartment, which the mice prefer more than light. In the acquisition trial, the time taken to enter the dark compartment was recorded (in seconds).Once the mouse was in the dark compartment, the sliding door was closed and an unavoidable electric shock (1mA for 1 seconds) delivered via the paws. The animal was then placed back in the home cage, the retention trial was carried out 24 h after the acquisition trial, by positioning the mouse in the light compartment and recording the time taken to enter the dark compartment (retention latency, cut-off 180 s). An increased retention latency indicates that the animal has learned the association between the shock and the dark compartment.

3.17 Novel Object Recognition test

Animals were habituated to the test arena for 10 min on the first day. After 1-day habituation, mice were subjected to familiarization (T1) and novel object recognition (T2). During the initial familiarization stage, two identical objects were placed in the centre of the arena equidistant from the walls and from each other. Each mouse was placed in the centre of the arena between the two objects for a maximum of 10 min or until it had completed 30 s of cumulative object exploration. Object recognition was scored when the animal was within 0.5 cm of an object with its nose toward the object. Exploration was not scored if a mouse reared above the object with its nose in the air or climbed on an object. Mice were returned to the home cage after familiarization and retested 120 min later, and in the arena a novel object (never seen before) took the place of one of the two familiar. Scoring of object recognition was performed in the same manner as during the familiarization phase. From mouse to mouse the role (familiar or new object) as well as the relative

position of the two objects were counterbalanced and randomly permuted. The objects for mice to discriminate consisted of white plastic cylinders, colored plastic Lego stacks of different shape and a metallic miniature car. The arena was cleaned with 70% ethanol after each trial. The basic measure was the time (in seconds) taken by the mice to explore the objects in the two trials. The performance was evaluated by calculating a discrimination index (N-F/N+F), where n= time spent exploring the new object during T2, F= time spent exploring the familiar object during T2 (Pitsikas, et al., 2001).

3.18 Immunohistochemistry on brain slices

The brain was embaded in paraffin and slices were taken onto SuperFrost Ultra Plus® glass slides, Menzel-Glaser. The sections were deparaffinised with two washes of xylene, 10 minute each. The sections were rehydrated in decreasing concentration of ethanol, 99% 95% 70% with 5 minute incubation in each dehydration step. Inhibition with peroxidase (3% in dH_2O of 30% Hydrogen peroxidase) was done for 15 minute, the slides were further washed with PBS buffer for 5 minutes. Two more washes were performed with PBST and the sections were blocked with 10% normal horse serum in PBS for 30 minutes in humid chamber, at RT. Primary antibody (GFAP and IBA1 in concentration 1:900) was incubated for 1 hr in blocking serum, at RT and the sections were further washed twice with PBST for 5 minutes. Secondary antibody Vector Lab BA-2000 biotinylated Anti-Mouse IgG (H+L), made in horse was used at dilution 1:200 in blocking serum, at room temperature in humid chamber for 30 minutes. The slides were washed 2 times with PBST. Biotin was complexes with peroxidase-labelled avidin, with Vector Lab, Vectastain Elite ABC kit PK-6100 and the reaction was carried out for 30 minutes. Slides were further washed with PBST twice. The chromogen reaction was carried out with Vector Lab DAB kit for the duration of 5- 10 minutes, depending upon the signal. The sections were rinsed with tap water and were counterstained with Mayer's hematoxylin for 1-2 minutes. The sections were again washed in tap water and dehydrated in increasing concentration of ethanol, 95%99%. Finally the sections were dehydrated in xylene for 10 minutes and were further mounted in the coverslip using mounting medium.

3.19 Dot Blot analysis

Dot blot analysis was done in cortical lysates of APPswe/PS1 using 6E10 antibody. 15 µg of protein from cortical tissues was spotted onto a nitrocellulose membrane that was then air-dried. The membranes were soaked in 5% milk in TBST, tween 0.01% for 1 h to block non-specific sites and were then incubated with the Aβ antibodies 6E10 (dilution 1:1500, mouse monoclonal; Covance,

San Diego, CA, USA) for 2hrs, the membrane were washed three times with TBST and then incubated with an secondary anti-mouse antibody that was conjugated with HRP (horseradish peroxidase; 1:40 000 dilution) for 1hr min at room temperature. The membrane was again washed three times with TBST and was developed by chemiluminescence reagent SuperSignal West Pierce ECL (Thermo Fisher Scientific Inc., Rockford, IL) and ECL film (Amersham, GE Healthcare limited, UK). The analysis of dot blot was done by Image J software.

3.20 Statistical Analysis

The data presented are mean ± SE. SigmaStat 3.5 (Jandel Scientific) software was used to do statistical analysis. After testing data for normal distribution, the appropriate statistical test has been used, as indicated in legends of figures. The differences were significant if $P<0.05$ and indicated by an asterisk and those at $P<0.01$ were indicated by a double asterisk.

4. RESULTS

4.1 Microglia-derived MVs in combination with Aβ 1–42 is neurotoxic in vitro

Recent evidence claims that natural lipids such as gangliosides and sphingolipids can lead to generation of highly toxic Aβ species by altering the equilibrium between insoluble and soluble Aβ towards neurotoxic soluble forms (Martin JC, et al., 2008; Fukunga S, et al., 2012). Given that microglia-derived MVs originate from lipid raft domains of the plasma membrane and contain bioactive lipids (Antonucci, et al., 2012) we investigated whether MVs may promote Aβ neurotoxicity. To this aim, the amyloidogenic peptide Aβ 1–42 (4 μM) dissolved in DMSO was incubated overnight with MVs derived from rat primary microglia (1 μg/100 μl) at 37°C in neuronal medium. The neurotoxic potential of Abeta exposed to MVs was then tested on two weeks old hippocampal rat neurons. Neurons were incubated with the mix of Aβ 1–42 and MVs or with Aβ 1–42 alone or MVs alone, and neuron viability was then assessed 24 h later by the propidium iodide calcein assay (Figure 4.1a). Overnight pre-incubation of Aβ 1–42 with MVs led to formation of a neurotoxic mixture that significantly increased the percentage of dead neurons. Milder toxic effects were observed upon shorter time periods of Aβ 1–42 pre-incubation with MVs (3-5h).

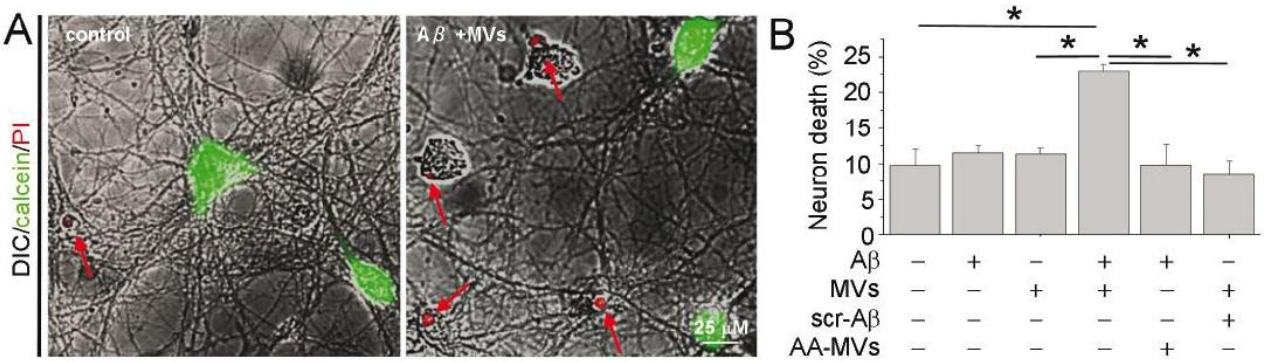

Figure 4.1 A Overlays of DIC and fluorescence microscopy images of neurons stained for calcein and propidium iodide (PI), after 24 h exposure to Aβ 1-42/MVs mixture or under control conditions. B Percentage of calcein-/PI+ neurons (dead cells) in cultures exposed to Aβ 1–42, scrambled Aβ 1–42 , MVs or Aβ 1–42/scrambled Aβ 1–42 incubated overnight with MVs. AA-MVs (Acutely Added-MVs),freshly isolated MVs added to Aβ 1–42, just before neuron challenge (Kruskal-Wallis ANOVA p<0.001; Dunn's test for comparison among groups *p<0.05).

After overnight incubation MVs alone, Aβ 1–42 alone do not significantly affected neuronal survival (Figure 4.1b). Electron microscopy revealed that after overnight incubation in neuronal medium Aβ 1–42 alone was mainly in a aggregated state (Figure 4.1b). No significant increase in the percentage of dead neurons was also observed when MVs were incubated with scrambled Aβ 1–42. Similarly Aβ 1–42 alone supplemented with MVs just before neuron challenge (Acutely Added-MVs, AA-MVs) barely affected neuronal viability. Altogether these data indicate that pre-treatment of Abeta 1-42 with MVs is necessary to cause neurotoxic damage.

4.2 Neurotoxicity caused by Microglia-derived MVs in combination with Aβ 1–42 is rapid.

We observed that the toxicity caused by Aβ 1–42 pre-incubated with MVs was rapid, as about 15-30% of neurons loaded with the calcium dye Fura-2 showed an abnormally high level of cytosolic calcium, one hour exposure to Aβ 1–42 pre-incubated with MVs. Basal $[Ca^{2+}]_i$ was measured in single neurons and expressed as ratio between F340/380 fluorescence (Figure 4.2a-b). We also stained neuronal cultures with the early apoptotic marker annexin-V and analysed the neurons positive for the annexin-V under the same experimental condition described above. By this approach we confirmed that MVs, pre-incubated overnight in neuronal medium with Abeta 1-42, induced a significant increase in annexin-V immunoreactivity (Figure 4.2c).

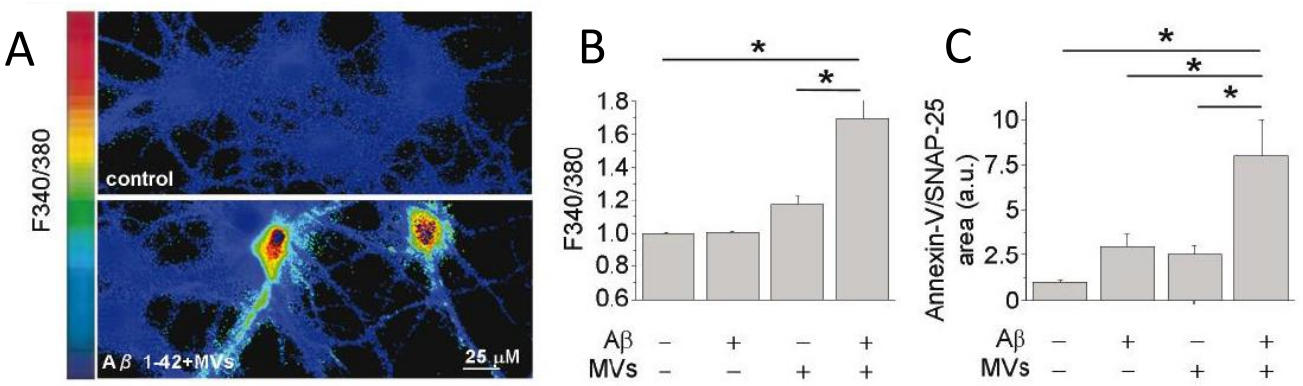

Figure 4.2 A Basal $[Ca^{2+}]_i$ was measured in single neurons loaded with the ratiometric calcium dye Fura-2 and expressed as F340/380 fluorescence. Representative pseudocolor images of 9DIV control neurons and neurons treated with Aβ1-42/MVs mixture for 1h. The color scale is shown on the left**, B** Quantification of basal $[Ca^{2+}]_i$ in neurons exposed to Aβ 1-42, MVs or Aβ 1-42 in combination with MVs. At least 100 neurons/condition were examined. Values are normalized to control (Kruskal-Wallis ANOVA p=0.002; Dunn's test for comparison among groups *p<0.05). **C** Quantification of early apoptotic damage, revealed by Annexin-V binding, normalized to SNAP-25 immunoreactive area, in neuron. (Kruskal-Wallis ANOVA p=0.001; Dunn's test for comparison among groups *p<0.05.

4.3 Microglia-derived MVs in combination with Aβ 1–42 induces fragmentation of dendrites and synaptic loss.

Immunofluorescence analysis for the neuronal marker β-3 tubulin and the pre- and post-synaptic markers V-Glut-1 and PSD-95, was performed in control hippocampal cultures and cultures exposed to MVs pretreated with abeta 1-42. We found that the processes of neurons treated with combined Aβ 1–42 and MVs were fragmented. Furthermore the density of excitatory synapses was significantly reduced in neurons exposed to abeta and MVs mixture, as indicated by the reduced number of vGLUT positive puncta per dendrite length (Figure 4.3a-b). We also observed a remarkable decrease in MAP-2 immunoreactivity, which is indicative of dendritic damage (Figure 4.3c-d).

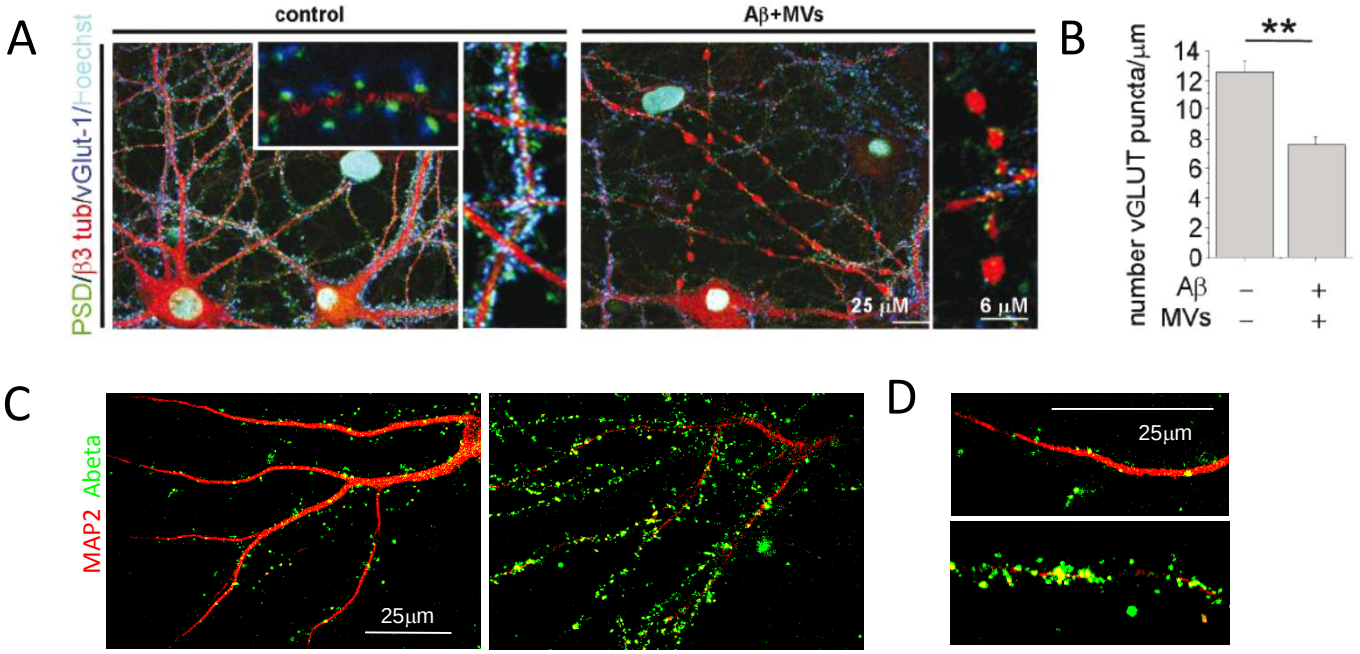

Figure 4.3 A Confocal microscopy images of 14DIV neurons untreated or pre-treated with Aβ 1-42 in combination with MVs and stained for beta-3 tubulin, the vesicular glutamate transporter vGlut-1 and the postsynaptic marker PSD-95. Nuclei are stained with Hoechst. Note fragmentation of neuronal processes and loss of excitatory synapses in neurons exposed to Aβ 1-42/ MVs mixture. Density of excitatory synaptic puncta is quantified in **B** (data follow normal distribution, student T test **p<0.001). **C** Decrease in immunoreactivity of neuronal marker MAP2, upon extensive binding to Hylite-488 Aβ 1-42 (right panel) as compared to less Aβ 1-42 binding to neuronal process (left). **D** Enlarged segment of images in panel C showing decrease in MAP-2 staining.

4.4 Aβ 1–42 in combination with MVs causes neuronal damage mainly by excitotoxicity

The toxic effect of Aβ 1–42 in combination with MVs was largely prevented when neurons were exposed to Abeta pre-treated with MVs in the presence of the glutamate receptors antagonists APV

(100 μM) and CNQX (20 μM), as evaluated by cytoplasmic calcium recordings. Protection by APV was confirmed by evaluation of neuron viability through the annexin-V or PI/ calcein assays (Figure4.4 a-c). These observations indicated excitotoxic damage as the cause of neuronal death.

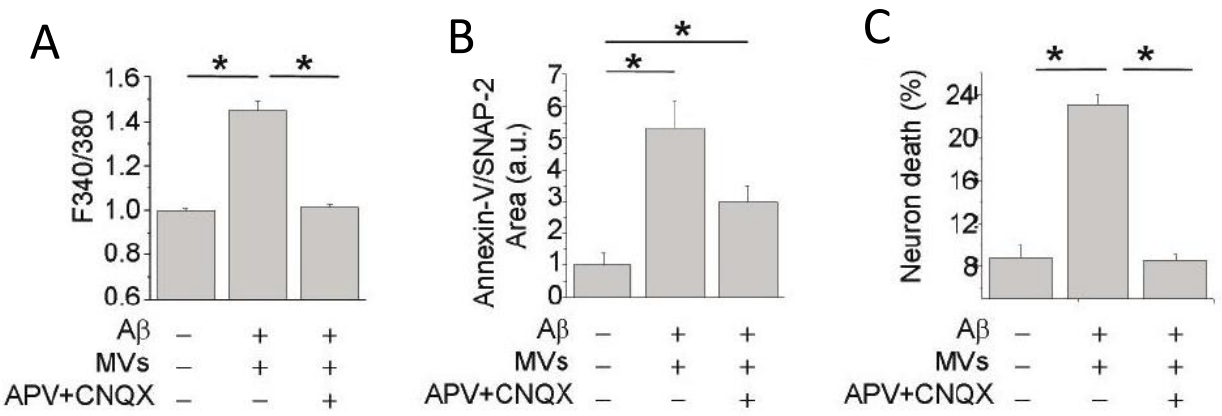

Figure 4.4 A-C Control cultures and cells treated with Aβ 1-42/MVs mixture analysed for basal $[Ca^{2+}]_i$ (H) (Kruskal-Wallis ANOVA p=0.001; Dunn's test for comparison among groups *p<0.05), early apoptotic damage (I) (Kruskal-Wallis ANOVA p=0.001; Dunn's test for comparison among groups *p<0.05) and calcein/PI staining (J, Kruskal-Wallis ANOVA p<0.001; Dunn's test for comparison among groups *p<0.05), either in the presence or in the absence of the glutamate receptor antagonists APV and CNQX.

4.5 Alterations in the aggregation of Ab1-42 induced by microglial derived MVs.

Recent evidence suggests that natural lipids solubilize inert Aβ 1–42 fibrils to neurotoxic protofibrillar species. To understand whether overnight incubation with microglial MVs can induce alterations in the content of aggregated Aβ 1–42 we performed the thioflavin T dye-binding assay. This assay showed a significant reduction (about 22± SE %) in the content of abeta fibrils (Figure4.8b, red lines) upon overnight incubation with MVs (ref). Furthermore there was a 39± SE % reduction of aggregated Aβ 1–42 species when a preparation of aggregated Aβ dissolved in DMSO and incubated overnight with microglial MVs at 37°c in neuronal medium was exposed to MVs (Figure4.5b, blu lines). No changes in Thioflavin-T spectra were detected upon acute MV addition, thus excluding possible interference of MV lipids on the Thioflavin-T binding site of Aβ1-42 (Figure 4.5c). We also performed time course analysis of Aβ 1–42 aggregation in the presence or on the absence of MVs. Results from time course experiment confirmed that shed MVs solubilize aggregated Aβ 1–42 and prevent its self-aggregation (Figure 4.5d). Consistent with these observations, we found that incubation with MVs reduced the fibril size of fluorescently-labeled

Aβ 1–42 fibrils, which were observed and analyzed by a confocal microscope (Figure 4.5e, left). Indeed exposure to MVs induced a shift towards smaller fibril size in the cumulative distribution (Figure 4.5e, right). Altogether these observations indicate that aggregated Aβ 1–42 disassembles into soluble species upon MV exposure.

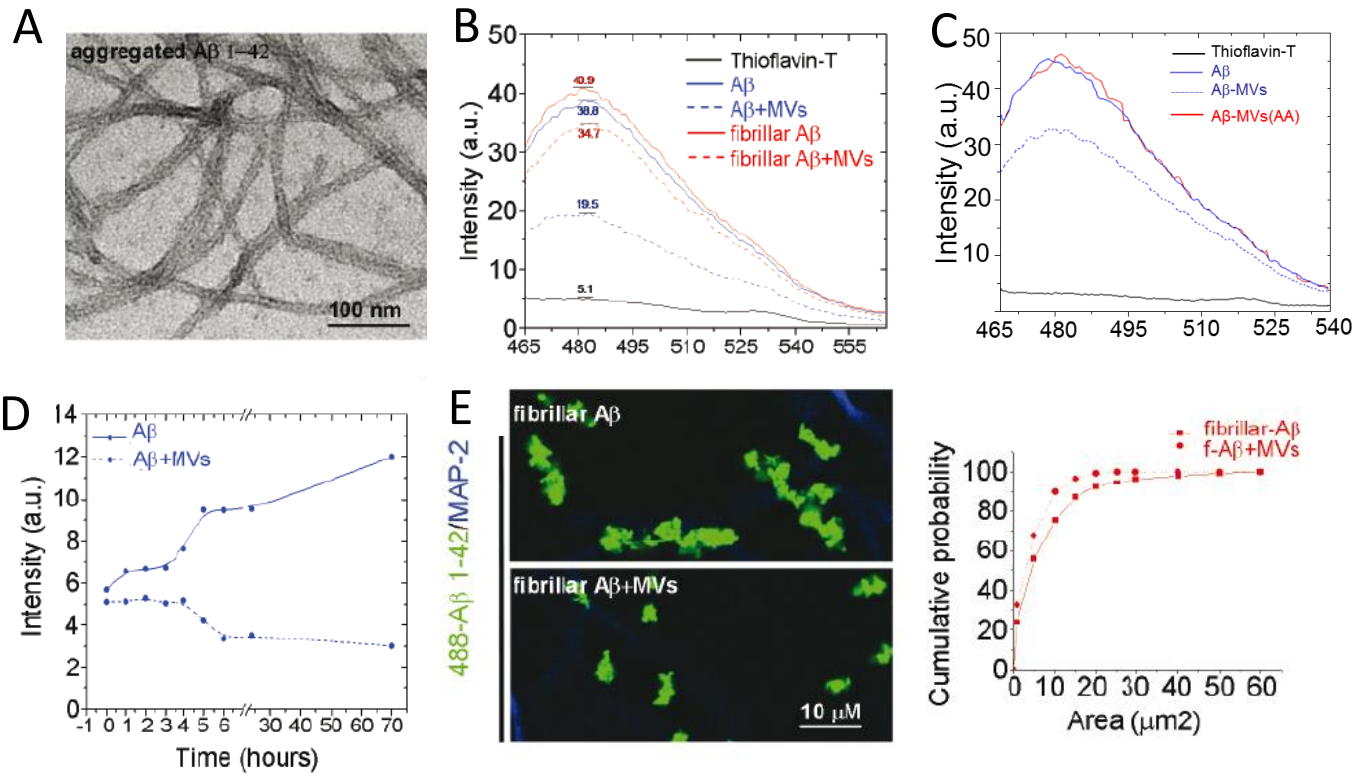

Figure 4.5 A Negative staining EM image of aggregated Aβ 1-42, incubated overnight in neuronal medium. **B**Thioflavin T emission spectra of aggregated Ab 1-42 (solid blue line), incubated overnight with MVs (dashed blue line) or acutely exposed to MVs. **C** Representative thioflavin-T fluorescence emission spectra of samples containing Aβ1–42 fibrils (dashed red lines) or aggregated Aβ 1-42 (dashed blue lines) exposed to MVs. **D** Time course of fibrilization of Aβ 1-42 in the presence (dashed line) or in the absence (solid line) of MVs. **E** Representative confocal images of Hylite-488-Aβ 1–42 (488-Aβ 1-42) fibrils untreated or treated overnight with MVs and exposed for 1h to neurons. Neurons are stained in blue for MAP-2 after fixation. Cumulative distribution of fibril size from control (solid line) and MV-treated (dashed line) 488-Aβ 1-42 fibril preparations is shown on the right.

Parallel analysis by SELDI-TOF mass spectrometry using 6E10 and 4G8 anti-Aβ antibodies indicated that microglia derived MVs induce a 50% decrease of Aβ1-42 monomers in the amyloid preparation (Figure 4.5f), with no significant peptide degradation. This is consistent with oligomerization and stabilization of Aβ1-42 monomers in the presence of EMVs, although the absence of antibodies to efficiently immuneo-isolate oligomers hampers their direct detection by mass spectrometry. Thus,

microglia-derived EMVs may favour solubilization of aggregated Aβ-1-42, but also induce formation of soluble oligomers from Aβ1-42 monomers.

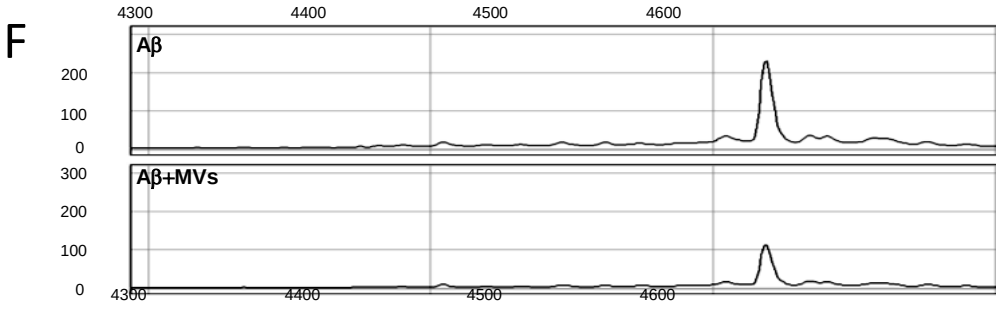

Figure 4.5 F Representative spectra of SELDI-TOF mass spectrometry using 6E10 and 4G8 anti-Ab antibodies indicating decrease in amount of Ab1-42 monomers in Ab1-42/MVs mix as compared to Ab1-42 peptide alone.

4.6 There is a transient interaction of Aβ 1-42 with MVs, but most of the soluble Aβ 1-42 generated is free.

To answer the possibility of interaction of Aβ 1-42 with MVs, Aβ 1-42 forms associated with MVs and soluble amyloid forms generated as consequence of this association were separated from insoluble species by sucrose gradient centrifugation at 100,000 *g* for 1 h (Martins JC., et al. 2008) in the samples incubated overnight with Aβ $1\text{–}42$ /MVs mix. The amount of Aβ 1-42 present was quantified by ELISA. We observed a fivefold increase in the fraction of soluble Aβ $1\text{–}42$ recovered at the top of the gradient and a parallel decrease in the fraction of insoluble Aβ $1\text{–}42$ at the bottom of the gradient, upon overnight incubation with MVs (Figure 4.6a). Interestingly acute addition of MVs even immediately before ultracentrifugation on sucrose gradient, partially promoted Aβ$1\text{–}42$ migration to the top of the gradient (Figure 4.6b), suggesting that MVs being light tend to move to the top fractions of the gradient and along with associate Aβ $1\text{–}42$ and contribute in part to Aβ $1\text{–}42$ redistribution to the top of the gradient.

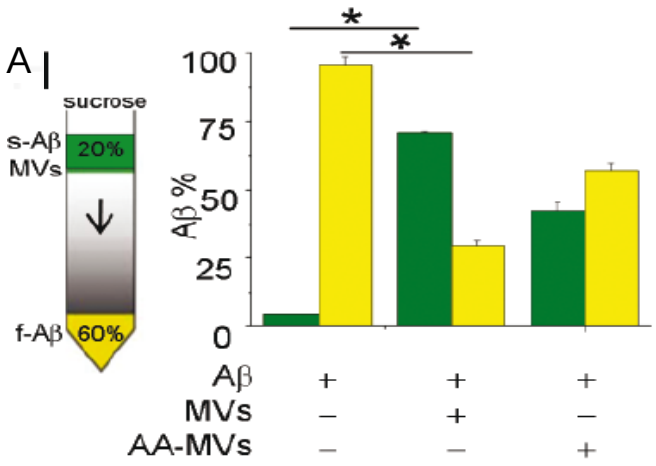

Figure 4.6 A "Floating assay" by ultracentrifugation reveals an increase of soluble Aβ 1-42 species in association with MVs.. As ELISA indicates, a higher fraction of Aβ 1-42 species is transported from the bottom to the top of the gradient in samples incubated overnight with MVs. Acute addition of MVs (AA-MVs) does not cause statistically significant changes in Aβ 1-42 distibution (Kruskal-Wallis ANOVA $p<0.001$; Tukey test for comparison among groups *$p<0.05$).

4.7 The neurotoxicity caused by Microglia-derived MVs is retained in the soup.

MVs incubated overnight with Aβ 1–42 in neuronal medium were centrifuged for 30 min at 10,000g to obtain a soup and a pellet fractions, with the soup containing soluble molecule released from MVs and soluble Aβ 1–42 species and the pellet containing aggregated Aβ 1–42, MVs, and Aβ 1–42 forms eventually associated with MVs. The neurotoxicity of these two fractions was analyzed by monitoring cytosolic calcium in cultured neurons. While the pellet was largely inert, most of the toxicity was retained in the supernatant (Figure 4.7a left). Similar results were obtained by quantification of neuronal death by PI/calcein assay (Figure 4.7a right). These findings suggested that soluble molecules not associated with MVs, were responsible for neuronal damage.

Next we investigated if soluble molecules released from MVs mediate neurotoxicity. We know that the inflammatory mediators IL-1β and TNFα are among the molecules contained in microglial MVs that, through potentiation of NMDA channel activity, may induce excitoxicity (Bianco F, et al., 2005; Turola E, et al., 2012). Since IL-1β and TNFα expression is up-regulated in M1 proinflammatory microglia, and down-regulated in M2 anti-inflammatory cells, neuronal viability was analyzed after exposure to Aβ 1–42 incubated with MVs produced by either LPS-primed M1 microglia or M2 cells, polarized with IL-4. We found similar alterations in cytosolic calcium levels in neurons exposed to Aβ 1–42 incubated with MVs derived from either M1 or M2 polarized microglia as compared to MVs produced by resting microglia (Figure 4.7b). In addition, Neuronal cultures were exposed to the

neurotoxic mixture in the presence of IL-1β and TNFα neutralizing antibodies. There was no change in the level of toxicity observed, measured as alterations in cytosolic calcium levels in neurons. (Figure 4.7c). These data rule out the possibility that excitotoxicity of Aβ 1-42 in combination with MVs depends on cytokine leakage from MVs.

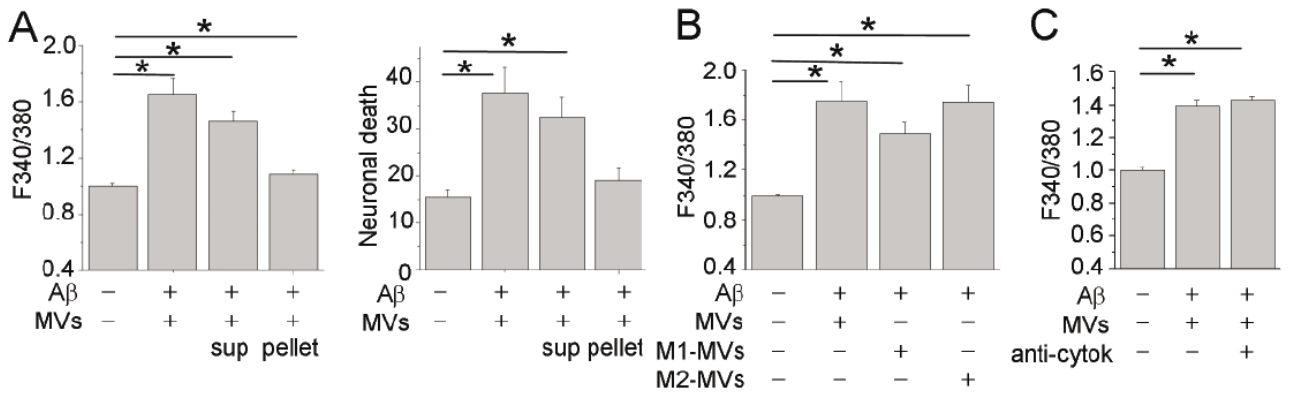

Figure4.7 A Basal $[Ca^{2+}]_i$ in neurons exposed for 1h either to Aβ 1-42/MVs mixture or soluble (sup)/insoluble (pellet) fractions (left panel, Kruskal-Wallis ANOVA p<0.001; Dunn's test for comparison among groups *p<0.05). Values are normalized to control. Right panel shows the percentage of calcein-/PI+ neurons under the same conditions (Kruskal-Wallis ANOVA p=0.002; Dunn's test for comparison among groups *p<0.05). **B** Basal $[Ca^{2+}]_i$ in neurons exposed for 1 h to MVs derived from resting, M1 or M2 microglia preincubated with extracellular Aβ 1-42. Values are normalized to control (Kruskal-Wallis ANOVA p<0.001; Dunn's test for comparison among groups *p<0.05). **C** Basal $[Ca^{2+}]_i$ in neurons exposed to Aβ 1-42 and/or MVs in the presence or in the absence of neutralizing antibodies for IL-1β and TNFα. Values are normalized to control.

4.8 The neurotoxicity caused by Aβ 1-42/MVs mixture is due to soluble Aβ forms.

We then investigated whether neurotoxic soluble Aβ forms could be present in Aβ 1-42/MVs mixture. Electron microscopy (EM) analysis revealed globular structures of diameter between 4 and 8 nm, similar oligomeric Aβ 1-42, together with thin fibrils of short length, likely representing soluble protofibrils, in the soup obtained after centrifugation at 10,000g for 30min of the Aβ 1-42/MVs mixture. 5-8 nm wide Aβ fibrils were instead observed in the pellet (Figure4.8a). Detection of globular/protofibrillar species in the soluble fraction from Aβ 1-42 and MVs mixture, prompted us to investigate by an array of techniques whether shed MVs change the equilibrium between soluble and insoluble Aβ $1{-}42$. (Figure 4.8b)

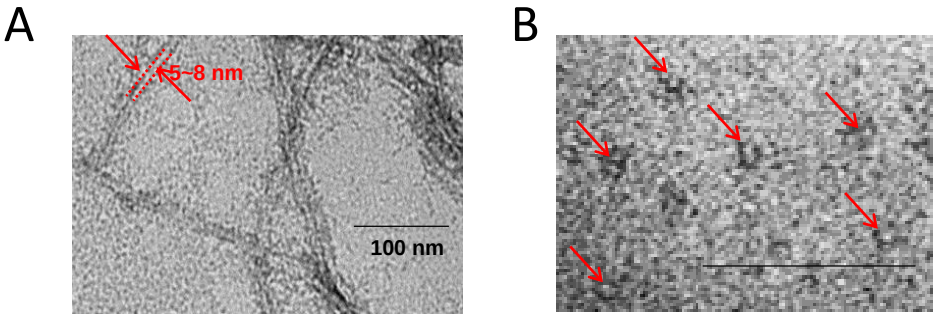

Figure 4.8 Representative TEM images of 5-8 nm wide Ab 1-42 fibrils retrieved in the pellet fraction (**A**) and of globular Ab 1-42 species, present in the supernatant (**B**)

4.9 Bio-detection of the Soluble Aβ 1–42 generated in Aβ 1-42/MVs mixture incubated overnight.

It is known that soluble Aβ but not fibrillar or monomeric Aβ forms activate NMDA receptors, enhancing calcium influx through the channel. Therefore we used neurons expressing functional NMDA receptors, loaded with FURA-2, as sensor cells to bioassay soluble Aβ 1-42 generated upon overnight incubation with MVs. We found that about 30% of neurons showed calcium responses to Aβ 1-42 in combination with MVs, but not to Aβ 1-42 or shed MVs alone (Figure 4.9a). Furthermore the NMDA receptor antagonist APV (100 μM) blocked completely the calcium responses evoked by Aβ 1-42 pre-treated with MVs. (Figure 4.9 b-c). HPLC measurements of glutamate content in MVs and Aβ 1-42/MVs mixture revealed concentration of glutamate lower than 1 μM, which is the minimum glutamate concentration able to induce calcium influx in our experimental conditions (mean glutamate concentration: 137± 70 nM, MVs alone; 196± 115 nM, Aβ 1-42/MVs mixtures). This finding exclude possible interference of ambient glutamate in the NMDA-dependent calcium response evoked by Abeta and Mvs mixture. We concluded that activation of NMDA calcium channels, which triggers neuron excitotoxicity, were caused by soluble Aβ 1-42 species generated in the presence of microglial MVs.

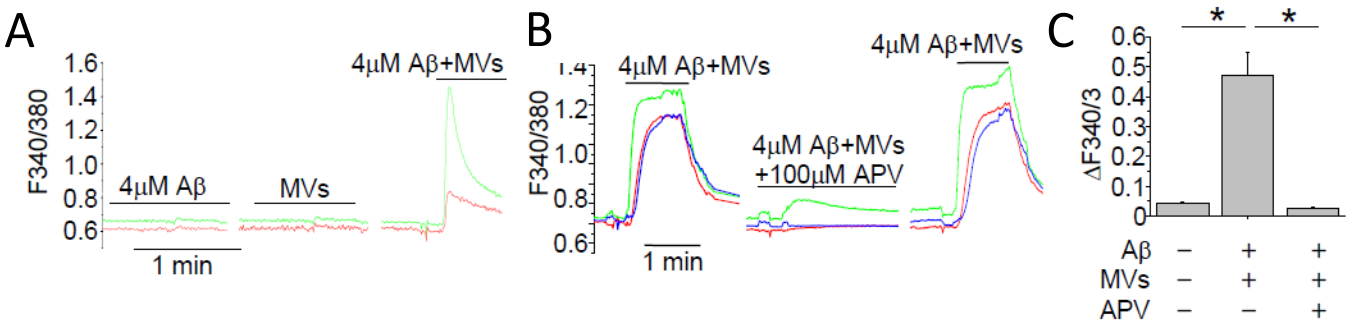

Figure4.9 Bio-detection of soluble Aβ 1-42 by fura-2-loaded sensor neurons, expressing functional NMDA receptors. Representative traces of $[Ca^{2+}]_i$ changes recorded in neurons upon exposure to KRH containing Aβ 1-42 alone (4 μM) or MVs alone (1 μg/100μl) or their combination (**A**). $[Ca^{2+}]_i$ responses induced by Aβ 1-42/MVs mixture are strongly inhibited by the NMDA receptor antagonist APV (**B**), as quantified in **C**. Values represent peak $[Ca^{2+}]_i$ increases (ΔF340/380 fluorescence) from about 30 neurons/condition (Kruskal-Wallis ANOVA $p<0.001$; Dunn's test for comparison among groups *$p<0.05$).

4.10 Microglia derived MVs lipid promote formation of neurotoxic Aβ-1-42 species

We then investigated whether lipids of shed MVs play an active role in the dissolution of insoluble Aβ1-42 species. We observed by thioflavin T assay that exposure to the lipid fraction extracted from MVs caused a reduction in amount of fibrillar (f-Aβ, red lines) or aggregated (Aβ, blue lines) Aβ1-42, similar to that induced by intact MVs (Figure4.10a). Furthermore, neuron viability analysis revealed a similar percentage of dead neurons in cultures exposed to Aβ 1-42 in combination with intact MVs or their lipid component (MV lipids, Figure4.10b). Interestingly, Aβ1-42 pre-incubated with synthetic liposomes, mimicking the phospholipid composition of the plasma membrane (60% PC, 20% cholesterol, 10% SM, 10% PS) and similar in size to MVs did not produce any increase in basal calcium concentration (Figure4.10b). These results demonstrated that the lipid component of microglial MVs was responsible for the dissolution of insoluble Aβ1-42 species. Thus interaction of Aβ1-42 with MVs lipids represents the mechanism by which MVs convert inert Aβ1-42 to neurotoxic forms.

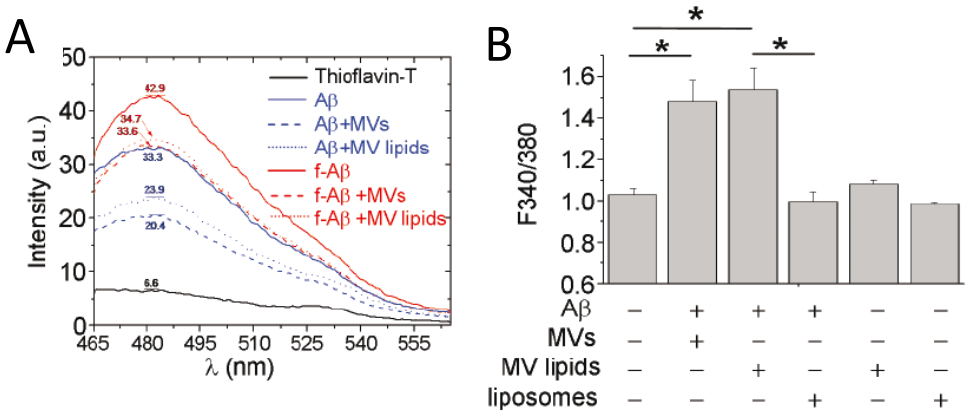

Figure4.10 A ThioflavinT fluorescence emission spectra of aggregated Aβ 1-42 (blue lines) or Aβ 1–42 fibrils (red lines), untreated (solid lines) or pre-treated (dashed lines) with shed MVs. Spectra of aggregated Aβ 1-42 or Aβ 1–42 fibrils exposed to MVs lipids (dotted lines) are also shown. **B** Basal $[Ca^{2+}]_i$ of neurons exposed for 1h to Aβ 1-42 pre-treated with intact MVs, small unilamellar vesicles of MV lipids (MV lipids) or artificial liposomes. Note that vesicles made by lipids extracted from shed MVs but not artificial liposomes significantly enhance basal $[Ca^{2+}]_i$.

4.11Binding of newly generated soluble Aβ-1-42-488 to neurons is competed by PrP^c

We then visualized soluble Aβ 1-42 forms, generated in the presence of MVs, by imaging their binding to hippocampal neurons. To this aim we exposed neuronal cultures for 1h to fluorescent Aβ 1-42 (488-Aβ 1-42), incubated or not overnight with MVs. Quantification of Aβ 1-42 fluorescent species bound to MAP-2 positive dendrites, revealed that MVs caused a strong increase in the Aβ 1-42 binding to neurons (Figure 4.11a-b). Notably, binding of 488-Aβ 1-42 to dendrites was paralleled by a marked reduction of MAP-2 immunoreactivity (Figure 4.11a), in line with previous observations (Jana A, et al., 2010). No preferential association of 488-Aβ1-42 with synapses was detected. Notably, there was competition between Aβ binding to dendrites and to PrP^c, a high affinity receptor for oligomeric Aβ (Lauren J, etal., 2009) . This competition resulted in decreased binding of soluble Aβ 1-42 forms to cultured neurons. Furthermore, we observed that soluble Aβ 1-42 binding can be abolished by pretreatment of 488-Aβ1-42 and MVs mixture with a cocktail of anti-Aβ antibodies, i.e. the A11 and 6E10 antibodies (Figure 4.11 a-b). Unlike the 89-230 truncated PrP^c,

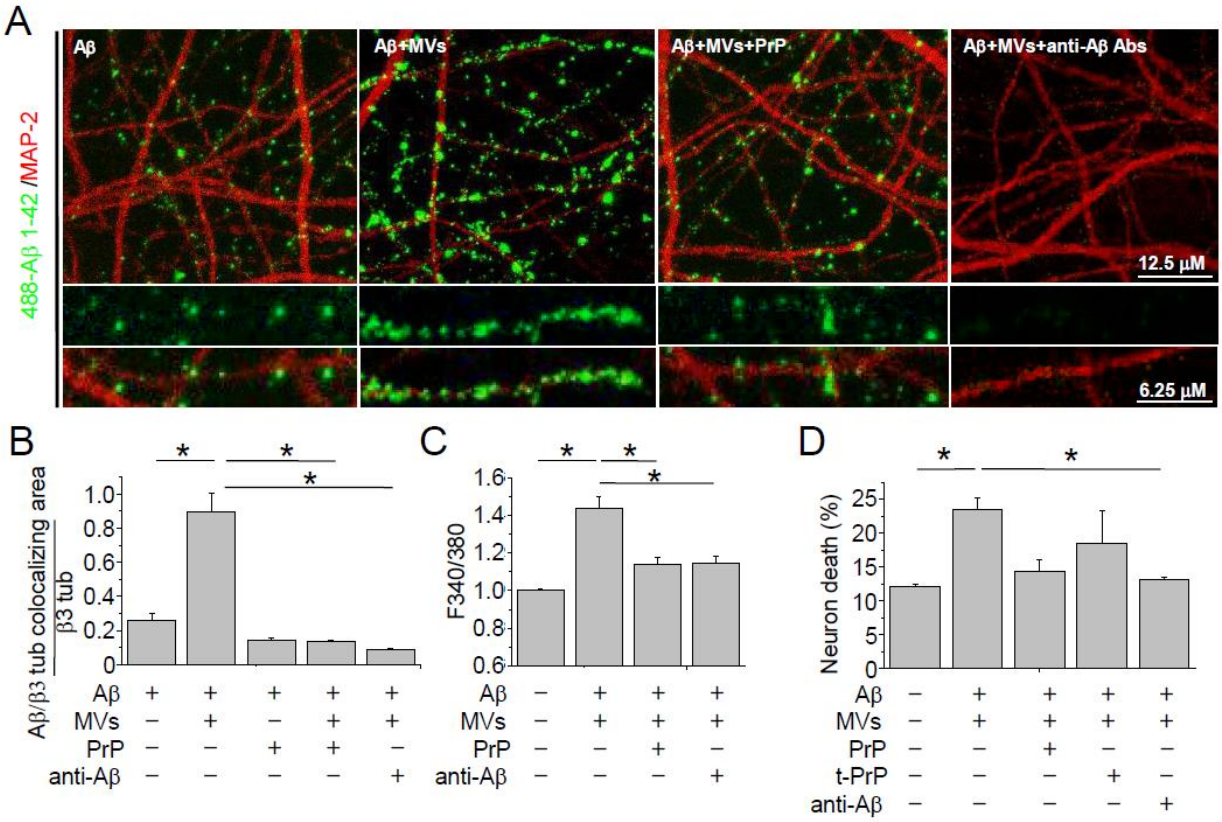

Figure4.11 A Representative confocal images of 14DIV neurons exposed to 488-Aβ 1-42 alone or in combination with MVs, with or without pretreatment with PrP or with the anti-Aβ antibodies A11 and 6E10. **B** Corresponding quantification of 488-Aβ 1-42 binding to cultured neurons expressed as colocalizing area between 488-Aβ and β tubulin, relative to total β tubulin (see methods) (Kruskal-Wallis ANOVA p<0.001; Dunn's test comparison among groups *p<0.05). **C-D** Basal $[Ca^{2+}]_i$ and percentage of calcein-/PI+ neurons in 9-14 DIV cultures exposed to different combinations of Aβ 1-42, MVs, A11 plus 6E10 antibodies, full-length or truncated ($tPrP^C$) PrP^C (Kruskal-Wallis ANOVA p<0.001; Dunn's test for comparison among groups *p<0.05).

both full- length folded PrP^C and anti-Aβ antibodies neutralized the toxicity of Aβ1-42/MVs mixture, as revealed by calcium recording (Figure 4.11c) and PI/calcein staining (Figure 4.11d)..

Figure 4.11 E-F Representative confocal images of neurons exposed to the supernatant (sup) (B) or to the pellet (C) fractions obtained after centrifugation of 488- Ab 1-42 / MVs mixture. Quantification of binding was performed D. (ANOVA, p<0.001, Holm-Sidak Method p<0.05).

Furthermore we observed that the soup, obtained after pelleting the mix of Aβ 1–42/ MVs by centrifuging at 10,000g, (speed for pelleting MVs) retained almost 70% of the total Aβ 1–42 soluble species (Figure 4.11e-left,f) that bound to the neuronal processes, and the pellet retained the species bound with MVs and more aggregated Aβ 1–42 species(Figure 4.11e-right,f)

4.12 MVs carry neurotoxic species generated from internalized Aβ 1-42

Microglia surrounding the amyloid plaques actively phagocyte and degrade Aβ. The MVs released from these activated microglia can potentially contain toxic Aβ species, generated from peptides internalized during phagocytosis. To investigate this possibility confocal analysis was done with microglia exposed to Aβ1-42 for 12-48h. The cells were washed extensively and stained with 6E10 anti-Aβ antibody, revealing intracellular Aβ aggregates. We observed that the Aβ1-42 uptake was fast. At 12 hr Aβ1-42 was clearly visible inside microglia cells, at 24hr large Aβ1-42 aggregates could be observed, a lot of which reached the plasma membrane, and were co-localized with the microglial surface stained by the isolectin IB4 (Figure 4.12a).

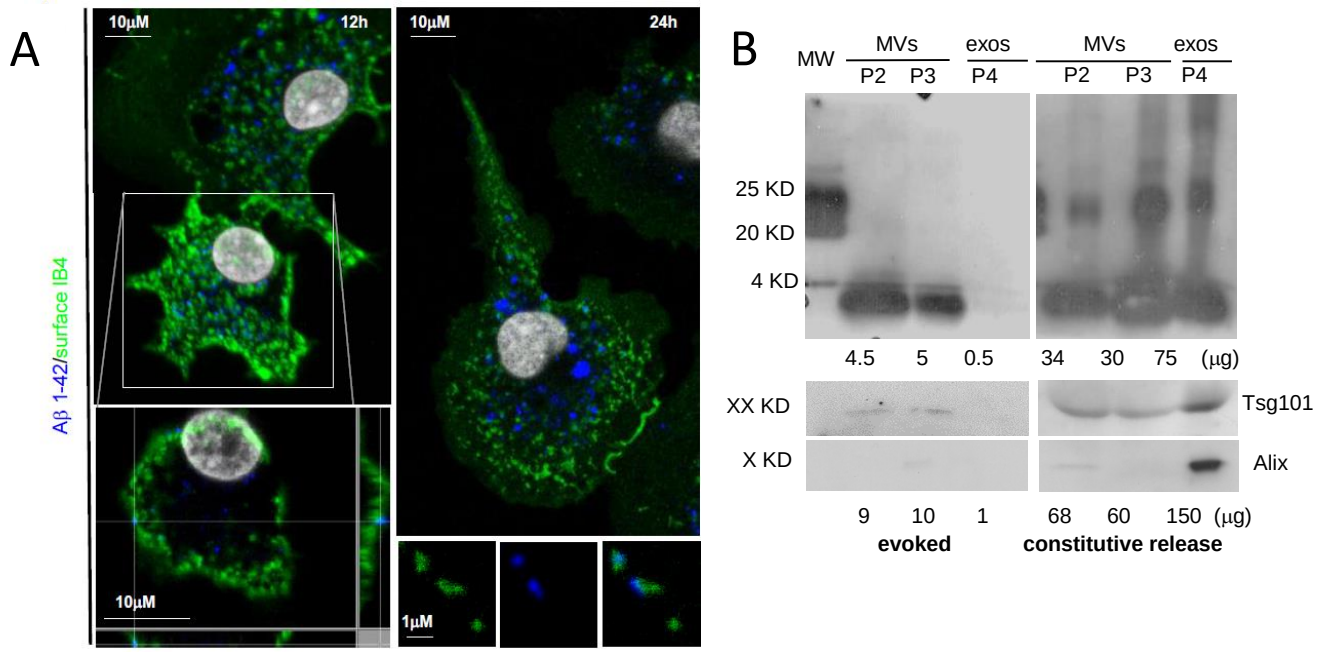

Figure 4.12 **A** Living rat microglia were exposed to human Aβ 1-42 for 12-48 h and stained with IB4-FITC to label the cell surface before being fixed and counterstained with 6E10 antibody, which recognizes human but not rat amyloids. Top left panel shows representative xy-plane maximum projection of microglia, revealing several 6E10 immunoreactive puncta inside the cells, some of which are double positive for surface IB4-FITC. Bottom left panel: single stack of the selected cell, shown at higher magnification, reveals a clear association of internalized Aβ 1-42 to the cell surface, further revealed by the z-axis scan. Note an increase in the size of internalized Aβ 1-42 after incubation for 48 h (top right panel). Examples of EMVs, double positive for 6E10 and IB4-FITC are shown in bottom right panels. **B** Western blot analysis of Aβ 1-42 species present in shed MVs (P2 and P3 fractions) and exosomes (P4 fraction) released upon 30 min ATP stimulation by $4X10^6$ microglia pre-exposed to biotinylated Aβ 1-42 (4μM). Blots were carried out using a 15% Tris-glycine gel and membranes were probed with streptavidine. Shed MVs and exosomes produced by $8X10^6$ donor microglia were

probed in parallel for the EMV markers Tsg101 and the exosomal marker Alix (lower panels). Numbers below each lane indicate the estimated amount of loaded proteins.

Notably, in the extracellular space, close to microglial cells a few Aβ and IB4 double positive particles were detected (Figure 4.12a bottom right panel). These observations suggested that Aβ species can be present inside EMVs produced from Aβ-loaded microglia. To verify this possibility we analyzed by western blotting the presence Aβ in MVs released from microglial cells preloaded with biotynilated Aβ1-42. To obtain the EMVs, the cells were washed properly after 24 hrs incubation to remove the free Aβ1-42, and were kept in ultracentrifuge medium, devoid of any vesicles for the next 24hrs to obtained MVs and exosomes released constitutively by microglial cells in the medium. After removal of the medium the cells were maintained for some hours in glial medium and were further stimulated with ATP for 30 min, a condition which mimics an inflammatory context and favours shedding of MVs (P2 and P3 fraction) versus exosome (P4 fraction) release (Bianco F, et al.,2009). Biotin-conjugated Aβ1-42 was recovered in both shed MV, and exosomes which were labelled by the EMV markers Tsg101 and Alix (Figure 4.12 b).

4.13 Internalized Aβ1-42 is processed by Microglia to other Aβ isoforms, as detected both in MVs and exosomes.

SELDI-TOF mass spectrometry using 6E10 and 4G8 anti-Aβ antibodies showed the presence of Aβ1-42 and of its cleavage product Aβ1-40, along with traces of other C-terminally truncated isoforms, in MVs shed from the plasma membrane (P2+P3 fractions) (Figure 4.13a). Similarly, Aβ1-42 and Aβ1-40 were recovered in exosomes (P4 fraction), but compared to MVs the amount was ten times less (Figure 4.13a).

By calcium recordings we found that MVs derived from microglia preloaded with 4 μM Aβ 1-42 (Aβ-MVs) were highly neurotoxic as compared to MVs derived from resting cells (Figure 4.13b). Neurotoxicity caused by MVs storing Aβ 1-42 was significantly decreased by anti-Aβ antibodies. We therefore concluded that microglia internalize and Aβ and sort neurotoxic abeta species to MVs. Neurotoxic Abeta species are likely exposed on the external membrane of the MVs, which are delivered to neurons and cause neurotoxicity.

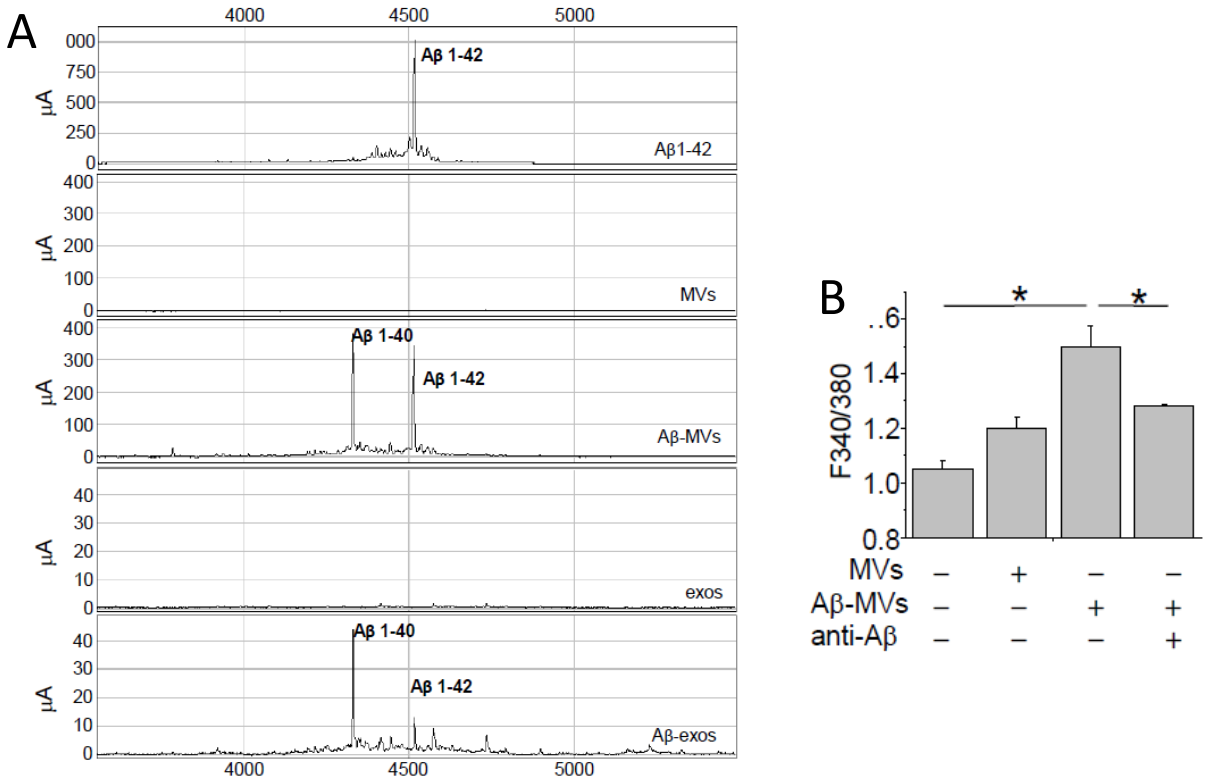

Figure 4.13 A Shed MVs and exosomes produced by 1X10^6 rat microglia pre-exposed to human Aβ 1-42 were analysed by a SELDI TOF MS immunoproteomic assay employing anti-human Aβ antibodies (4G8 and 6E10) on PS20 chip array to capture Aβ 1-42 and C-terminally truncated abeta isoforms. The following representative spectra of samples in NP40 1% lysis buffer are shown (from top to bottom): 4µM Aβ1-42 peptide incubated overnight in KRH; MVs from control microglia, not exposed to Aβ1-42; MVs from Aβ1-42 preloaded microglia (Aβ-MVs); exosomes from control microglia (exos); exosomes from Aβ1-42 preloaded microglia (Aβ-exos). **B** Basal $[Ca^{2+}]_i$ recorded from neurons exposed to MVs produced from microglia either resting or pre-treated for 48 h with Aβ 1-42 (Aβ-MVs), in the presence or in the absence of anti-Aβ antibodies (A11+6E10) (Kruskal-Wallis ANOVA p<0.001; Dunn's test for comparison among groups *p<0.05). See also Figure S1.

4.14 Elevation of Microglia derived MVs in AD patients.

Recently studies done in our lab indicates that the extent of microglia activation in the course of neuroinflammation can be reflected by the amount of microglia-derived MVs detected in the CSF of humans (Verderio C, et al., 2012). To understand if the production of MVs from microglia could be elevated in AD, where neuroinflamation correlates with cognitive defects, we collected the CSF from patients with mild cognitive impairment (MCI) or AD, as well as from age- and gender-matched healthy controls (HC). We performed flow cytometry analysis for MVs positive for the myeloid marker IB4 and observed strikingly higher levels (more than ten-fold) of MVs in MCI and AD patients than in control subjects (Figure 4.14a). Approximately 65% of total EMVs detectable by flow cytometry were IB4-positive. Furthermore, we found that MV concentration correlated with Tau protein levels in the CSF, a marker of neurodegeneration (Figure 4.14b; p<0.0001) (Holtzman DM, et al., 2011).

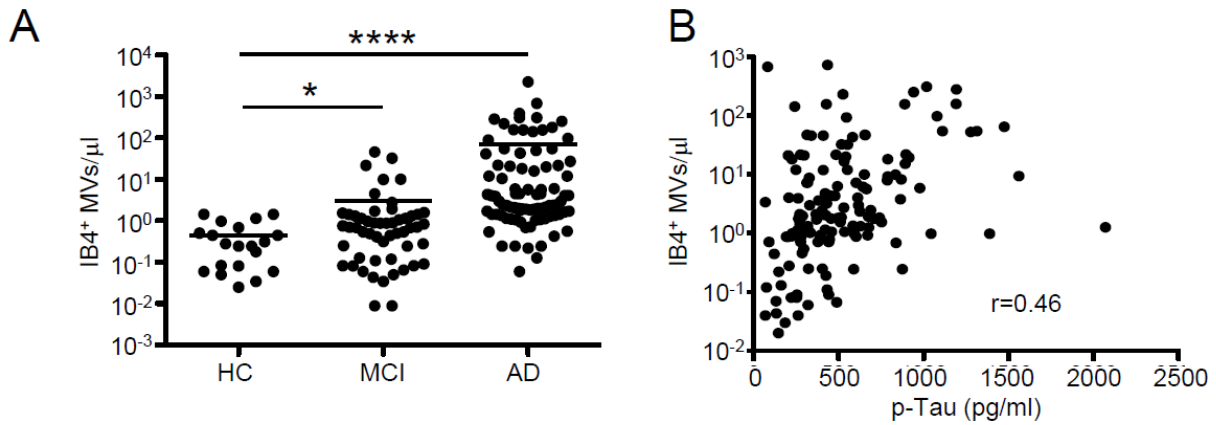

Figure 4.14A Quantitative flow cytometry analysis of IB4⁺ MVs in CSF collected from MCI patients (n= 53), AD patients (n = 89), and age- and gender-matched controls (HC; n= 20) (Mann–Whitney p<0.0001 AD versus HC; p<0.0329 MCI versus HC). **B** Correlation between IB4⁺ MVs and total tau protein in the CSF of MCI and AD patients, (rho = 0.46, p<0.0001 Spearman correlation).

4.15 Microglia derived MVs from AD patient's effects the equilibrium between soluble and insoluble Aβ 1-42 species and cause neurotoxicity.

To verify whether MVs from AD patients affect the equilibrium between soluble and insoluble A 1-42 specie we collected the CSF from AD patients and isolated MVs by centrifugation at 10,000g. Confocal analysis of neurons exposed to 488-Aβ 1-42 pre-incubated overnight with AD MVs revealed a three-fold decrease in the content of fluorescent Aβ aggregates (Figure 4.15Ia,b) thus indicating that AD MVs break up insoluble Aβ 1-42 species. We also observed that AD MVs induced a parallel increase in the fluorescent Aβ species bound to dendrites (Figure 4.15Ia,c)

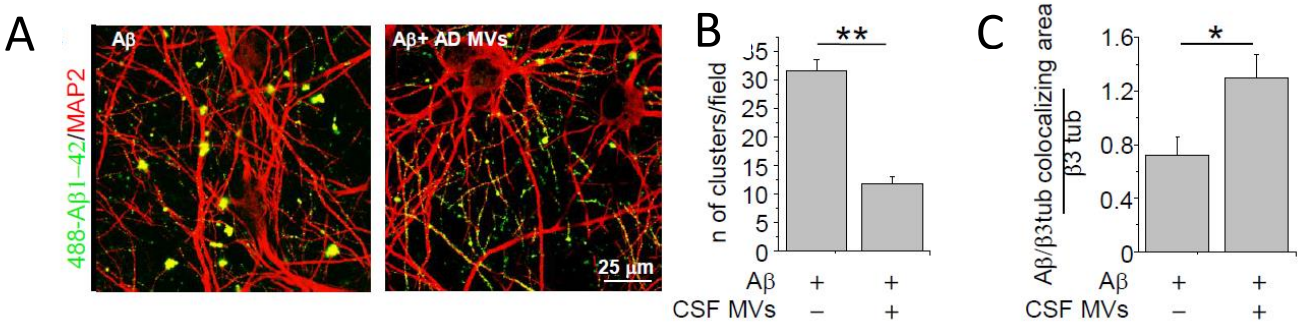

Figure 4.15 I A Representative confocal images of cultured neurons, exposed to aggregated 488-Aβ 1-42 untreated or pre-treated overnight with MVs from AD patients and stained for MAP-2 after fixation (red). Aβ species bind to MAP-2 dendrites. Note the decrease in the number of large fluorescent Aβ clusters in neurons exposed to 488-Aβ 1-42 in combination with AD MVs. **B** Quantification of 488-Aβ 1-42 aggregates (larger than 5 µm) per field (data follow normal distribution, student T test **p<0.001). **C** Quantification of 488-Aβ 1-42 binding to cultured neurons, expressed as colocalizing area between 488-Aβ and βtubulin, relative to total β tubulin (see methods) (data follow normal distribution, Student T test **p<0.001).

Table 4.1. Clinical features of MCI and AD patients

	Gender (F/M)	Age (average ± S.D.)
HC	10/10	68.0 ± 6.3
MCI	27/26	68.8 ± 6.5
AD	50/39	64.6 ± 7.1

In line with our *in vitro* results indicating that microglial MVs carry neurotoxic abeta species, we demonstrated that MVs recovered from AD patients were highly toxic and eventually lead to neuronal death, as quantified by calcein-/PI+ dead neurons. Interestingly MVs isolated from the CSF of AD patients were more toxic with respect to MVs isolated from patients with multiple sclerosis, (MS) a neuroinflammaory disease characterized by increased level of microglial MVs, (Figure 4.15IId,e,f). There was a significant decrease in neurotoxicity of AD MVs with pre-treatment with anti-Aβ antibodies, 6E10 and A11 (Figure4.15IIg), suggesting that the toxicity was in part mediated by Aβ 1-42 carried by the MVs.

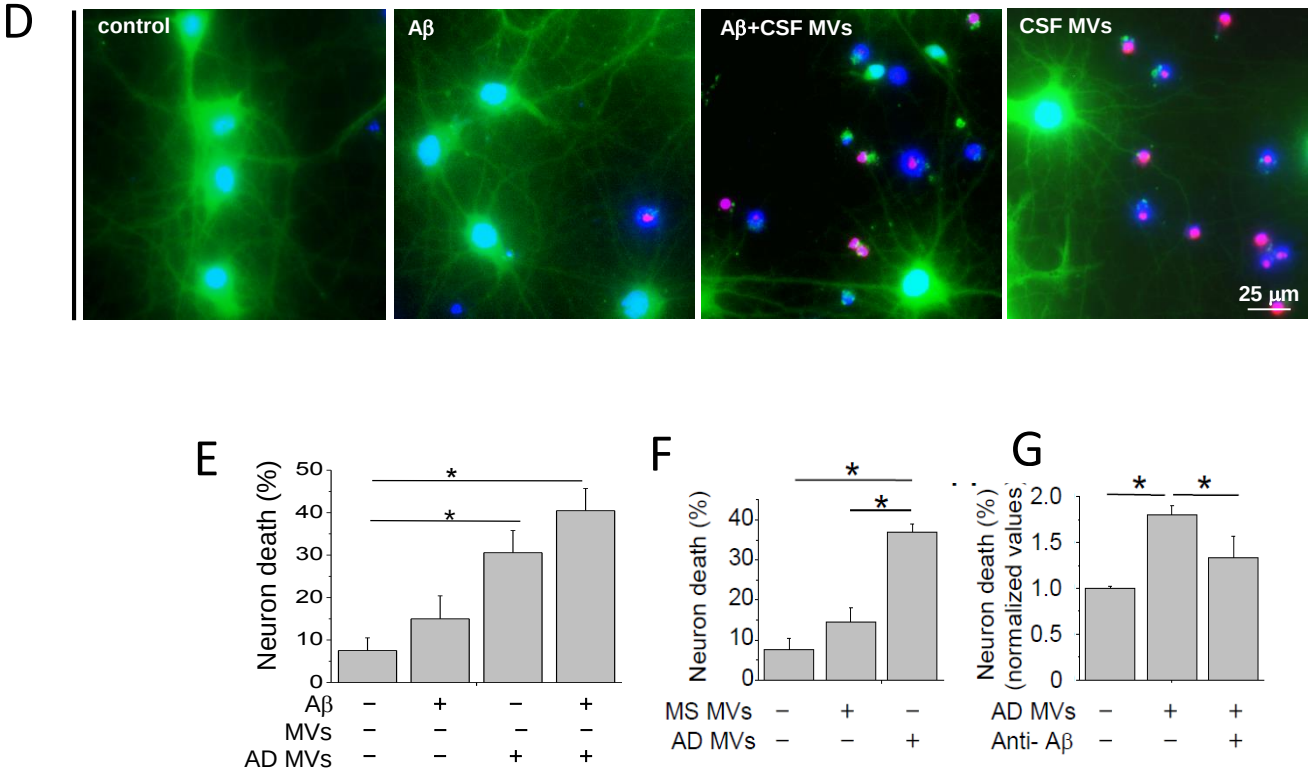

Figure 4.15 II D Representative fluorescence microscopy images of 14DIV neurons triple stained for calcein, PI and Hoechst 24 h after exposure to AD MVs or maintained in control conditions **E-F** Quantification of the percentage of calcein-/PI+ neurons (dead cells) in cultures exposed to AD MVs or MVs isolated from patients with multiple sclerosis (MS) or Aβ alone (Kruskal-Wallis ANOVA $p<0.001$; Dunn's test for comparison among groups *$p<0.05$). **G** Percentage of dead neurons in cultures exposed to MVs isolated from the CSF of AD patients in the presence of anti-Aβ antibodies A11 and 6E10 (ANOVA, $p<0.001$, Holm-Sidak Method $p<0.05$).

Interestingly, Aβ 1-40, Aβ 1-42 and other truncated Aβ peptides were detected by SELDI-TOF mass spectrometry in CSF MVs of a patient affected by AD (Figure 4.15 III).

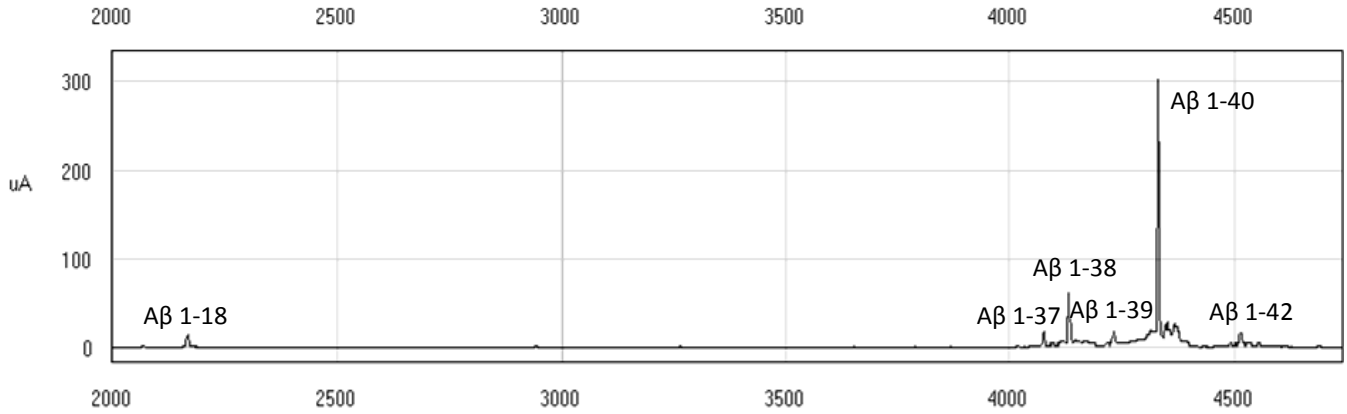

Figure 4.15III Representative SELDI TOF MS spectra of MVs isolated from the CSF of a patient with AD showing the most common Aβ peptides captured by immunoproteomic assay employing 6E10 and 4G8 monoclonal antibodies.

4.16 Subchronic treatment with the MV shedding inhibitor FTY720 improves memory performance in APP/PS1 transgenic mice model for AD.

It has been previously shown by our lab that MV shedding is inhibited by blockers of acid sphingomyelinase (A-SMase), such as imipramine or FTY720 and is almost abolished in A-SMase knock out glial cells *in vitro* and *in vivo* (Bianco, et al., 2009; Verderio et al., 2012). To explore the therapeutic potential of inhibition *of* MV shedding *in vivo*, FTY720 (1mg/Kg) or plain water were administered by oral gavage to 12 months-old APPswe/PS1 and their littermates for 6 weeks. Pre-drug and post-drug behavioural tasks were carried out to test learning and different forms of memory performance, i.e., reference, object and innate memory, using the passive avoidance, the object recognition and the nest building tasks, respectively. As expected, male APPswe/PS1 mice showed severe deficits in reference memory in the passive avoidance task and after 5 weeks of treatment with plain water performed significantly worse, as indicated by the decreased latency to enter the dark room, where mice receive a mild foot shock, while their cognitive performance was preserved upon treatment with FTY720 (Figure 4.16b-c; blue bars). These results were supported by object recognition memory testing, which showed reduced recognition index in vehicle-treated APPswe/PS1mice and improved recognition index in FTY720-treated double transgenic mice (Figure 4.16b-c; blue bars). Female APPSwe/PS1 mice were partially protected from memory impairment

(Figure 4.16b-c; red bars). They were never impaired in the passive avoidance task, but became impaired in the object recognition task after 5 weeks of treatment with plain water, while maintained performance similar to wild type littermates upon FTY720 administration. Consistent with a therapeutic action of FTY720, in the nest building task a significantly higher percentage of APPSwe/PS1 mice was able to complete the nest after treatment with the drug, as compared with pre-drug behavioural analysis (Figure 4.16d). In this task, no major difference in the behaviour of male and female APPSwe/PS1 mice was observed.

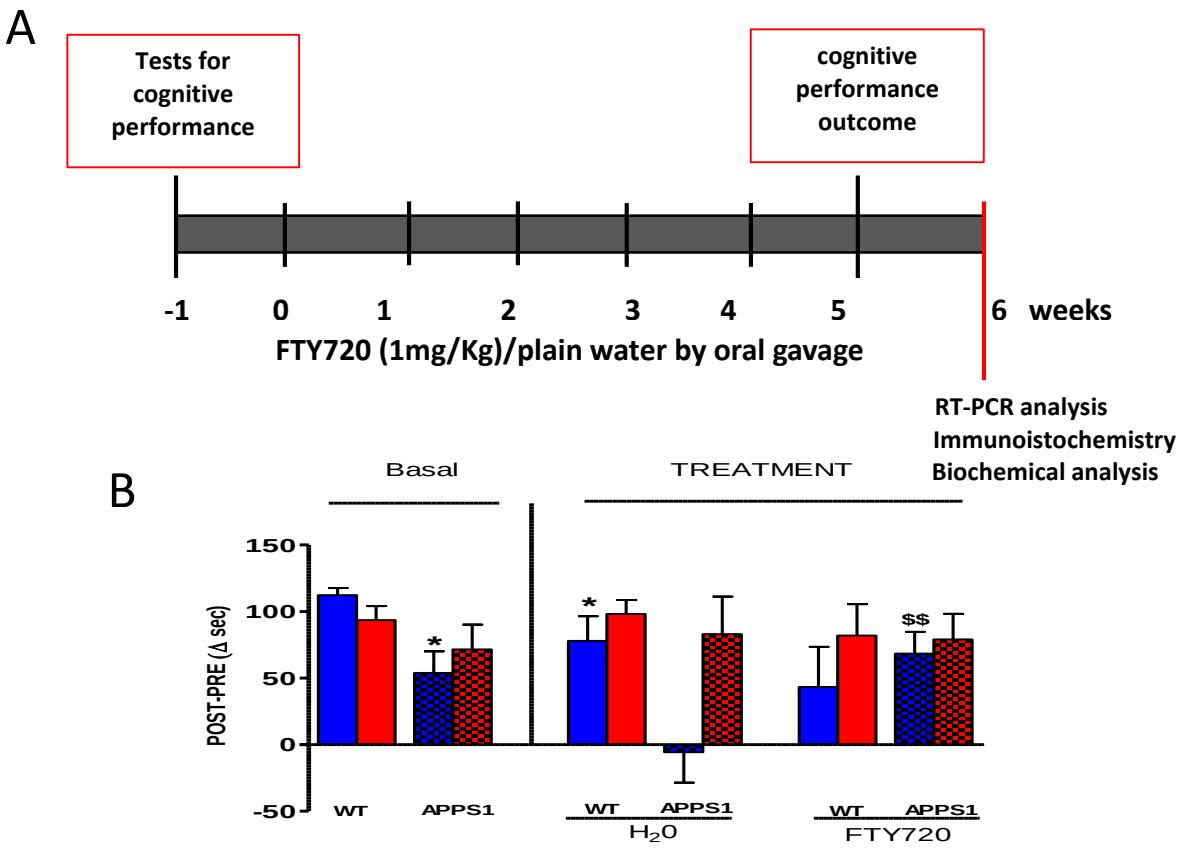

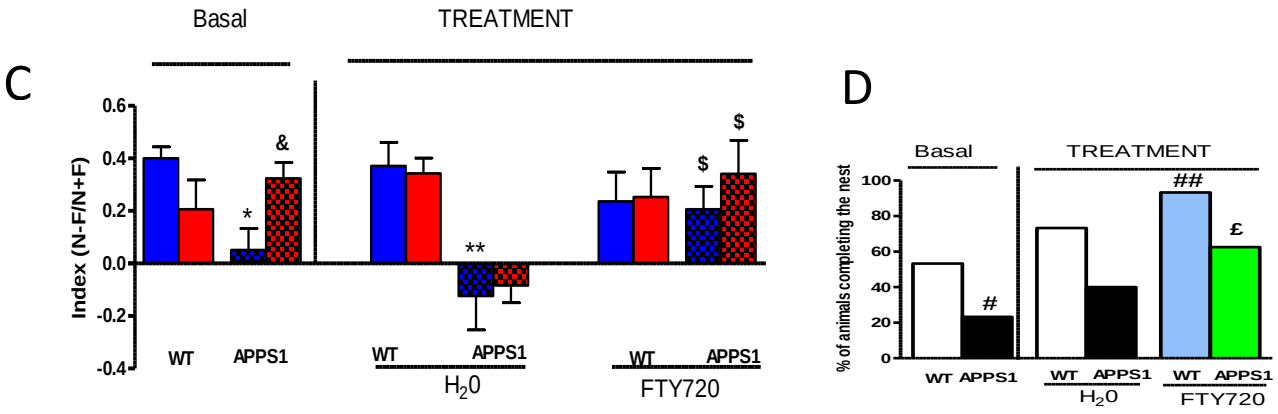

Figure 4.16 Transgenic APPPS1 Mice administered with FTY and observed for behavior tasks related to memory. **A** Diagrammatic representation of the scheme followed for drug administration and further experiments .The mice were initially checked for their general health, reflex, sensory abilities and then tested for motor activity and learning and memory performance before drug administration. APPswe/PS1 displayed normal gross behavior and motor activity. **B** Passive avoidance test showed improvement with FTY720 administration, in case of APPPS1 transgenic males. Females were not impaired for this test and performed like WT female controls. **C** Object Recognition Test was performed, initially only the transgenic male were impaired compared to WT control males, in course of drug/vehicle administration for 5 weeks both male and female transgenic animals, which received water as vehicle were impaired with respect to respective controls but transgenic animals administered with FTY720 showed significant improvement in their performance. **D** In case of Nest building, there was impairment in performance of Transgenic APPPS1 mice, both male female as compared to respective WT controls. We further observed improvement in performance in transgenic mice after FTY720 administration as compared to WT controls. The results obtained in case of male and female were similar, so the data was pooled and grouped as WT and APPPS1.

4.17 FTY720 reduces inflammation in APPPS1 transgenic mice brain

We next examined the impact of subchronic FTY720 treatment on brain inflammation. As a measure of astrogliosis we analyzed the mRNA (Figure 4.17a) and protein (Figure 4.17c) expression of the astrocytic marker GFAP in the cortex of mice. Due to differences in the behavior responses we analysed separately male and female both in wild type and transgenic mice. The transgenic mice, especially females, showed increased levels of GFAP transcript. Interestingly, we observed that GFAP was significantly decrease both at mRNA and protein levels in case of male and female transgenic mice administered with FTY720 as compared to transgenic mice receiving vehicle alone. We also performed immunostaining for GFAP of the cortical slices of transgenic and wild type mice (Figure 4.17b). Tthis analysis was performed only in male transgenic and wild type mice and further indicated a significant increase in astrogliosis in transgenic mice administered with vehicle, and a significant decrease in GFAP protein expression upon FTY720 treatment in transgenic mice.

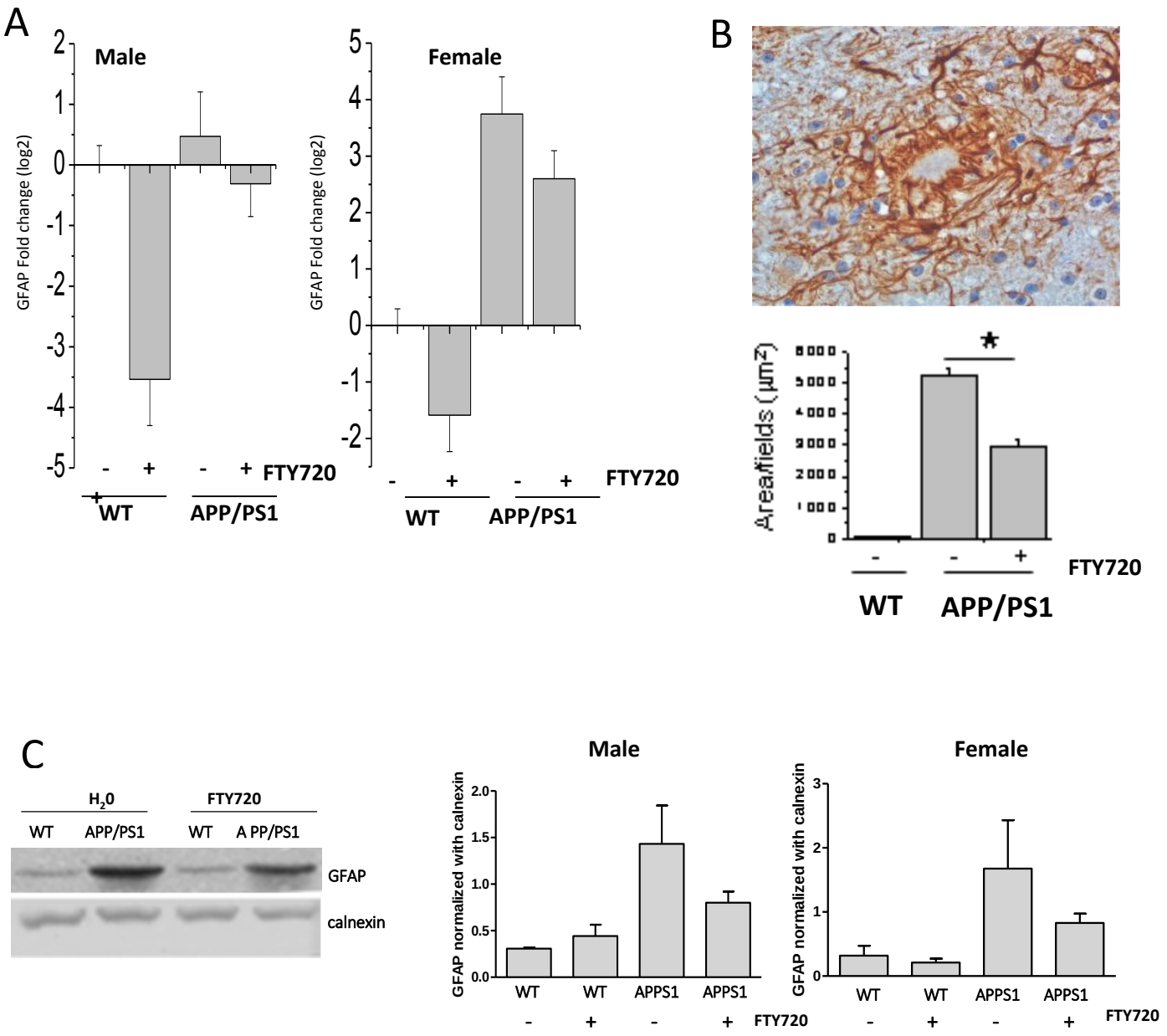

Figure 4.17 I A Increased mRNA expression of GFAP in APPSwe/PS1 transgenic mice as compared to wild type control, which was decreased both in case of male and female upon FTY administration. **B** Representative image of cortical section for transgenic mice showing astogliosis, the results are in accordance with GFAP mRNA expression. **C** Representative western blot for GFAP, the values obtained were normalized with Calnexin. We observed increased astogliosis in transgenic mice compared to wild type both in case of male and female, and decreased significantly with FTY720.

We also observed that APPSwe/PS1 mice, especially females (Figure 4.17IIa), displayed higher mRNA expression of the microglial marker IBA1 in the cortex as compared to wild type littermates, and that upon FTY720 administration this expression was decreased. However, immunohystochemical analysis revealed no changes in IBA1 expression in the cortex of APPSwe/PS1mice treated with

FTY720 as compared to vehicle-treated mice (Figure 4.17IIb). We also analyzed by western blotting MCH class II molecules expression to quantify the activation of microglial towards M1 phenotype. A marked increase in MHCII levels was observed in female APPSwe/PS1 mice as compared to wild type animals. Administration of FTY720 significantly decreased MHCII expression in APPSwe/PS1 mice. Male APPSwe/PS1 mice showed no changed in MHCII expression with respect to control male mice (Figure 4.17IIc).

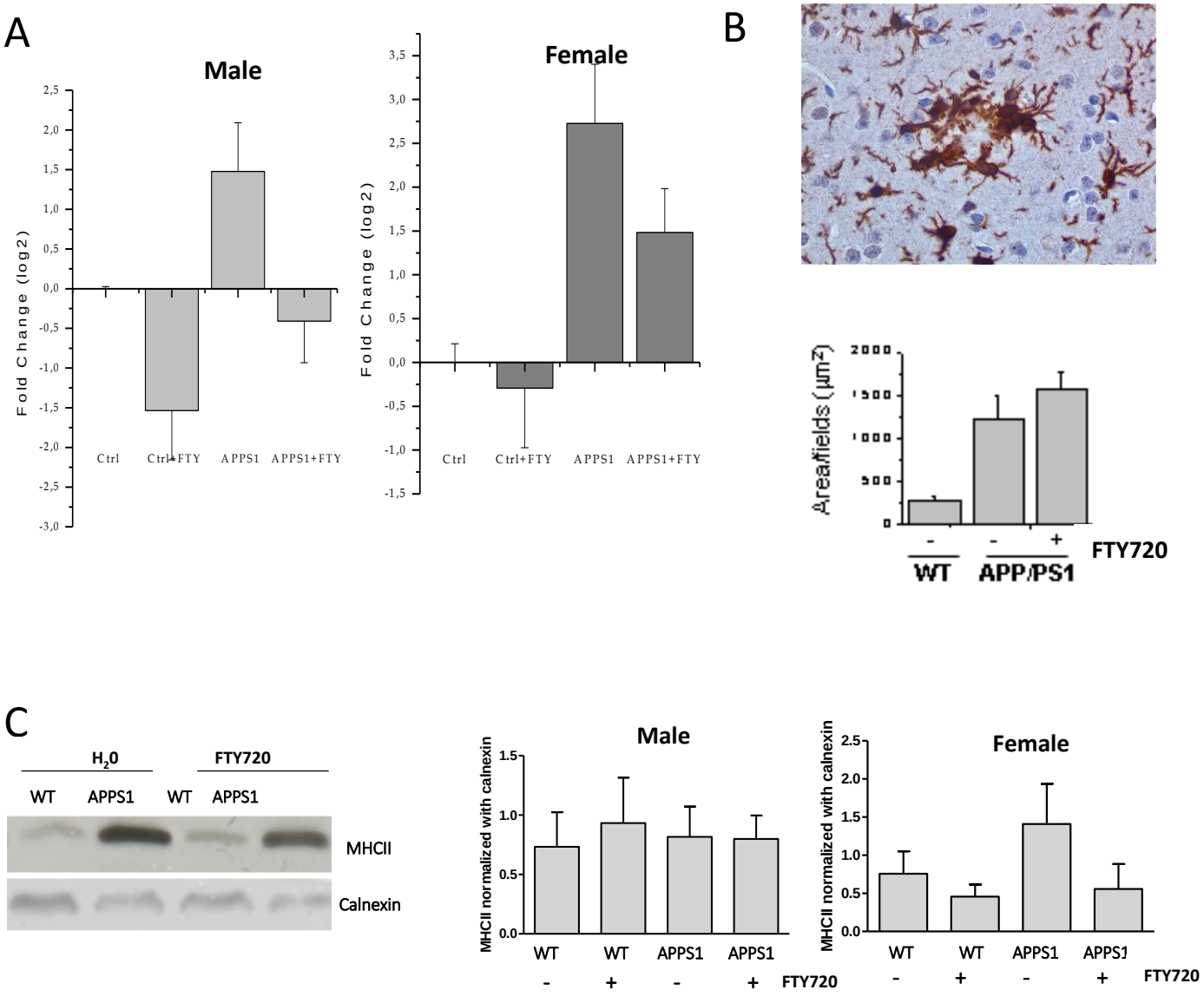

Figure 4.17 I A Increased mRNA expression of IBA1 in APPSwe/PS1 transgenic mice as compared to wild type control, which was decreased both in case of male and female upon FTY administration. **B** Representative image of cortical section for transgenic male mice showing microgliosis. Quantification of images revealed significant increase in IBA positive cells around the plaque in transgenic mice as compared to wild type, but no decrease was observed upon FTY administration. **C** Representative western blot for MHCII, a marker to study microglial activation. The values obtained were normalized with Calnexin. We observed increased microglial activation in female transgenic mice compared to wild type which decreased significantly with FTY720. No changes were observed for MHCII in male transgenic and wild type mice.

Treatment with FTY720 also lead to a significant reduction in the mRNA expression of typical inflammatory markers, i.e. iNOs, COX-2 IL-1β and IL-6 as observed independently in male and female in wild type and double transgenic mice. (Figure 4.16 IIIa).

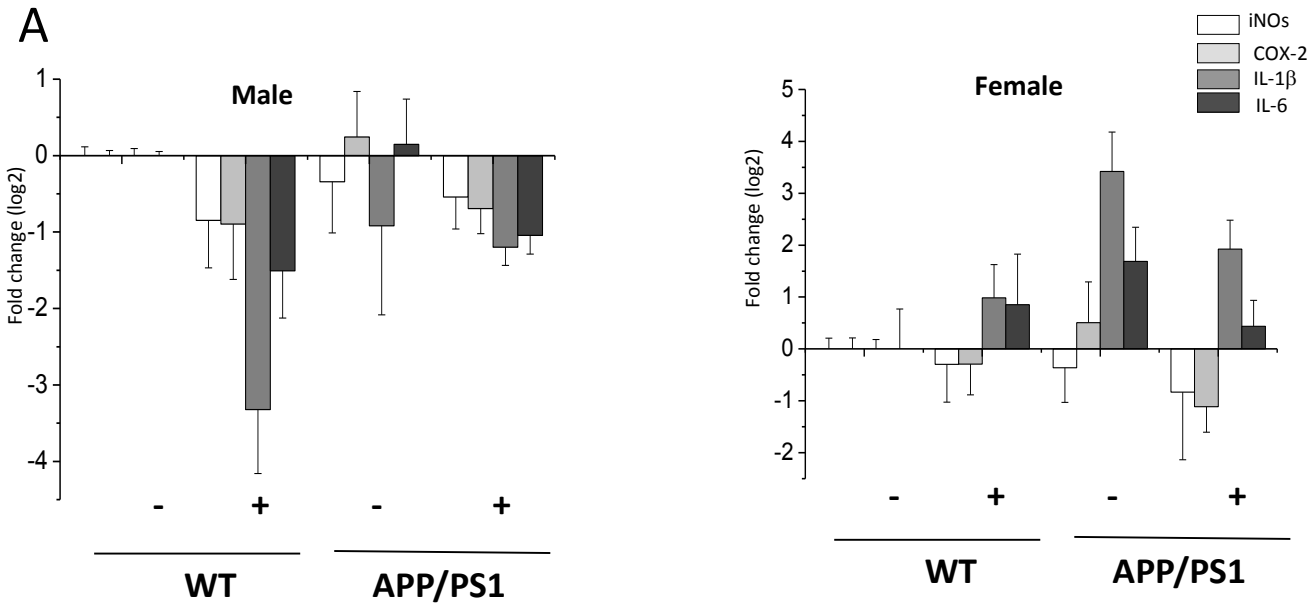

Figure 4.16 III A FTY induces reduction in mRNA expression of inflammatory markers in male and female both in case of wild type and APPSwe/PS1 transgenic mice.

4.18 FTY720 decreases Aβ 1-42 load in APPPS1 transgenic mice brain.

We further investigated if FTY720 influences the Aβ levels in APPSwe/PS1 transgenic mice. To evaluate the changes in total Abeta 1-42 levels we performed dot blot analysis from the total protein isolated from the cortices of transgenic mice treated or not with FTY720. We observed that Aβ levels decreased both in male and female APPSwe/PS1 mice administered with FTY720 (Figure 4.18a) Next we analysed by Elisa the levels of Aβ in the soluble fraction isolated in detergent-free buffer from the hippocampus of APPSwe/PS1 mice chronically administered with FTY720 or plain water. This analysis revealed a significant decrease in soluble Aβ levels in female transgenic mice administered with FTY720. No significant changes were observed in male transgenic mice upon FTY720 administration (Figure 4.18b).

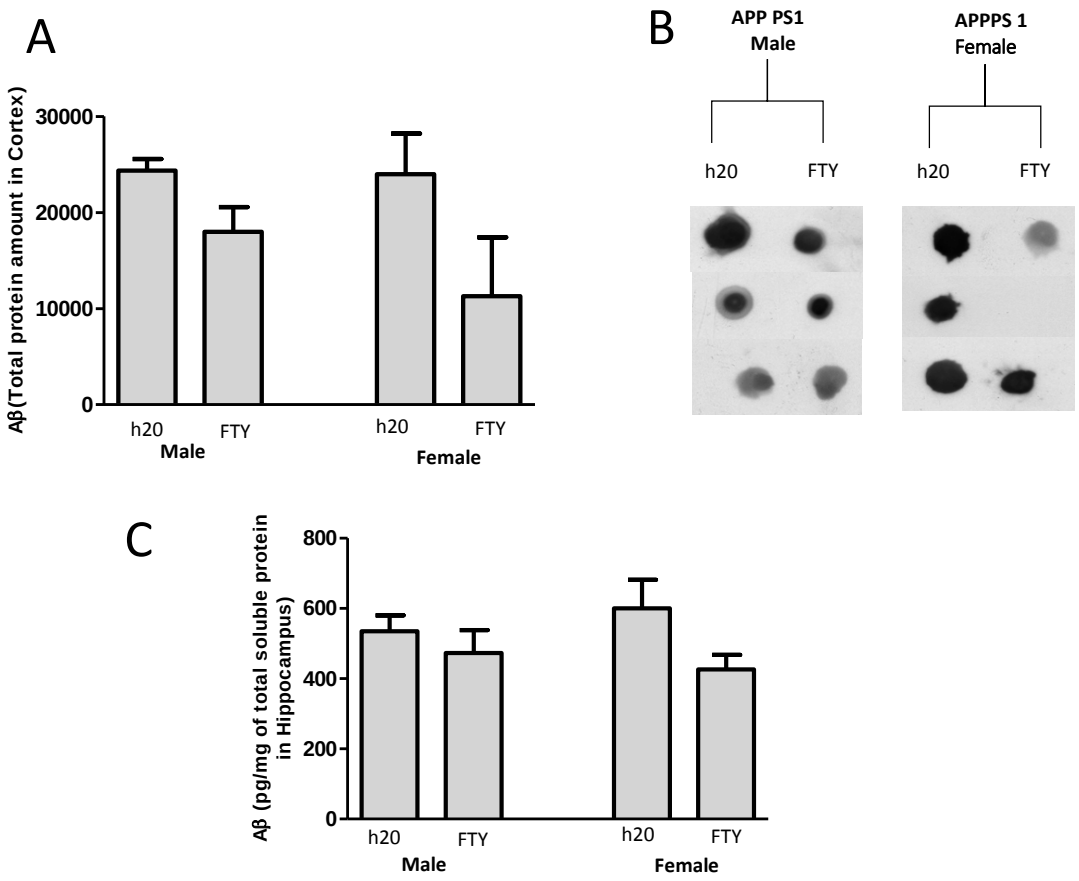

Figure 4.18 A Quantification for the total amount of Aβ through dot blot in cortex of transgenic male and female mice revealed a decrease upon FTY administration. **B** Representative image of the Dot Blot. **C** Quantification for soluble Aβ through ELISA in the hippocampus of transgenic male and female mice. We observed a significant decrease in female transgenic mice upon FTY administration, whereas male transgenic mice with and without FTY administration showed no differences in soluble Aβ levels.

5. DISUSSION

In the present study, we unveil a novel mechanism by which microglia derived MVs contribute to neuronal damage in AD. The effect is mediated by lipid component of MVs which changes the equilibrium of soluble and insoluble Aβ 1-42, promoting formation of soluble neurotoxic species. The species of Aβ 1-42 so generated bind efficiently to subpopulation of neuronal cultures, increasing NMDA receptor permeability and excitotoxicity. This binding was greatly prevented by pre-incubations with PrP^C and anti-Aβ antibodies. We also demonstrated that Microglial MVs contains neurotoxic Aβ generated from Aβ 1-42 internalized by phagocytising microglia. These MVs can act as carrier of toxic Aβ and eventually may be toxic to neurons they encounter on their way. Furthermore we observed increased level of IB4 positive MVs in CSF obtained from AD patients. In line with our in-vitro data MVs from CSF of AD patients were able to promote formation of soluble Aβ 1-42 and were toxic to cultured neurons. Administration of FTY720, an inhibitor of MVs shedding for a period of 5 weeks improved cognitive impairment in APPSwe/PS1 transgenic mice by decreasing level of neuroinflammation and plaque load.

5.1 Microglia derived MVs increased the toxicity of Aβ 1-42 which is mediated by the lipid component of MVs.

Microglial MVs can play physiological role by modulating synaptic activity and neurotransmission (Antonucci, et al., 2012; Turola, et al., 2012). Moreover MVs have been identified as a novel biomarker of brain inflammation in humans (Verderio C, et al., 2012; Colombo E,et al., 2012). Recent literature suggests alterations in metabolism of natural sphingolipids and gangliosides in AD patients (Mielke M M, et al., 2011) altered levels of these bioactive lipids can destabilize and rapidly resolubilize long Aβ fibrils to neurotoxic amyloid species. We demonstrated for the first time that MVs, extracellularly released by cultured microglia, strongly increase Aβ 1-42 neurotoxicity *in vitro*. This effect is due to the lipid components of MVs, which promote formation of small soluble neurotoxic species from Aβ 1-42 extracellular aggregates. We observed that overnight incubation of inert Aβ 1-42 peptide with microglial MVs promoted formation of soluble neurotoxic species, whereas Aβ 1-42 alone became aggregated and displayed low toxicity. The Aβ 1-42 species generated in Aβ 1-42/MVs mix induced fragmentation of dendrites and reduced synaptic density as

compared to control cultures. Our data suggest that a transient interaction takes place between MVs and Abeta species, as suggested by increased Aβ flotation on sucrose gradient upon acute addition of MVs. However this interaction is not stable as the neurotoxic forms generated in the presence of MVs are recovered in the soup after fractionation of Abeta/MVs mixture at 10000g, while the pellet, containing MV-associated Aβ 1-42 along with aggregated Aβ 1-42 forms displayed low toxicity and little neuronal binding capacity. This indicates that most of neurotoxic forms do not bind to MVs strongly. We therefore identified microglial MVs as the endogenous source of bioactive lipids, which are able to shift the equilibrium towards toxic Aβ species. This argument is in line with previous studies that demonstrated that brain membrane lipids, including phosho- and (glycol)sphingolipids, favour formation of soluble forms, either promoting solubilization of inert fibrils (Martins JC, et al., 2008), or hindering their conversion to insoluble fibrils (Johansson A S, et al., 2007). Interestingly, neuronal exosomes have been found to promote rather than reduce Aβ fibrillogenesis (Yuyama K, et al., 2012), thus indicating that lipid composition of MVs generated from distinct cell types may have different effects on Aβ extracellular assembly and can influence the kind of species generated. Notably, MVs have a distinct repertoire of lipids not only compared to exosomes (our unpublished data) (Thery C., et al. 2009) but also to the plasma membrane of origin. MVs are enriched in cholesterol, sphingomyelin and ceramide and contain lipid raft elements (Del Conde I, et al., 2005), including GM1 and GM3 gangliosides and flotillin-2 (Han X, et al., 2003). Interestingly, artificial liposomes, that mimic the phospholipids composition of the plasma membrane, neither induce fibril solubilization nor promote Aβ neurotoxicity. Lipidomic profiling of microglial MVs will be of help to better characterize the endogenous lipids responsible for the generation of neurotoxic Aβ species, which could themselves represent putative AD biomarkers (Serrano-Pozo A, et al., 2012; Han X, et al., 2003; Malnar M, at al., 2012).

5.2 Toxicity of Aβ 1-42/MVs mixture is due to soluble Aβ 1-42 species, and is neutralized by PrP^C and anti- Aβ 1-42 antibodies.

The majority of neurotoxic Aβ 1-42 generated in Aβ 1-42/ MVs mix, is retained in the soup after partitioning of Aβ 1-42/ MVs in two fraction by ultracentrifugation. They are soluble, non-aggregated Aβ 1-42 species, which are not associated to MVs as indicated by our previous observations. Electron microscopic images confirmed the presence of globular structures of diameter between 4 and 8 nm, similar to those of oligomeric Aβ 1-42. The toxicity of small soluble $A\beta 1{-}42$species has been proposed to depend on their interaction with specific neuronal proteins,

such as the NMDA receptor (Synder E M, et al., 2005) or the prion protein PrP^C (Lauren J, et al.,2009), which modulates NMDA receptors through Fyn kinase (Um JW, et al., 2012). Alternatively, soluble Aβ $1{-}42$ oligomers may damage neurons by binding to multiple membrane components, including lipids, thereby changing membrane permeability and causing calcium ion leakage into the cell (Benilova I, et al.,2012; Verdier Y., et al., 2004) We demonstrated that the soluble forms generated in Aβ 1-42/ MVs mix, bind efficiently to a subpopulation of neurons *in vitro*, and increase NMDA receptor permeability causing an excitotoxic damage. This response was blocked when the antagonist of NMDA receptor APV was administered to the neuronal cultures. We excluded that toxicity could be due to glutamate content of MVs or Aβ 1-42/MVs preparation, as we detected a glutamate concentration in Aβ 1-42/MVs much below the minimum required for activation NMDA response. We observed significant reduction in binding of soluble Aβ 1-42 to neurons in the presence of PrP^C thanks to the competition between Aβ $1{-}42$ binding to dendrites and to PrP^C, which is a high affinity receptor for oligomeric Aβ $1{-}42$. Binding of soluble Aβ 1-42 was completely abolished by a cocktail of anti-Aβ antibodies. This reduction in binding of soluble Aβ 1-42 by PrP^C and anti- Aβ antibodies could neutralize the neurotoxicity caused by Aβ 1-42/MVs mix.

5.3 Microglial MVs contain toxic A forms generated from internalized Aβ 1-42.

First we demonstrated that microglia-derived MV mediate extracellular Aβ processing, leading to neurotoxicity. Then, we could show that microglial MVs also contain toxic forms generated from internalized Aβ $1{-}42$. Previous literature indicates that exosomes derived from neurons and oligodendrocytes carry a fraction of intracellular Aβ (Rajendran L., et al.,2006; Gidhoni R, et al.,2011; Vingtdeux V, et al., 2007) and that phagocytosed Aβ can be re-secreted from microglia, although through an unknown mechanism (Yamamoto, et al., 2008). In our study we demonstrated that microglia release neurotoxic Aβ 1-42 and Aβ 1-40 species in association with MVs. This is the first evidence that microglia, which phagocytize and degrade extracellular Aβ fibrils (Aguzzi A, et al., 2013; Prinz M, et al.,2011) or cause macropinocytosis of soluble Aβ (Paresce DM., et al.1997; Lee CY., et al. 2010) can favour seeding and formation of neurotoxic amyloids throughout the brain. We assume that when there is saturation of Aβ degradation pathways, due to excessive abeta load, beyond the clearing capacity of microglia, these cells can eliminate undigested Aβ through the release of MVs. In this way, MV-mediated release of neurotoxic Aβ forms may occur. Neurotoxic Aβ species may be processed in early to late endosomes and lysosomes (Rajendran L, et al.,2012), after

disassembly of phagocytosed Aβ. Sorting to the external surface of MVs can occur through association with the GPI-anchored protein PrP^C or GM1 gangliosides, all of which are localized to raft domains (Mattei V, et al., 2009) and bind tightly to Aβ oligomers (Ariga T., et al 2001). Alternatively, neurotoxic forms may be generated at the plasma memnbrane of microglial cells. Indeed the microglial surface contains components of the ɣ-secretase complex -also localized inside lipids rafts (Rajendran L, et al., 2012) and can cleave the carboxyl terminal of Aβ 1-42 at position 40 (Kiyota T, et al., 2009), resulting in the generation of neurotoxic Aβ species. This sorting mechanism may be consistent with the proposed role of lipid rafts in setting up platforms to concentrate into MVs proteins destined to secretion (Shen B, et al., 2011; Del Conde I, et al., 2005). The fact that we observed significant decrease in neurotoxicity upon pretreatment with anti-Aβ antibodies strongly supports the theory that neurotoxic Aβ forms are localized to the outer lipid bilayer of MVs. Finally, we cannot exclude that processing of Aβ1-42 to Aβ1-40 may even proceed within MVs. Indeed, previous evidence showed that neuron-derived EMVs contain some components of the ɣ -secretase complex (Sharples RA, et al.,2008), while the Insulin Degrading Enzyme IDE, which proteolyzes Aβ 1-42 and Aβ 1-40, has been detected among cargo proteins of microglial EMVs (Tamboli IY, et al., 2010). However, further studies are required to unequivocally define the topology of Aβ species and to clarify whether Aβ forms are actually associated to the extracellular membrane of shed MVs.

5.4 Microglial MVs in CSF of AD patients.

The in-vitro findings of my thesis work has clear clinical implications. The main idea behind the hypothesis that microglia-derived MVs can lead to neurotoxicity came from the fact that both in AD patients and mice models for AD there are activated microglial cells surrounding the plaque. Recent studies demonstrates that activation of microglia increases linearly throughout the disease course and correlates with AD neurodegeneration (Serrano-Pozo A, et al., 2011). These activated microglia cells release MVs, so we were interested in investigating the production of MVs in AD patients. Interestingly we found that microglial MVs were very high in MCI and AD patients, reflecting microgliosis (Verderio C, et al., 2012), which typically characterizes the disease (Serrano-Pozo A, et al., 2011). In accordance with our in-vitro results we observed that MVs collected from the CSF of AD patients promote extra-cellular formation of neurotoxic Aβ species, similarly to MVs shed from cultured cells. We also found that the MVs from AD patients were extremely toxic to cultured neurons, more than Mvs collected from patients with other neuroinflammatory disorders, and by the use of anti-Aβ antibodies we could partially block this toxicity. These results suggest that the

toxicity of MVs from AD patients is at least in part, associated to their Aβ cargo. Further analysis of the various Aβ species present in the MVs obtained from the CSF of a large cohort of AD and healthy subjects will clarify whether changes in the conformation and/or in the amount of Aβ forms may account for higher neurotoxicity of MVs from dementia patients. Furthermore, lipidomic profiling of human MVs from AD and healthy subjects will help to understand if possible alterations in lipid components can in part account for neurotoxicity caused by MVs from AD patients and may be used as a new putative AD biomarkers, thus increasing the diagnostic potential of MVs in AD. Finally, it should be pointed out that it is still to be defined whether MVs may associate with Abeta present in the parenchyma/blood vessel as well as plaques during their travel to CSF. In this case the content of Abeta present in MVs collected from dementia patients does not merely reflect Abeta trafficking inside donor microglial cells.

In agreement with their pathogenic role, levels of microglia-derived MVs are positively correlated with classical biomarkers of neuronal injury such as tau in the CSF (Holtzma D, et al., 2011) of MCI and AD subjects, and with damage to white matter structures of the temporal lobe in MCI patients, as revealed by MRI scans (Dalla Libera, et al., manuscript in preparation). These observations suggest that MVs may play a critical role in AD pathogenesis and open the way for new therapies targeting MVs to prevent neurotoxicity of Aβ species in the brain. Moreover our study suggests that MVs may represent as a novel companion tool for AD diagnosis.

5.5 Treatment with the inhibitor of MV shedding FTY720 improves cognitive impairment in APPSwe/PS1 transgenic mice by decreasing neuro-inflammation and plaque load.

We further observed that treatment with the pharmacological drug FTY720, which is known to exert therapeutic benefit in MS (Cohen JA, et al.,2011) and various CNS injuries, such as stroke and trauma (Aktas O, et al., 2010; Wei Y, et al., 2011) could ameliorate the pathophysiology and cognitive defects in APPSwe/PS1 AD mouse model. Recent reports suggest that FTY720 is a specific inhibitor of A-SMase (Dawson G, et al., 2011), the enzyme that controls MV production. Work from our lab further demonstrated that FTY720 completely abolished release of MVs evoked by ATP in vitro and decreased MV concentration to baseline levels in the CSF of EAE mice upon chronic treatment (Verderio C, et al., 2012). Thus, we were interested to explore the possibility that inhibition of MV shedding by FTY720 may contribute, at least in part, to the therapeutic action of FTY720 in the brain. To investigate this possibility we used APPSwe/PS1 transgenic mice as a model of AD.

As expected, we observed cognitive impairment in male APPswe/PS1 mice in passive avoidance and object recognition memory tests as compared to wild type mice. Transgenic females were not impaired in passive avoidance, but became impaired in object recognition during the course of treatment with the vehicle. Notably we observed a promising improvement in the cognitive behaviour of transgenic male and female mice upon FTY 720 administration for 5 weeks. However we could not correlate amelioration of cognitive behaviour to variation in MV production by the drug, as in the old mice used in these experiments we did not collected sufficient amount of CSF to analyse MV concentration by FACS.

Consistent with the known immunosuppressive properties of the drug (S Suzuki, et al., 1996), we found a significant reduction in astrogliosis and microgliosis in the brain of transgenic mice treated with FTY720, which tipically display increased protein and mRNA levels of the astrogliosis and microgliosis marker GFAP and IBA1. Indeed there was a significant reduction in mRNA expression of these inflammatory markers in transgenic mice upon FTY treatment. The wild type mice administered with FTY performed poorly in behaviour and there was further reduction in glial cells along with decrease in inflammatory marker as compared to wild type littermates administered with water. There is evidence showing that S1P influences inflammatory responses and induces neuronal apoptosis in a concentration-dependent manner (Hagen, et al., *2009*). Therefore, it may be hypothesized that administration of FTY720 to non-AD mice enhances the S1P signalling to pathologic levels. In addition, we observed decreased level of total abeta load upon FTY720 treatment in transgenic mice, while soluble abeta brain content was significantly decreased in case of transgenic female.

Recently a lot of reports point to multiple molecular targets of FTY720 neuroprotective action. The phosphorylated form of FTY is an analog of S1P. In AD patients, levels of SIP are significantly reduced compared with the age-matched normal controls. FTY720 also decreases the levels of ceramides (S Lahiri, et al.,2009), which have been shown to promote beta amyloid peptide formation and are also linked to neurotoxicity via activation of pro-apoptotic pathways (X. He, et al., 2010) Furthermore SPK1 (S1P producing enzyme) overexpression, promotes neuronal survival upon Aβ exposure (A. Gomez-Brouchet, et al., 2007). Ex vivo study, demonstrates that S1P possesses neuroprotective effects against soluble Aβ oligomer-induced cell death by inhibiting the activation of acid sphingomyelinase (Gómez-Muñoz, et al., *2003*). The balance between the levels of ceramide and S1P, the 'ceramide/S1P rheostat', contributes to the fate of cells (Cuvillier, et al., 1996). Therefore, the potential ability of FTY720 to recapitulate the function of S1P might also underlie its protective

mechanism against Aβ neurotoxicity, which can account for behavioural improvement in transgenic mice treated with FTY.

Recent reports also indicate that FTY720 may also act directly on neural and non-neural CNS cells to reduce Abeta neurodegeneration and to promote reparative mechanisms through upregulation of BDNF production (Doi Y, et al., 2013). In parallel to our study, other groups observed that chronic treatment with FTY720 decreases the $A\beta_{42}$-induced activation of caspase-3 and protects against hippocampal neuronal loss in vitro (Fatemeh Hemmati, et al. 2013). The protective actions of FTY720 also manifest as improved spatial learning and memory formation in AD model rats. It has been suggested that FTY720 administration improves passive avoidance memory retrieval through mechanisms which alter the overall inflammatory and apoptotic mechanisms toward less brain damage and memory loss (Fatemeh Hemmati, et al. 2013).

In conclusion, although we observed a clear improvement in the pathophysiology and cognitive defects of APPSwe/PS1 AD mice upon FTY720 administration, due to the multiple targets of the drug, we could not ascribe its neuroprotective action to its ability to inhibit MV shedding. Actually we believe that FTY720 may induce beneficial effects in AD by multiple pathways and either improving or preventing the patology from father progression.

5.6 Conclusion

Our study clearly demonstrates that MVs derived from microglial cells, surrounding the plaque may act as a carrier of neurotoxic species and have potential to convert extracellular inert A to neurotoxic. The increase in level of myeloid MVs in CSF of AD patient, identifies MVs as a novel therapeutic target and companion tool for AD diagnosis.

6. REFERENCES

Glass CK, Saijo K, Winner B, Marchetto MC, Gage FH 2010. Mechanisms underlying inflammation in neurodegeneration. Cell 140: 918-34.

Werner P, Mittelman MS, Goldstein D, Heinik J 2012. Family stigma and caregiver burden in Alzheimer's disease Gerontologist 52: 89-97.

Terry RD, Masliah E, Salmon DP, Butters N, DeTeresa R, Hill R, Hansen LA, Katzman R 1991. Physical basis of cognitive alterations in Alzheimer's disease: Synapse loss is the major correlate of cognitive impairment. Ann Neurol 30: 572–580

Mandelkow EM, Mandelkow E 1998. Tau in Alzheimer's disease. Trends Cell Biol 8: 425–427.

Trojanowski JQ, Lee VM 1998. Aggregation of neurofilament and α-synuclein proteins in Lewy bodies: Implications for the pathogenesis of Parkinson disease and Lewy body dementia. Arch Neurol 55: 151–152.

Iqbal K, Grundke-Iqbal I 2002. Neurofibrillary pathology leads to synaptic loss and not the other way around in Alzheimer disease. J Alzheimers Dis 4: 235–238.

Masliah E 2000. The role of synaptic proteins in Alzheimer's disease. Ann NY Acad Sci924: 68–75.

Beach T, Walker R, McGeer E 1989. Patterns of gliosis in Alzheimer's disease and aging cerebrum. Glia 2: 420–436.

Itagaki S, McGeer PL, Akiyama H, Zhu S, Selkoe D 1989. Relationship of microglia and astrocytes to amyloid deposits of Alzheimer disease. J Neuroimmunol 24: 173–182.

Rogers J, Luber-Narod J, Styren S, Civin W 1988. Expression of immune system-associated antigens by cells of the human central nervous system: Relationship to the pathology of Alzheimer's disease. Neurobiol Aging 9: 339–349.

Masliah E, Rockenstein E, Veinbergs I, Sagara Y, Mallory M, Hashimoto M, Mucke L 2001b. β-amyloid peptides enhance α-synuclein accumulation and neuronal deficits in a transgenic mouse model linking Alzheimer's disease and Parkinson's disease.Proc Natl Acad Sci 98: 12245–12250.

Gibson PH, Tomlison BE 1977. Numbers of Hirano bodies in the hippocampus of normal and demented people with Alzheimer's disease. J Neurol Sci 33: 199–206.

Gómez-Isla T, Price JL, McKeel DW Jr, Morris JC, Growdon JH, Hyman BT 1996.Profound loss of layer II entorhinal cortex neurons occurs in very mild Alzheimer's disease. J Neurosci 16: 4491–4500

Iqbal K, Grundke-Iqbal I 2002. Neurofibrillary pathology leads to synaptic loss and not the other way around in Alzheimer disease. J Alzheimers Dis 4: 235–238.

Bussière T, Gold G, Kövari E, Giannakopoulos P, Bouras C, Perl DP, Morrison JH, Hof PR 2003. Stereologic analysis of neurofibrillary tangle formation in prefrontal cortex area 9 in aging and Alzheimer's disease. Neuroscience 117: 577–592.

Hof PR, Bussière T, Gold G, Kövari E, Giannakopoulos P, Bouras C, Perl DP, Morrison JH 2003. Stereologic evidence for persistence of viable neurons in layer II of the entorhinal cortex and the CA1 field in Alzheimer disease. J Neuropathol Exp Neurol62: 55–67.

Yoshiyama Y, Higucho M, Zhang B, Huang SM, Iwata N, Saido TC, Maeda J, Suhara T, Trojanowski JQ, Lee VM 2007. Synapse loss and microglial activation precede tangles in a P301S tauopathy mouse model. J Neuron 53: 337–351.

Spires-Jones TL, de Calignon A, Matsui T, Zehr C, Pitstick R, Wu HY, Osetek JD, Jones PB, Bacskai BJ, Feany MB, et al. 2007. In vivo imaging reveals dissociation between caspase activation and acute neuronal death in tangle-bearing neurons. J Neurosci28: 862–867.

de Calignon A, Fox LM, Pitstick R, Carlson GA, Bacskai BJ, Spires-Jones TL, Hyman BT 2010. Caspase activation precedes and leads to tangles. Nature 464: 1201–1204.

Kimura T, Fukuda T, Sahara N, Yamashita S, Murayama M, Mirozoki T, Yoshiike Y, Lee B, Sotiropoulos I, Maeda S, et al. 2010. Aggregation of detergent-insoluble tau is involved in neuronal loss but not in synaptic loss. J Biol Chem 285: 38692–38699.

R. Vassar, B.D. Bennett, S. Babu-Khan, S. Kahn, E.A. Mendiaz, P. Denis, D.B. Teplow, S. Ross, P. Amarante, R. Loeloff, Y. Luo, S. Fisher, J. Fuller, S. Edenson, J. Lile, M.A. Jarosinski, A.L. Biere, E. Curran, T. Burgess, J.C. Louis, F. Collins, J. Treanor, G. Rogers, M. Citron 1999. Beta-secretase cleavage of Alzheimer's amyloid precursor protein by the transmembrane aspartic protease BACE. Science (New York, NY), 286: 735–741

D. Edbauer, C. Kaether, H. Steiner, C. Haass 2004. Co-expression of nicastrin and presenilin rescues a loss of function mutant of APH-1. J Biol Chem 279: 37311–37315.

Xu H, Sweeney D, Wang R, Thinakaran G, Lo AC, Sisodia SS, Greengard P, Gandy S 1997. Generationof Alzheimer beta-amyloid protein in the trans-Golgi network in the apparent absence of vesicle formation. Proc Natl Acad Sci 94: 3748-52.

Hartmann T, Bieger SC, Brühl B, Tienari PJ, Ida N, Allsop D, Roberts GW, Masters CL, Dotti CG, Unsicker K, Beyreuther K 1997.Distinct sites of intracellular production for Alzheimer's disease A beta40/42 amyloid peptides. Nat Med. :1016-20.

Greenfield JP, Tsai J, Gouras GK, Hai B, Thinakaran G, Checler F, Sisodia SS, Greengard P, Xu H 1999. Endoplasmic reticulum and trans-Golgi network generate distinct populations of Alzheimer beta-amyloid peptides. Proc Natl Acad Sci 96:742-7.

Berridge M. J 1998. Neuronal calcium signaling. Neuron 21: 13–26.

Khachaturian ZS, Monjan AA, Radebaugh TS 1989. The future of Alzheimer's disease research.Prog Clin Biol Res 317:13-21.

Ohyagi Y., Asahara H., Chui D. H. et al 2005. Intracellular Abeta42 activates p53 promoter: a pathway to neurodegeneration in Alzheimer's disease. FASEB J. 19, 255–257.

Pearson H. A. and Peers C 2006. Physiological roles for amyloid β peptides. J. Physiol. 575, 5–10.

Hardy J 2007. Does Aβ 42 have a function related to blood homeostasis? Neurochem. Res. 32, 833–835.

Bailey J. A., Maloney B., Ge Y. W. and Lahiri D. K. 2011. Functional activity of the novel Alzheimer's amyloid β-peptide interacting domain (AβID) in the APP and BACE1 promoter sequences and implications in activating apoptotic genes and in amyloidogenesis. Gene 488, 13–22.

Cao X. and Sudhof T. C 2001. A transcriptively active complex of APP with Fe65 and histone acetyltransferase Tip60. Science 293,115–120.

Pardossi-Piquard R., Petit A., Kawarai T. et al 2005. Presenilin-dependent transcriptional control of the Abeta-degrading enzyme neprilysin by intracellular domains of βAPP and APLP. Neuron 46, 541–554.

Müller T., Concannon C. G., Ward M. W., Walsh C. M., Tirniceriu A. L., Tribl F., Kogel D., Prehn J. H. and Egensperger R 2007. Modulation of gene expression and cytoskeletal dynamics by the amyloid precursor protein intracellular domain (AICD). Mol. Biol. Cell 18, 201–210

Belyaev N. D., Nalivaeva N. N., Makova N. Z. and Turner A. J 2009. Neprilysin gene expression requires binding of the amyloid precursor protein intracellular domain to its promoter: implications for Alzheimer disease. EMBO Rep. 10, 94–100.

Belyaev N. D., Kellett K. A., Beckett C., Makova N. Z., Revett T. J., Nalivaeva N. N., Hooper N. M. and Turner A. J 2010. The transcriptionally active amyloid precursor protein (APP) intracellular domain is preferentially produced from the 695 isoform of APP in a β-secretase-dependent pathway. J. Biol. Chem. 285, 41443–41454.

Kitazume S, Tachida Y, Kato M, Yamaguchi Y, Honda T, Hashimoto Y, Wada Y, Saito T, Iwata N, Saido T, Taniguchi N 2010. Brain endothelial cells produce amyloid {beta} from amyloid precursor protein 770 and preferentially secrete the O-glycosylated form. J Biol Chem 285:40097-103

Schmitt TL, Steiner E, Klingler P, Lassmann H, Grubeck-Loebenstein B 1995. Thyroid epithelial cells produce large amounts of the Alzheimer beta-amyloid precursor protein (APP) and generate potentially amyloidogenic APP fragments. J Clin Endocrinol Metab.80:3513-9.

Fukumoto H, Tomita T, Matsunaga H, Ishibashi Y, Saido TC, Iwatsubo T 1999. Primary cultures of neuronal and non-neuronal rat brain cells secrete similar proportions of amyloid β peptides ending at Aβ40 and Aβ42. NeuroReport 10:2965–2969.

Giuffrida ML, Caraci F, De Bona P, Pappalardo G, Nicoletti F, Rizzarelli E, Copani A 2010. The monomer state of beta-amyloid: where the Alzheimer's disease protein meets physiology.Rev Neurosci 21:83-93.

Schilling, S., Lauber, T., Schaupp, M., Manhart, S., Scheel, E., Bohm, G., and Demuth, H.U 2006. On the seeding and oligomerization of pGlu-amyloid peptides (in vitro). Biochemistry 45:12393-12399

Bieschke, J., Herbst, M., Wiglenda, T., Friedrich, R.P., Boeddrich, A., Schiele, F., Kleckers, D., Lopez del Amo, J.M., Gruning, B.A., Wang, Q., et al 2012. Small-molecule conversion of toxic oligomers to nontoxic beta-sheet-rich amyloid fibrils. Nature chemical biology 8:93-101

Caughey B, Lansbury PT 2003. Protofibrils, pores, fibrils, and neurodegeneration: separating the responsible protein aggregates from the innocent bystanders. Annu Rev Neurosci.26:267-98..

Glabe CG 2006. Common mechanisms of amyloid oligomer pathogenesis in degenerative disease. Neurobiol Aging27:570-5

Roychaudhuri R, Yang M, Hoshi MM, Teplow DB 2009, Amyloid beta-protein assembly and Alzheimer disease. J Biol Chem. 284:4749-53.

Lambert M.P., Barlow A.K., Chromy B.A., Edwards C., Freed R., Liosatos M., Morgan T.E., Rozovsky I., Trommer B., Viola K.L., et al 1998. Diffusible, nonfibrillar ligands derived from Aβ1-42 are potent central nervous system neurotoxins. Proc. Natl. Acad. Sci. USA 95:6448–6453.

Gonzalez-Velasquez F.J., Kotarek J.A., Moss M.A 2008. Soluble aggregates of the amyloid-β protein selectively stimulate permeability in human brain microvascular endothelial monolayers. J. Neurochem 107:466–477.

Hartley D.M., Walsh D.M., Ye C.P., Diehl T., Vasquez S., Vassilev P.M., Teplow D.B., Selkoe D.J 1999. Protofibrillar intermediates of amyloid β-protein induce acute electrophysiological changes and progressive neurotoxicity in cortical neurons. J. Neurosci 19:8876–8884.

Lesne S., Koh M.T., Kotilinek L., Kayed R., Glabe C.G., Yang A., Gallagher M., Ashe K.H 2006. A specific amyloid-β protein assembly in the brain impairs memory. Nature 440:352–357.

Walsh D.M., Klyubin I., Fadeeva J.V., Rowan M.J., Selkoe D.J 2002. Amyloid-β oligomers: Their production, toxicity and therapeutic inhibition. Biochem. Soc. Trans 30:552–557.

Westerman M., Cooper-Blacketer D., Mariash A., Kotilinek L., Kawarabayashi T., Younkin L., Carlson G., Younkin S., Ashe K 2002. The relationship between aβ and memory in the tg2576 mouse model of alzheimer's disease. J. Neurosci 22:1858–1867.

Snyder EM, Nong Y, Almeida CG, Paul S, Moran T, Choi EY, Nairn AC, Salter MW, Lombroso PJ, Gouras GK, Greengard P 2005. Regulation of NMDA receptor trafficking by amyloid-beta.Nat Neurosci.8:1051-8.

Lauren, J., Gimbel, D.A., Nygaard, H.B., Gilbert, J.W., and Strittmatter, S.M 2009. Cellular prion protein mediates impairment of synaptic plasticity by amyloid-beta oligomers. Nature 457:1128-1132.

Um, J.W., Nygaard, H.B., Heiss, J.K., Kostylev, M.A., Stagi, M., Vortmeyer, A., Wisniewski, T., Gunther, E.C., and Strittmatter, S.M 2012. Alzheimer amyloid-beta oligomer bound to postsynaptic prion protein activates Fyn to impair neurons. Nature neuroscience 15:1227-1235.

Benilova, I., Karran, E., and De Strooper, B 2012. The toxic Abeta oligomer and Alzheimer's disease: an emperor in need of clothes. Nature neuroscience 15:349-357.

Verdier, Y., Zarandi, M., and Penke, B 2004. Amyloid beta-peptide interactions with neuronal and glial cell plasma membrane: binding sites and implications for Alzheimer's disease. Journal of peptide science : an official publication of the European Peptide Society 10:229-248.

Tanzi R. E., Kovacs D. M., Kim T. W., Moir R. D., Guenette S. Y. and Wasco W 1996. The gene defects responsible for familial Alzheimer's disease. Neurobiol. Dis. **3**, 159–168.

Hardy J 1997. Amyloid, the presenilins and Alzheimer's disease. Trends Neurosci. **20**:154–159.

Tanzi R. E. and Bertram L. 2005. Twenty years of the Alzheimer's disease amyloid hypothesis: a genetic perspective. Cell **120**:545–555.

De Strooper B. 2003 Aph-1, Pen-2, and Nicastrin with Presenilin generate an active gamma-secretase complex. Neuron 38: 9–12.

Edbauer D., Winkler E., Regula J. T., Pesold B., Steiner H. and Haass C 2003.Reconstitution of gamma-secretase activity. Nat. Cell Biol 5:486–488.

Hardy J, Selkoe DJ 2002 The amyloid hypothesis of Alzheimer's disease: progress and problems on the road to therapeutics.Science 297:353-6

Goate A, Hardy J 2012. Twenty years of Alzheimer's disease-causing mutations J Neurochem 120 Suppl 1:3-8.

Potter H, Wisniewski T 2012. Apolipoprotein e: essential catalyst of the Alzheimer amyloid cascade Int J Alzheimers Dis 489428.

Liu and Hong, 2003 B. Liu, J.S. Hong 2003. Role of microglia in inflammation-mediated neurodegenerative diseases: mechanisms and strategies for therapeutic intervention Journal of Pharmacology and Experimental Therapeutics 304: 1–7.

F. Al Nimer, A.D. Beyeen, R. Lindblom, M. Strom, S. Aeinehband, O. Lidman, F. Piehl 2011. Both MHC and non-MHC genes regulate inflammation and T-cell response after traumatic brain injury Brain, Behavior, and Immunity, 25 : 981–990.

Alzheimer A., Stelzmann R. A., Schnitzlein H. N., Murtagh F. R 1995. An English translation of Alzheimer's 1907 paper, “Uber eine eigenartige Erkankung der Hirnrinde.” Clin. Anat. 8, 429–431.

T. Wyss-Coray, J.D. Loike, T.C. Brionne, E. Lu, R. Anankov, F. Yan, S.C. Silverstein, J. Husemann 2003.Adult mouse astrocytes degrade amyloid-beta in vitro and in situ Nat. Med., 9 :453–457.

Nikolaev, T. McLaughlin, D.D.M. O'Leary, M. Tessier-Lavigne 2009.APP binds DR6 to trigger axon pruning and neuron death via distinct caspases Nature, 457: 981–989.

Carrero I, Gonzalo MR, Martin B, Sanz-Anquela JM, Arévalo-Serrano J, Gonzalo-Ruiz A 2012 Oligomers of β-amyloid protein (Aβ1-42) induce the activation of cyclooxygenase-2 in astrocytes via an interaction with interleukin-1β, tumour necrosis factor-α, and a nuclear factor κ-B mechanism in the rat brain.Exp Neurol 236 :215-27.

Vinet, H.R. Weering, A. Heinrich, R.E. Kalin, A. Wegner, N. Brouwer, F.L. Heppner, N. Rooijen, H.W. Boddeke, K. Biber 2012. Neuroprotective function for ramified microglia in hippocampal excitotoxicity Journal of Neuroinflammation, 9: 27

C. Lauro, R. Cipriani, M. Catalano, F. Trettel, G. Chece, V. Brusadin, L. Antonilli, N. van Rooijen, F. Eusebi, B.B. Fredholm, C. Limatola 2010. Adenosine A1 receptors and microglial cells mediate CX3CL1-induced protection of hippocampal neurons against Glu-induced death Neuropsychopharmacology, 35: 1550–1559.

Medeiros R, Figueiredo CP, Pandolfo P, Duarte FS, Prediger RD, Passos GF, Calixto JB. 2010.The role of TNF-alpha signaling pathway on COX-2 upregulation and cognitive decline induced by beta-amyloid peptide. Behav Brain Res 209:165-73

Smits HA, Rijsmus A, van Loon JH, Wat JW, Verhoef J, Boven LA, Nottet HS 2002. Amyloid-beta-induced chemokine production in primary human macrophages and astrocytes. J Neuroimmunol. 127:160-8

Lue, L.F., Brachova, L., Civin, W.H., and Rogers, J 1996. Inflammation, A beta deposition, and neurofibrillary tangle formation as correlates of Alzheimer's disease neurodegeneration. Journal of neuropathology and experimental neurology 55:1083-1088.

Edison, P., Archer, H.A., Gerhard, A., Hinz, R., Pavese, N., Turkheimer, F.E., Hammers, A., Tai, Y.F., Fox, N., Kennedy, A., et al 2008. Microglia, amyloid, and cognition in Alzheimer's disease: An [11C](R)PK11195-PET and [11C]PIB-PET study. Neurobiology of disease 32:412-419.

Okello, A., Edison, P., Archer, H.A., Turkheimer, F.E., Kennedy, J., Bullock, R., Walker, Z., Kennedy, A., Fox, N., Rossor, M., et al 2009. Microglial activation and amyloid deposition in mild cognitive impairment: a PET study. Neurology 72:56-62.

Serrano-Pozo, A., Mielke, M.L., Gomez-Isla, T., Betensky, R.A., Growdon, J.H., Frosch, M.P., and Hyman, B.T 2011. Reactive glia not only associates with plaques but also parallels tangles in Alzheimer's disease. The American journal of pathology 179:1373-1384.

Hollingworth, P., Harold, D., Sims, R., Gerrish, A., Lambert, J.C., Carrasquillo, M.M., Abraham, R., Hamshere, M.L., Pahwa, J.S., Moskvina, V., et al. 2011. Common variants at ABCA7, MS4A6A/MS4A4E, EPHA1, CD33 and CD2AP are associated with Alzheimer's disease. Nature genetics 43:429-435.

Guerreiro, R., Wojtas, A., Bras, J., Carrasquillo, M., Rogaeva, E., Majounie, E., Cruchaga, C., Sassi, C., Kauwe, J.S., Younkin, S., et al 2013. TREM2 variants in Alzheimer's disease. The New England journal of medicine 368:117-127.

Giulian, D., Haverkamp, L.J., Yu, J.H., Karshin, W., Tom, D., Li, J., Kirkpatrick, J., Kuo, L.M., and Roher, A.E 1996. Specific domains of beta-amyloid from Alzheimer plaque elicit neuron killing in human microglia. The Journal of neuroscience : the official journal of the Society for Neuroscience 16:6021-6037.

Fuhrmann, M., Bittner, T., Jung, C.K., Burgold, S., Page, R.M., Mitteregger, G., Haass, C., LaFerla, F.M., Kretzschmar, H., and Herms, J 2010. Microglial Cx3cr1 knockout prevents neuron loss in a mouse model of Alzheimer's disease. Nature neuroscience 13:411-413.

Tan, B., Choi, R.H., Chin, T.J., Kaur, C., and Ling, E.A 2012. Manipulation of microglial activity as a therapy for Alzheimer's disease. Frontiers in bioscience 4:1402-1412.

Weitz, T.M., and Town, T 2012. Microglia in Alzheimer's Disease: It's All About Context. International journal of Alzheimer's disease 2012:314185.

Mathivanan S, Ji H, Simpson RJ 2010. Exosomes: extracellular organelles important in intercellular communication. J Proteomics 73: 1907-1920.

Hanson PI, Shim S, Merrill SA 2009. Cell biology of the ESCRT machinery. Curr Opin Cell Biol 21: 568-574.

Wollert T, Hurley JH 2010. Molecular mechanism of multivesicular body biogenesis by ESCRT complexes. Nature 464: 864-869.

Wollert T, Yang D, Ren X, Lee HH, Im YJ, Hurley JH 2009. The ESCRT machinery at a glance. JCell Sci 122: 2163-2166.

Babst M 2005. A protein's final ESCRT. Traffic 6: 2-9.

Kosaka N, Iguchi H, Yoshioka Y, Takeshita F, Matsuki Y, Ochiya T 2010. Secretory mechanisms and intercellular transfer of microRNAs in living cells. J Biol Chem 285: 17442-17452

Trajkovic K, Hsu C, Chiantia S, Rajendran L, Wenzel D, Wieland F, Schwille P, Brugger B, Simons M 2008. Ceramide triggers budding of exosome vesicles into multivesicular endosomes.Science 319: 1244-1247

Simons M, Raposo G 2009. Exosomes--vesicular carriers for intercellular communication. Curr Opin Cell Biol 21: 575-581

Sadallah S, Eken C, Martin PJ, Schifferli JA 2011. Microparticles (ectosomes) shed by stored human platelets downregulate macrophages and modify the development of dendritic cells. JImmunol 186: 6543-6552

Bernimoulin M, Stern M, Tichelli A, Jotterand M, Gratwohl A, Nissen C 2008. Leukemic cluster growth in culture is an independent risk factor for acute myeloid leukemia and short survival in patients with myelodysplastic syndrome. Acta Haematol 119: 226-235

Cocucci E, Racchetti G, Meldolesi J 2009. Shedding microvesicles: artefacts no more. Trends Cell Biol 19: 43-51

Thery C, Ostrowski M, Segura E 2009. Membrane vesicles as conveyors of immune responses. Nat Rev Immunol 9: 581-593

Emmanouilidou E, Melachroinou K, Roumeliotis T, Garbis SD, Ntzouni M, Margaritis LH, Stefanis L, Vekrellis K 2010. Cell-produced alpha-synuclein is secreted in a calcium-dependent manner by exosomes and impacts neuronal survival. J Neurosci 30: 6838-6851

Bianco F, Pravettoni E, Colombo A, Schenk U, Moller T, Matteoli M, Verderio C 2005.Astrocyte-derived ATP induces vesicle shedding and IL-1 beta release from microglia. J Immunol174: 7268-7277.

Bianco F, Perrotta C, Novellino L, Francolini M, Riganti L, Menna E, Saglietti L, Schuchman EH,

Furlan R, Clementi E, Matteoli M, Verderio C 2009. Acid sphingomyelinase activity triggers

microparticle release from glial cells. EMBO J 28: 1043-1054.

Verderio, C., Muzio, L., Turola, E., Bergami, A., Novellino, L., Ruffini, F., et al 2012. Myeloid microvesicles are a marker and therapeutic target for neuroinflammation.Ann. Neurol. 72, 610–624.

Antonucci, F., Turola, E., Riganti, L., Caleo, M., Gabrielli, M., Perrotta, C., et al 2012. Microvesicles released from microglia stimulate synaptic activity via enhanced sphingolipid metabolism. EMBO J. 31, 1231–1240.

Turola, E., Furlan, R., Bianco, F., Matteoli, M., and Verderio, C 2012. Microglial microvesicle secretion and intercellular signaling. Front. Physiol. 3:149.

McKhann G, Drachman D, Folstein M, Katzman R, Price D, Stadlan EM 1984. Clinical diagnosis of Alzheimer's disease: report of the NINCDS-ADRDA work group under the auspices of department of health and human services task force on Alzheimer's disease. Neurology. 8:939–944.

Knopman DS, DeKosky ST, Cummings JL, Chui H, Corey-Bloom J, Relkin N, Small GW, Miller B, Stevens JC. Practice parameter: diagnosis of dementia (an evidence-based review). Report of the

Quality Standards Subcommittee of the American Academy of Neurology. Neurology. 2001 8:1143–1153.

Jack CR Jr, Albert MS, Knopman DS, McKhann GM, Sperling RA, Carrillo MC, Thies B, Phelps CH 2011.Introduction to the recommendations from the national institute on aging-Alzheimer's association workgroups on diagnostic guidelines for Alzheimer's disease. Alzheimer's dementia j Alzheimer's Assoc 8:257–262.

Blennow K, Hampel H, Weiner M, Zetterberg H 2010. Cerebrospinal fluid and plasma biomarkers in Alzheimer disease. Nat Rev Neurol 8:131–144.

Price JL, Morris JC 1999.Tangles and plaques in nondemented aging and "preclinical" Alzheimer's disease. Ann Neurol 8:358–368.

Jack CR Jr, Knopman DS, Jagust WJ, Shaw LM, Aisen PS, Weiner MW, Petersen RC, Trojanowski JQ 2010.Hypothetical model of dynamic biomarkers of the Alzheimer's pathological cascade. Lancet Neurol 8:119–128.

Camussi G, Deregibus MC, Bruno S, Cantaluppi V, Biancone L (2010) Exosomes/microvesicles as a mechanism of cell-to-cell communication. Kidney Int 78: 838-848.

Colombo, E., Borgiani, B., Verderio, C., and Furlan, R. 2012. Microvesicles: novel biomarkers for neurological disorders. Frontiers in physiology 3:63.

Rajendran, L., Honsho, M., Zahn, T.R., Keller, P., Geiger, K.D., Verkade, P., and Simons, K 2006. Alzheimer's disease beta-amyloid peptides are released in association with exosomes. Proceedings of the National Academy of Sciences of the United States of America 103:11172-11177.

de Calignon A, Polydoro M, Suárez-Calvet M, William C, Adamowicz DH, Kopeikina KJ, Pitstick R, Sahara N, Ashe KH, Carlson GA, Spires-Jones TL, Hyman BT 2012. Propagation of tau pathology in a model of early Alzheimer's disease. Neuron 73:685-97.

J.A. Harris, N. Devidze, L. Verret, K. Ho, B. Halabisky, M.T. Thwin, D. Kim, P. Hamto, I. Lo, G.Q. Yu et al 2010. Transsynaptic progression of amyloid-β-induced neuronal dysfunction within the entorhinal-hippocampal network Neuron 68: 428–441

Luk KC, Kehm V, Carroll J, Zhang B, O'Brien P, Trojanowski JQ, Lee VM 2012. Pathological α-synuclein transmission initiates Parkinson-like neurodegeneration in nontransgenic mice. Science 338 :949-53.

Mielke, M.M., Haughey, N.J., Bandaru, V.V., Weinberg, D.D., Darby, E., Zaidi, N., Pavlik, V., Doody, R.S., and Lyketsos, C.G 2011. Plasma sphingomyelins are associated with cognitive progression in Alzheimer's disease. Journal of Alzheimer's disease 27:259-269.

Martins, I.C., Kuperstein, I., Wilkinson, H., Maes, E., Vanbrabant, M., Jonckheere, W., Van Gelder, P., Hartmann, D., D'Hooge, R., De Strooper, B., et al 2008. Lipids revert inert Abeta amyloid fibrils to neurotoxic protofibrils that affect learning in mice. EMBO journal 27:224-233.

Johansson, A.S., Garlind, A., Berglind-Dehlin, F., Karlsson, G., Edwards, K., Gellerfors, P., Ekholm-Pettersson, F., Palmblad, J., and Lannfelt, L 2007. Docosahexaenoic acid stabilizes soluble amyloid-beta protofibrils and sustains amyloid-beta-induced neurotoxicity in vitro. The FEBS journal 274:990-1000.

Zhao L.N., Chiu S.W., Benoit J., Chew L.Y., Mu Y 2011. Amyloid β peptide aggregation in a mixed membrane bilayer: A molecule dynamic study. J. Phys. Chem. B 115:12247–12256

Wakabayashi M., Matsuzaki K 2009. Ganglioside-induced amyloid formation by human islet amyloid polypeptide in lipid rafts. FEBS Lett 583:2854–2858.

Wakabayashi M., Okada T., Kozutsumi Y., Matsuzaki K 2005. GM1 ganglioside-mediated accumulation of amyloid beta-protein on cell membranes. Biochem. Biophys. Res. Commun 328:1019–1023

Miron, V. E., Schubart, A., and Antel, J. P 2008. Central nervous system-directed effects of FTY720 (fingolimod) J. Neurol. Sci 274, 13–17

J.A. Cohen, J. Chun 2011. Mechanisms of fingolimod's efficacy and adverse effects in multiple sclerosis Annals of Neurology 69: 759–777

Dawson G, Qin J 2011. Gilenya (FTY720) inhibits acid sphingomyelinase by a mechanism similar to tricyclic antidepressants.Biochem Biophys Res Commun 404: 321–323.

Gómez-Muñoz A, Kong J, Salh B, Steinbrecher UP 2003. Sphingosine-1-phosphate inhibits acid sphingomyelinase and blocks apoptosis in macrophages. FEBS Lett 539:56–60

A. Gomez-Brouchet, D. Pchejetski, L. Brizuela, V. Garcia, M.-F. Altié, M.-L. Maddelein et al. 2007. Critical role for sphingosine kinase-1 in regulating survival of neuroblastoma cells exposed to amyloid-β peptide Molecular Pharmacology 72: 341–349

Doi Y, Takeuchi H, Horiuchi H, Hanyu T, Kawanokuchi J, Jin S, Parajuli B, Sonobe Y, Mizuno T, Suzumura A 2013. Fingolimod phosphate attenuates oligomeric amyloid β-induced neurotoxicity via increased brain-derived neurotrophic factor expression in neurons. PLoS One 8 :e61988.

S. Lahiri, H. Park, E.L. Laviad, X. Lu, R. Bittman, A.H. Futerman Ceramide synthesis is modulated by the sphingosine analog 2009.FTY720 via a mixture of uncompetitive and noncompetitive inhibition in an Acyl-CoA chain length-dependent manner Journal of Biological Chemistry, 284: 16090–16098

Fatemeh Hemmati, Leila Dargahi, Sanaz Nasoohi,Rana Omidbakhsh, Zahurin Mohamed, Zamri Chik, Murali Naidu, Abolhassan Ahmadiani 2013. Neurorestorative effect of FTY720 in a rat model of Alzheimer's disease: Comparison with Memantine Behavioural Brain Research 252: 415–421

J. L. Jankowsky, D. J. Fadale, J. Anderson et al 2004. Mutant presenilins specifically elevate the levels of the 42 residue β-amyloid peptide in vivo: evidence for augmentation of a 42-specific γsecretase. Human Molecular Genetics 13: 159–170.

H. Xiong, D. Callaghan, J. Wodzinska, et al 2011. Biochemical and behavioral characterization of the double transgenic mouse model (APPswe/PS1dE9) of Alzheimer's disease. Neuroscience Bull 27 :221–232,.

M. Garcia-Alloza, L. A. Borrelli, B. T. Hyman, and B. J. Bacskai, 2010 Antioxidants have a rapid and long-lasting effect on neuritic abnormalities in APP:PS1 mice. Neurobiology of Aging, vol. 31, no. 12, pp. 2058–2068,

M. Meyer-Luehmann, M. Mielke, T. L. Spires-Jones et al 2009. A reporter of local dendritic translocation shows plaque-related loss of neural system function in APP-transgenic mice. Journal of Neuroscience 29: 12636–12640.

R. Minkeviciene, S. Rheims, M. B. Dobszay et al 2009. Amyloid β-induced neuronal hyperexcitability triggers progressive epilepsy.Journal of Neuroscience 29: 3453–3462.

E. Machová, V. Rudajev, H. Smyčková, H. Koivisto, H. Tanila, and V. Doležal 2010 Functional cholinergic damage develops with amyloid accumulation in young adult APPswe/PS1dE9 transgenic mice. Neurobiology of Disease 38: 27–35.

W. Zhang, J. Hao, R. Liu et al 2011. Soluble Aβ levels correlate with cognitive deficits in the 12-month-old APPswe/PS1dE9 mouse model of Alzheimer's disease," Behavioural Brain Research 222: 342–350.

Riboni L, Viani P, Tettamanti G 2000. Estimating sphingolipid metabolism and trafficking in cultured cells using radiolabeled compounds. Methods Enzymol 311: 656–682

De Felice, F.G., Wu, D., Lambert, M.P., Fernandez, S.J., Velasco, P.T., Lacor, P.N., Bigio, E.H., Jerecic, J., Acton, P.J., Shughrue, P.J., et al. 2008. Alzheimer's disease-type neuronal tau hyperphosphorylation induced by A beta oligomers. Neurobiology of aging 29:1334-1347

Klein, W.L 2002. Abeta toxicity in Alzheimer's disease: globular oligomers (ADDLs) as new vaccine and drug targets. Neurochemistry international 41:345-352.

Fukunaga, S., Ueno, H., Yamaguchi, T., Yano, Y., Hoshino, M., and Matsuzaki, K 2012. GM1 cluster mediates formation of toxic Abeta fibrils by providing hydrophobic environments. Biochemistry 51:8125-8131.

Jana, A., and Pahan, K 2010. Fibrillar amyloid-beta-activated human astroglia kill primary human neurons via neutral sphingomyelinase: implications for Alzheimer's disease. The Journal of neuroscience : the official journal of the Society for Neuroscience 30:12676-12689.

Lauren, J., Gimbel, D.A., Nygaard, H.B., Gilbert, J.W., and Strittmatter, S.M 2009. Cellular prion protein mediates impairment of synaptic plasticity by amyloid-beta oligomers. Nature 457:1128-1132.

Holtzman, D.M 2011. CSF biomarkers for Alzheimer's disease: current utility and potential future use. Neurobiology of aging 32 Suppl 1:S4-9.

Del Conde, I., Shrimpton, C.N., Thiagarajan, P., and Lopez, J.A 2005. Tissue-factor-bearing microvesicles arise from lipid rafts and fuse with activated platelets to initiate coagulation. Blood 106:1604-1611.

Han, X., Fagan, A.M., Cheng, H., Morris, J.C., Xiong, C., and Holtzman, D.M 2003. Cerebrospinal fluid sulfatide is decreased in subjects with incipient dementia. Annals of neurology 54:115-119.

Malnar, M., Kosicek, M., Bene, R., Tarnik, I.P., Pavelin, S., Babic, I., Brajenovic-Milic, B., Hecimovic, H., Titlic, M., Trkanjec, Z., et al 2012. Use of cerebrospinal fluid biomarker analysis for improving Alzheimer's disease diagnosis in a non-specialized setting. Acta neurobiologiae experimentalis 72:264-271.

Ghidoni, R., Paterlini, A., Albertini, V., Glionna, M., Monti, E., Schiaffonati, L., Benussi, L., Levy, E., and Binetti, G. 2011. Cystatin C is released in association with exosomes: a new tool of neuronal communication which is unbalanced in Alzheimer's disease. Neurobiology of aging 32:1435-1442.

Vingtdeux, V., Hamdane, M., Begard, S., Loyens, A., Delacourte, A., Beauvillain, J.C., Buee, L., Marambaud, P., and Sergeant, N. 2007. Intracellular pH regulates amyloid precursor protein intracellular domain accumulation. Neurobiology of disease 25:686-696.

Aguzzi, A., Barres, B.A., and Bennett, M.L. 2013. Microglia: scapegoat, saboteur, or something else? Science 339:156-161.

Prinz, M., Priller, J., Sisodia, S.S., and Ransohoff, R.M 2011. Heterogeneity of CNS myeloid cells and their roles in neurodegeneration. Nature neuroscience 14:1227-1235.

Paresce, D.M., Chung, H., and Maxfield, F.R 1997. Slow degradation of aggregates of the Alzheimer's disease amyloid beta-protein by microglial cells. The Journal of biological chemistry 272:29390-29397.

Lee, C.Y., and Landreth, G.E 2010. The role of microglia in amyloid clearance from the AD brain. Journal of neural transmission 117:949-960

Mattei, V., Barenco, M.G., Tasciotti, V., Garofalo, T., Longo, A., Boller, K., Lower, J., Misasi, R., Montrasio, F., and Sorice, M 2009. Paracrine diffusion of PrP(C) and propagation of prion infectivity by plasma membrane-derived microvesicles. PloS one 4:e5057.

Ariga, T., Kobayashi, K., Hasegawa, A., Kiso, M., Ishida, H., and Miyatake, T 2001. Characterization of high-affinity binding between gangliosides and amyloid beta-protein. Archives of biochemistry and biophysics 388:225-230.

Kiyota, T., Yamamoto, M., Xiong, H., Lambert, M.P., Klein, W.L., Gendelman, H.E., Ransohoff, R.M., and Ikezu, T 2009. CCL2 accelerates microglia-mediated Abeta oligomer formation and progression of neurocognitive dysfunction. PloS one 4:e6197.

Shen, B., Wu, N., Yang, J.M., and Gould, S.J 2011. Protein targeting to exosomes/microvesicles by plasma membrane anchors. The Journal of biological chemistry 286:14383-14395.

Sharples RA, Vella LJ, Nisbet RM, Naylor R, Perez K, Barnham KJ, Masters CL, Hill AF 2008.Inhibition of gamma-secretase causes increased secretion of amyloid precursor protein C-terminal fragments in association with exosomes.FASEB J 22:1469-78

Tamboli IY, Barth E, Christian L, Siepmann M, Kumar S, Singh S, Tolksdorf K, Heneka MT, Lütjohann D, Wunderlich P, Walter J 2010. Statins promote the degradation of extracellular amyloid {beta}-peptide by microglia via stimulation of exosome-associated insulin-degrading enzyme (IDE) secretion.J Biol Chem. 285 :37405-14.

O. Aktas, P. Küry, B. Kieseier, H. P. Hartung 2010. Fingolimod is a potential novel therapy for multiple sclerosis Nature Reviews Neurology 6: 373–382

Y. Wei, M. Yemisci, H.H. Kim, L.M. Yung, H.K. Shin, S.K. Hwang et al 2011.Fingolimod provides long-term protection in rodent models of cerebral ischemia Annals of Neurology 69: 119–129

S. Suzuki, S. Enosawa, T. Kakefuda, T. Shinomiya, M. Amari, S. Naoe et al 1996. A novel immunosuppressant, Fty720, with a unique mechanism of action, induces long-term graft acceptance in rat and dog allotransplantation 1. Transplantation 61: 200–205

Hagen N, Van Veldhoven PP, Proia RL, Park H, Merrill AH Jr, van Echten-Deckert G 2009.Subcellular origin of sphingosine 1-phosphate is essential for its toxic effect in lyase-deficient neurons. J Biol Chem 284:11346-53.

O. Cuvillier, G. Pirianov, B. Kleuser, P.G. Vanek, O.A. Coso, S. Gutkind, S. Spiegel 1996. Suppression of ceramide-mediated programmed cell death by sphingosine-1-phosphateNature, 381 : 800–803.

7. ACKNOWLEDGEMENT

It's always a mentor's job to guide their students, in the best possible way and if you are lucky one you can be blessed to have mentors who can become a part of your life. Since childhood, it was cake ride for me, with my teachers and well-wishers to always support and encourage me. A special thanks to all my teachers in school and college. I would specially like to thank Dr Rajnish Chaturvedi, under whose guidance I did my master's thesis and who made me believe in myself and introduced me to the field of Neurobiology.

I still remember my first skype talk with Prof Michela Matteoli, before joining her lab. After the talk I had no double thoughts, if given a chance to work with her I would undoubtedly be more than happy to be a part. Since landing in Milan till the date I am writing this acknowledgement it has been a pleasure to work under her. I really thank her for all her moral and emotional support during my times of need, and her encouragement and valuable discussions during the course of my PhD.

There are no words to express my gratitude for Dr. Claudia Verderio, who guided me throughout my PhD. I appreciate a lot her enthusiasm, her passion and devotion for science, her scientific aptitude and her ability to always keep encouraging and bringing out the best from her students. I thank her a lot to be there for me during times of profession and personal crises, which she use to welcome with a smile that was so comforting that for me she will always remain as a motherly figure. The efforts she put to groom me all the way till now and all the patience she kept with me I will always acknowledge. I also take opportunity to apologize for all the times I could not give my best. I wish all success to her and wish that she gets what she deserves.

I take opportunity to thank all the Lab members, without whom I surely would have had nightmares being a foreigner in this country. Since my first day in laboratory, I was so lucky to have met enthusiastic batch-mates in Guliana Fossati and Stefania Zambetti, grateful to Raffaella Morini for helping me all through the bureaucratic procedure. Working along with Elena during the first year of my PhD was a great experience, who helped me to understand the work and with the basics in the experiments. It was fun to share personal and professional experience with Ana Maria Ruiz. I am thankful to her for her guidance and all the possible help in experiments and discussions. Days spend working in Filarete were always special,, of course being near to my apartment in Milan I was always happy to work there, but more so the company of Ana, Cinzia Camoglli, Matteo, lorena and Stefania the blond one!!!! for lunch and coffee and chatting sessions in between experiments will

be always memorable. Special thanks to Matteo who helped a lot with the brain sectioning and immunostaining, it was always special to share working space with you Matteo, with all funny moments and scientific blunders we did together… :p I raise a toast of RUM!!!! But I really appreciate you as a crazy person who is motivated to make any impossible thing happen. I miss not meeting you often, but at same time I wish you all success in life. Big thanks to Cinzia for always being there to organise and making it easy to work in Filarete, and helping through dissections and some of the experiments.

There are no words to thank the support from Verderio's Lab members. It is always a relief to have lab members who are understanding and willing to help personally and professionally. I would appreciate Martina Gabrilla for her willingness to take care of Patients sample in my absence and would like to apologize for moments of arguments (thought only 2 :p) but it was always fun to exchange our cultural background, your disliking for my Bollywood music… and our endless relationship talks!!!!

Special thanks to Loredana for taking care of all the orders and rescuing me from Evelena :p and all her assistance being the most senior most member of the group. It was always nice to get expert advice from Ilaria Prada and to share the mantra of life. I really appreciate your encouragement to push me to speak in Italian… I day will come when I will speak Ila ;). I would like to further thank Marta for taking care of the animal colony in my absence. Martina, the student assisting me with the experiments, I would like to thank her for her valuable help for immunostaining and organising for experiments along with helping in all possible assistance in preparation of medium, coated flasks and petri. I further thank her for bearing with me when I use to be short tempered.

A special thanks to all the lab members of Michela's group: Elezabeta, Irene, Flavia, Elisa, Lucrezia, Stefania, Guliana, Davide, Romana, for being there for discussions in the lab meeting and giving there critical comments and suggestions. I am in debt to Elezabetta who personally help me when I was ill and encouraged me. I would further like to thank Sonia who helped in performing Elisa and gave her valuable suggestions in animal experiments conducted with transgenic mice for AD.

I would like to thank all the people in Roberto Furlan's lab who helped us with the Patient CSF analysis and providing us with the significant data. A special thanks to Annamaria who always is kind to organise the availability of CSF samples. Special thanks to Roberta Gidhoni for the analysis of

Mass Spectrometry and Annamaria Rosa for lending us spetroflorimeter to do thioflavin assay. The behaviour test was done in co-laboration with Prof. Mariavina Sala and I would like to thank Andria for his help to perform the experiments.

Lastly I would like to thank Stefania, who always helped me through the procedures of University from time of enrolment till the time I will submit my thesis…. ☺ it is always refreshing to talk to you be it related to experiments or personal life… I will rember the small Pooja ;) will miss you dear!

I am very grateful to know in person Fabia, who is an amazing person, always there to help, even when I was ill or any other personal problems she has always been the first person who came out of comfort zone and helped me to make my life smooth and beautiful. I always wish her the best in all aspects of her life,, and am grateful to have found a friend like her,, no matter where I will be in future I will always try to be in touch with you,,,, a lot of kissesss and huggss!!!! Thanks to your family for the wonderful dinner I shared with them.

Finally… Dannnii…. Danialla how can I forget you…. Ohhh grl I so miss you!!! But at same time happy for you that you are doing great and living up to your dreams… the times me you Martina, Matteo spent together will always remain as beautiful memories. Thanks for being there.

Having said about Milan, life is just incomplete without mentioning my Indian friends and flatmates. I was blessed to have such wonderful friends cum family…a mini India in Milan and I never thought I will follow the rituals and celebrations in the same way as we do in India. Special thanks to Ajay Vikram Singh who helped me settle in the initial days along with his motivational talks. I am thankful to the support and care provided by Rashmi, Sheetal, Sonia, Rama, Jaya and Shruti. I would like to thank Madhu, Ajay for scientific discussion. Will always remember the talks shared over cup of tea with Vimal and Dinesh. The person whom I would will always remember for being there for me in the department, with whom I could open my heart and talk endless…Vijay it was amazing to know you.I wish you all the success in life. The refreshing talks with Pawan, Pallavi, Sonu, Prem, Miland, Rama, Prasitha, Raj, Yatish, Vivek, Ashish, Amit during the Indian parties, always will be cherished.
I will miss a lot the times spent with Neethu, with whom I spend some of the memorable days in the residence. Talking about residence always gives good feelings, as even in Milan because of all the Indians it always felt we are in India,, the endless cooking, the Friday and Saturday

nights….sometimes extending to Sundays…and then hangover till the nextweek end!!! Debolina, Riti, Ganesh, Arun, Vivek, Rohan, Guru, Gopi.. it was amazing the times we spend and I am glad to have met people like you all,, hopefully till I am in Milan, I will always love to be “MOM” to all :p. Thanks Riti Ganesh and Rashmi for being there to support me when I was ill it means a lot.

I feel short of words to thank you Ramveer, though it’s not a long time that we are friends, but I feel lucky to have met you and must say influenced by you,, you are an amazing person. Sometimes life bring you in a situation where you no more can think for yourself, no matter you know how much important it is to be strong and believe in yourself,,,,,,,.I am really thankful to you and owe you a lot for helping me through the crucial times while I was writing my thesis. I was blessed to have you around, to motivate me and take care of me. I wish that you get all happiness and care along with a very successful life,, best wishes for your future endure.

Though we keep on getting older and older but the kid inside us always gives us the energy to live every moment of life. As life becomes more and more complicated not all are able to keep this kid alive, but I was blessed to have Prakhar, with whom my life became so much worth to live… I have no complains if I groomed with you. I am happy the changes you brought in me, as I leant that life is not to regret for..but to let go yourself free and feel every moment of it. You mean happiness to me..,, and I am thankfull to you for always being there for me in my hour of need, in my crises,,to listen to all my problems,,, to critically put you view point, which offends me but at same time I respect it. I have no words to express my gratitude for your parents, who are always there with endless love, care and affection. It feels blessed when people around you make you feel that you are an important part in their lives. Thanks for everything.. I love u ☺

Mommaaa,, Dadyyyy..Nids and Saku.. I consider myself the luckiest person having you all in my life.. The every day I spend here in Milan, every single day moma you made it special with your messages, I have no words to express how much happiness and relief it gives I read them. I am so proud of you mom k aapne koi chez nai chode jis se aap mujh se touch me reh sako….and moma mafi un sab time ke liye jab main aapko reply nai kar paya..but aap mere bahut badi strength ho… jab main bimar bhi huva tab bhi aap hanesha mujhe feel karaya main fit hoon and kush rahoon…aapke jaisa to nai ban sakta but ma I promise main hamesha khush rahunga aapko…I miss you so so so so much…. Jaldi se run run karke ek baar aap bhi milan aajao fir bahut sari masti karenge… ☺:* bahut sari kissiii….yaar but u know ma jab main thesis likhing… aapke stickers in FB yaar maza aajata tha.. kaha se lato ho…bilkul aapke jaise they are so fuuny and made me so happy…Thanks for everything moma..and I love u the most,,,what all I am today Is bcz of your and dad support encouragement and strictness

I pray to god to bless you will good health and at same time I wish to spend some more time with you…jaha main aapke moma banu :p. Papa…you are the best hanesha kuch rahte ho and always gave me stranght and courage.. aapne hum sab ko hamesha support kiya to do what all we wanted to,,,really I respect all you did for us…and hope we will never let you down ..love you dad!!!!

Bhai chillar party,,, kya bolu ab if I will write emotional tum log hasoge,, but yaar staying here alone the small small things you guys did for me meant a lot to me,,, my bday celebration,, sending gifts for me,, mere bakvas sunna and being there for all times I was feeling down… love you behno….and yaar it's rare to have younger sisters you actually make you as feel the youngest one,,,with all pampering and troubleshoot that you guys do!!! May god give you both what u deserve.. Lastly I would thank all my relatives and friends who were always in touch and I thank to all the people who helped me or their gesture made my life beautiful. ☺

A note of thanks to all…….

There are times in life, we take a step back,
Laden in the memories of past, we recollect,
Words sometimes become short to express,
Things that mark the meaning of our present.

How much I am in-depth, is not my concern,
As nothing can pay back the emotions,
What I believe, I could demand nothing more,
For God has already blessed me with all!!!!!

Someday more wiser I may become,
To realize how much I may be wrong,
For the judgements made by me,
I apologise for not carrying my best.

In the cascade sometimes important it becomes
To realize who stood by in your need,
To acknowledge of course I will,
The people who accepted me with all my greed!!!

Life keeps on going and it never ends,
With few chances to look back and recollect,
Moments that mark the meaning of present,
I owe you all for bringing me through this.

-----POOJA JOSHI, 12th Dec 2013

8. ABBREVIATIONS

1. AD: Alzhheimer's Disease
2. Aβ: Amyloid beta
3. MVs: Microvesicles
4. CAA: Congophilic amyloid angiopathy
5. ER: Endoplasmic Reticulum
6. APP: Amyloid precursor protein
7. BACE-1: β-site APP-cleaving enzyme
8. CTF: C-terminal APP fragment
9. APH-1: Anterior pharynx-defective phenotype 1
10. PEN-2: PS-enhancer 2
11. AICD: APP intracellular domain
12. GAGs: Glycosaminoglycans
13. apoE : apolipoprotein E
14. SAP : Serum amyloid P
15. IFN : Interferon
16. MHC : Major histocompatibility complex,
17. TNF-α : Tumor necrosis factor-α
18. MVBs : Multivesicular bodies
19. ESCRT: Endosomal sorting complex required for transport
20. CHMPs : Charged multivesicular body proteins
21. IL-1β: Interleukin-1β
22. IL-6: Inteleukin-6
23. CNS: Central nervous system
24. mEPSC: Miniature excitatory post-synaptic current
25. CSF: Cerebrospinal fluid
26. MCI: Mild cognitive impairment

27. BBB: blood−brain barrier
28. BDNF: Brain-derieved neutotrophic factor
29. MWM: Morris water maze
30. DMSO: dimethyl sulfoxide
31. HFP: hexafluoroisopropanol
32. ThT: Thioflavin-T
33. PI : propidium iodide
34. TBST: tris buffered saline with tween-20
35. CHCA: α-cyano-4-hydroxy cinnamic acid
36. SSc: side-scatter
37. EM: Electron microscopy
38. HC: healthy controls

Cell Death and Differentiation (2013), 1–12

www.nature.com/cdd

Microglia convert aggregated amyloid-β into neurotoxic forms through the shedding of microvesicles

P Joshi[1,2], E Turola[1,2], A Ruiz[1], A Bergami[3], DD Libera[3], L Benussi[4], P Giussani[1], G Magnani[3], G Comi[3], G Legname[5], R Ghidoni[4], R Furlan[3], M Matteoli*[,1,6,7] and C Verderio*[,2,3,4,5,6,7]

Alzheimer's disease (AD) is characterized by extracellular amyloid-β (Aβ) deposition, which activates microglia, induces neuroinflammation and drives neurodegeneration. Recent evidence indicates that soluble pre-fibrillar Aβ species, rather than insoluble fibrils, are the most toxic forms of Aβ. Preventing soluble Aβ formation represents, therefore, a major goal in AD. We investigated whether microvesicles (MVs) released extracellularly by reactive microglia may contribute to AD degeneration. We found that production of myeloid MVs, likely of microglial origin, is strikingly high in AD patients and in subjects with mild cognitive impairment and that AD MVs are toxic for cultured neurons. The mechanism responsible for MV neurotoxicity was defined *in vitro* using MVs produced by primary microglia. We demonstrated that neurotoxicity of MVs results from (i) the capability of MV lipids to promote formation of soluble Aβ species from extracellular insoluble aggregates and (ii) from the presence of neurotoxic Aβ forms trafficked to MVs after Aβ internalization into microglia. MV neurotoxicity was neutralized by the Aβ-interacting protein PrP and anti-Aβ antibodies, which prevented binding to neurons of neurotoxic soluble Aβ species. This study identifies microglia-derived MVs as a novel mechanism by which microglia participate in AD degeneration, and suggest new therapeutic strategies for the treatment of the disease.
Cell Death and Differentiation (2013) **0**, 000–000. doi:10.1038/cdd.2013.180

Alzheimer's disease (AD) is the major cause of dementia in humans. Neuronal loss and cognitive decline occurring in AD patients are traditionally linked to the accumulation in the brain of extracellular plaques consisting of short amyloid-β (Aβ) peptides of 39–42 amino acids, generated by amyloidogenic cleavage of the amyloid precursor protein.[1] Among Aβ peptides, Aβ 1–42 and pyroglutamate-modified Aβ very rapidly aggregate and initiate the complex multistep process that leads to mature fibrils and plaque.[2,3]

Although association of amyloid plaques with AD has long been assumed, Aβ load does not correlate with neuronal loss[4,5] and high plaque burden does not necessarily lead to dementia in humans.[6,7] Accordingly, recent evidence clearly showed that the amyloid load reaches a plateau early after the onset of clinical symptoms in AD patients[8] and does not substantially increase in size during clinical progression.[9] These observations agree with the current view that small, soluble pre-fibrillar Aβ species, rather than plaques formed by insoluble Aβ fibrils, are the most toxic forms of Aβ.[10] These cause synaptic dysfunction and spine loss, and correlate most closely with the severity of human AD.[5,8,11] Recent biochemical studies indicated that natural sphingolipids and gangliosides, whose metabolism has been shown to be altered in AD patients,[12] destabilize and rapidly resolubilize long Aβ fibrils to neurotoxic species.[13] These studies also showed that phospholipids stabilize toxic oligomers from monomeric peptides.[14]

The toxicity of small soluble Aβ species has been proposed to depend on the interaction with specific neuronal proteins, such as the NMDA receptor[15] or the prion protein (PrP^C),[16] which modulates NMDA receptors through Fyn kinase.[17] Alternatively, soluble Aβ oligomers may damage neurons by binding to multiple membrane components, including lipids, thereby changing membrane permeability and causing calcium ion leakage into the cell.[5,18]

Neuroinflammation arguably has a role in promoting neurotoxicity of Aβ plaques. This is suggested by several lines of evidence: (i) subjects with high plaque burden without dementia show virtually no evidence of neuroinflammation;[6] (ii) recent PET studies[19,20] showed an inverse correlation between the cognitive status and activation of microglia, the immune cells of the nervous system, in AD patients;

Q1 [1]Department of Biotechnology and Translational Medicine, University of Milano, via Vanvitelli 32, Milano 20129, Italy; [2]CNR Institute of Neuroscience, via Vanvitelli 32, Milano 20129, Italy; [3]INSPE, Division of Neuroscience, San Raffaele Scientific Institute, via Olgettina 60, Milano 20132, Italy; [4]Proteomics Unit, IRCCS Istituto centro San Giovanni di Dio Fatebenefratelli, via Pilastroni, Brescia 4 25125, Italy; [5]SISSA, Department of Neuroscience, Via Bonomea 265, Trieste I-34136, Italy and [6]IRCCS Humanitas,via Manzoni 56, Rozzano 20089, Italy

Q2 *Corresponding authors: M Matteoli, Department of Biotechnology and Translational Medicine, Via Vanvitelli 32, Milano 20129, Italy. E-mail: michela.matteoli@unimi.it or C Verderio, CNR Institute of Neuroscience, Via Vanvitelli 32, Milano 20129, Italy.Tel: +00390250317098; E-mail: c.verderio@in.cnr.it
[7]Joint senior authors.

Q3 **Keywords:** microglia; extracellular microvesicles; ectosomes; neurodegeneration; Abeta 1–42; prion protein; bioactive lipids; Alzheimer's disease

Abbreviations: EMVs, extracellular membrane microvesicles; MVs, microvesicles; AA-MVs, acutely added MVs; Aβ, amyloid-β; AD, Alzheimer's disease; MCI, mild cognitive impairment; PrP^c, prion protein; CSF, cerebrospinal fluid; PI, propidium iodide; KRH, Krebs–Ringer solution; ThT, thioflavin-T

Received 18.6.13; revised 15.10.13; accepted 30.10.13; Edited by L Greene

(iii) activation of microglia increases linearly throughout the disease course and correlates with AD neurodegeneration.[8] Moreover, recent studies demonstrating that variants of TREM2 and CD33, two receptors expressed in microglial cells, increase the risk for late-onset AD[21,22] have refocused the spotlight on microglia as a major contributing factor in AD. Although multiple preclinical evidence indicates that microglia activation promotes neuronal dysfunction and neuron elimination[23,24] and accelerates AD progression,[19,25,26] the molecular mechanisms by which microglia exert neurotoxicity remain largely unknown.

We have recently described a novel mechanism of cell-to-cell communication in the brain, by which reactive microglia propagate an inflammatory signal through the release of extracellular membrane microvesicles (EMVs), which bud from the cell surface, called shed microvesicles (MVs) or ectosomes. MVs are shed by microglia upon ATP activation[27] and originate from lipid rafts,[28] where the ATP receptor $P2X_7$ is localized.[29] Shed MVs selectively accumulate various cellular components, including soluble and integral proteins, lipids and nucleic acids and their composition reflects the activation state of donor microglia. Notably, microglia-derived MVs in the cerebrospinal fluid (CSF) have been recently identified as a novel biomarker of brain inflammation in humans.[30,31]

The observation that typical proteins of EMVs, like flotilin, accumulate in the plaques of AD brain,[32] together with evidence that activated microglia constantly surround amyloid deposits,[33] prompted us to investigate whether EMVs may be involved in the spatiotemporal propagation of Aβ pathology through the brain. Here we show that production of MVs is extremely high in patients with AD and that microglial MVs, either shed *in vitro* or isolated from the CSF of AD patients, promote generation of soluble neurotoxic Aβ species, thereby acting as potent drivers of neuronal damage.

Results

The combination of Aβ 1–42 and microglia-derived MVs is neurotoxic *in vitro*. The evidence that natural lipids may shift the equilibrium between insoluble and soluble Aβ toward highly toxic soluble species[13,34] prompted us to test whether MVs shed from microglial cells may promote Aβ neurotoxicity. Aβ 1–42 (4 μM) dissolved in dimethyl sulfoxide (DMSO) was incubated overnight with MVs derived from rat primary microglia (1 μg/100 μl) at 37 °C in neuronal medium and subsequently exposed to cultured hippocampal neurons for 1 h. Overnight pre-incubation of Aβ 1–42 with MVs yielded a neurotoxic mixture that significantly increased the percentage of dead neurons, as assessed 24 h later by propidium iodide (PI) and calcein staining (Figures 1a and b; number of experiments = 4). Notably, neither MVs alone nor MVs incubated overnight with scrambled Aβ 1–42 significantly affected neuronal survival (Figure 1b). Aβ 1–42 alone, dissolved in DMSO and incubated overnight at 37 °C in neuronal medium in the absence of MVs, from now on called aggregated Aβ 1–42 barely affected neuronal viability, even when supplemented with MVs just before neuron challenge (acutely added MVs, AA-MVs- Figure 1b). Collectively, these findings indicate that overnight pre-incubation of aggregated Aβ 1–42 with MVs is required for the development of neurotoxicity. Aβ 1–42 pre-incubated with MVs induced cell death very rapidly. One hour after exposure to Aβ 1–42 pre-incubated with MVs, about 15–30% of neurons loaded with the calcium dye Fura-2 displayed an abnormally high level of cytosolic calcium (Figures 1b and c; $n = 10$) and were positive for the early apoptotic marker annexin-V (Figure 1e; $n = 6$). MVs alone, pre-incubated overnight in neuronal medium, also induced a slight increase in intracellular calcium concentrations (Figure 1d). Immunofluorescence analysis with the neuronal marker β-3 tubulin and the pre- and post-synaptic markers V-Glut-1 and PSD-95 revealed that processes of neurons treated with combined Aβ 1–42 and MVs were fragmented and showed reduced synaptic density (Figures 1f and g). Dendrite damage was associated to a marked decrease of MAP-2 immunoreactivity (Figure 3f). The toxic effect of Aβ 1–42 in combination with MVs was largely prevented when neurons were exposed to the mixture in the presence of the glutamate receptors antagonists APV (100 μM) and CNQX (20 μM), as evaluated by quantification of cytoplasmic calcium ($n = 4$), annexin-V ($n = 2$) or PI/calcein ($n = 2$) staining (Figures 1h–j). This suggests excitotoxic damage as the cause of neuronal death.

Shed MVs promote formation of soluble forms of Aβ 1–42. Aβ 1–42 pre-incubated overnight with MVs was partitioned into two phases by centrifugation for 30 min at 10 000 × *g*. The neurotoxicity of the two fractions was analyzed by monitoring cytosolic calcium in cultured neurons. Whereas the supernatant retained a high degree of toxicity, the pellet was largely inert (Figure 2a left; $n = 3$). Similar results were obtained by quantification of dead neurons by PI/calcein assay (Figure 2a right; $n = 3$). This suggested that soluble molecules, not associated to MVs, either generated from Aβ 1–42 synthetic peptides or deriving from MVs were mainly responsible for toxicity.

The inflammatory mediators IL-1β and TNFα are among the molecules contained in microglial MVs that, through potentiation of NMDA channel activity, may induce excitoxicity.[27,35] As IL-1β and TNFα expression is upregulated in M1 proinflammatory microglia, and downregulated in M2 anti-inflammatory cells, we analyzed neuron viability after exposure to Aβ 1–42 incubated with MVs produced by either LPS-primed M1 microglia or M2 cells, polarized with IL-4. Similar alterations of cytoplasmic calcium were observed in neurons exposed to Aβ 1–42 in combination with MVs derived from M1 or M2 microglia (Figure 2b; $n = 3$) or exposed to the neurotoxic mixture in the presence of IL-1β- and TNFα-neutralizing antibodies (Figure 2c; $n = 4$). These data rule out the possibility that excitotoxicity of Aβ 1–42 in combination with MVs depends on cytokine leakage from MVs.

We then investigated whether neurotoxicity of Aβ 1–42/MVs mixture could be due to the presence of neurotoxic soluble Aβ forms. Negative staining electron microscopic analysis revealed the presence of both globular structures of diameter between 4 and 8 and 5–8 nm wide Aβ fibrils in samples of aggregated Aβ 1–42 incubated overnight with MVs. After fractionation into two phases by centrifugation, fibrils were retrieved in the pellet (Supplementary Figure S1A), whereas globular structures were mostly observed in the

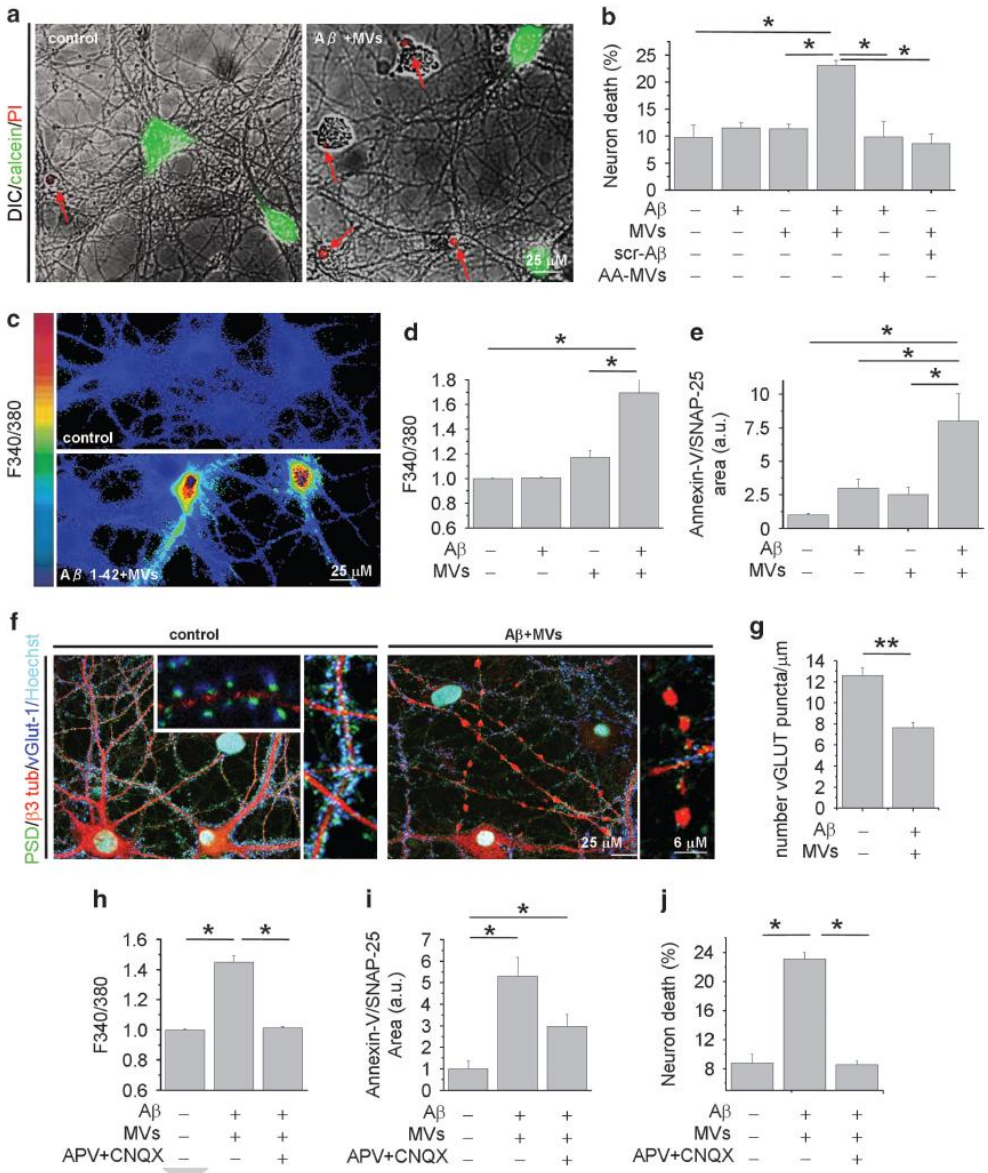

Figure 1 Microglia-derived MVs promote Aβ neurotoxicity. Fourteen DIV hippocampal neurons were exposed for 1 h to Aβ 1–42 or scrambled Aβ 1–42 (4 μM) pre-incubated with MVs (1 μg/100 μl) overnight in neuronal medium. (**a**) Overlays of DIC and fluorescence microscopic images of neurons stained for calcein and propidium iodide (PI), after 24 h exposure to Aβ 1–42/MVs mixture or under control conditions. (**b**) Percentage of calcein − /PI + neurons (dead cells) in cultures exposed to Aβ 1–42, scrambled Aβ 1–42, MVs or Aβ 1–42/scrambled Aβ 1–42 incubated overnight with MVs. AA-MVs refer to freshly isolated MVs added to Aβ 1–42, just before neuron challenge (the Kruskal–Wallis ANOVA, $P<0.001$; Dunn's test for comparison among groups, $^*P<0.05$). (**c**) Basal $[Ca^{2+}]_i$ was measured in single neurons loaded with the ratiometric calcium dye Fura-2 and expressed as F340/380 fluorescence. Representative pseudocolor images of 9DIV control neurons and neurons treated with Aβ1–42/MVs mixture for 1 h. The color scale is shown on the left. (**d**) Quantification of basal $[Ca^{2+}]_i$ in neurons exposed to Aβ 1–42, MVs or Aβ 1–42 in combination with MVs. At least 100 neurons/condition were examined. Values are normalized to control (the Kruskal–Wallis ANOVA, $P=0.002$; Dunn's test for comparison among groups, $^*P<0.05$). (**e**) Quantification of early apoptotic damage, revealed by Annexin-V binding, normalized to SNAP-25 immunoreactive area, in neurons treated as in **d**. (the Kruskal–Wallis ANOVA, $P=0.001$; Dunn's test for comparison among groups, $^*P<0.05$). (**f**) Confocal microscopic images of 14DIV neurons untreated or pretreated with Aβ 1–42 in combination with MVs and stained for β-3 tubulin, the vesicular glutamate transporter vGlut-1 and the postsynaptic marker PSD-95. Nuclei are stained with Hoechst. Note, fragmentation of neuronal processes and loss of excitatory synapses in neurons exposed to Aβ 1–42/ MVs mixture. Density of excitatory synaptic puncta is quantified in **g** (data follow normal distribution, Student's *t*-test, $^{**}P<0.001$). (**h–j**) Control cultures and cells treated with Aβ 1–42/MVs mixture analyzed for basal $[Ca^{2+}]_i$ (**h**, the Kruskal–Wallis ANOVA, $P=0.001$; Dunn's test for comparison among groups, $^*P<0.05$), early apoptotic damage (**i**, the Kruskal–Wallis ANOVA, $P=0.001$; Dunn's test for comparison among groups, $^*P<0.05$) and calcein/PI staining (**j**, the Kruskal–Wallis ANOVA $P<0.001$; Dunn's test for comparison among groups, $^*P<0.05$), either in the presence or in the absence of the glutamate receptor antagonists APV and CNQX

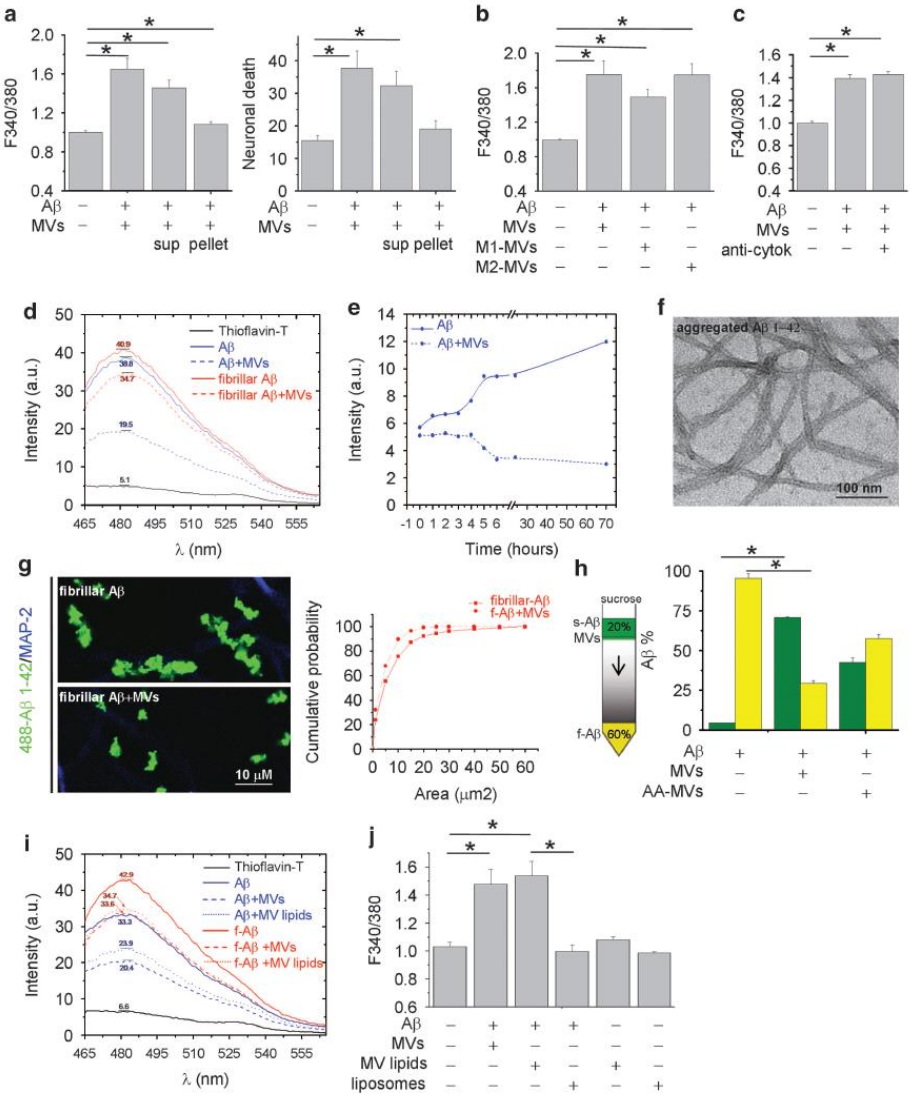

Figure 2 Shed MVs promote formation of soluble forms of Aβ 1–42. (**a**) Basal $[Ca^{2+}]_i$ in neurons exposed for 1 h either to Aβ 1–42/MVs mixture or soluble (sup)/insoluble (pellet) fractions (left panel, the Kruskal–Wallis ANOVA, $P<0.001$; Dunn's test for comparison among groups, $^*P<0.05$). Values are normalized to control. Right panel shows the percentage of calcein −/PI+ neurons under the same conditions (the Kruskal–Wallis ANOVA, $P=0.002$; Dunn's test for comparison among groups, $^*P<0.05$). (**b**) Basal $[Ca^{2+}]_i$ in neurons exposed for 1 h to MVs derived from resting, M1 or M2 microglia pre-incubated with extracellular Aβ 1–42. Values are normalized to control (the Kruskal–Wallis ANOVA, $P<0.001$; Dunn's test for comparison among groups, $^*P<0.05$). (**c**) Basal $[Ca^{2+}]_i$ in neurons exposed to Aβ 1–42 and/or MVs in the presence or in the absence of neutralizing antibodies for IL-1β and TNFα. Values are normalized to control. (**d**) Representative ThT fluorescence emission spectra of samples containing Aβ1–42 fibrils (dashed red lines) or aggregated Aβ 1–42 (dashed blue lines) exposed to MVs. (**e**) Time course of fibrilization of Aβ 1–42 in the presence (dashed line) or in the absence (solid line) of MVs. (**f**) Negative staining electron microscopic image of aggregated Aβ 1–42, incubated ovemight in neuronal medium. (**g**) Representative confocal images of Hylite-488-Aβ 1–42–488-Aβ 1–42) fibrils untreated or treated overnight with MVs and exposed for 1 h to neurons. Neurons are stained in blue for MAP-2 after fixation. Cumulative distribution of fibril size from control (solid line) and MV-treated (dashed line) 488-Aβ 1–42 fibril preparations is shown on the right. (**h**) 'Floating assay' by ultracentrifugation reveals an increase of soluble Aβ 1–42 species in association with MVs. After centrifugation for 1 h at 150 000 × *g*, MVs are expected in the top fraction, whereas Aβ 1–42 aggregates are expected in the pellet. As ELISA indicates, a higher fraction of Aβ 1–42 species is transported from the bottom to the top of the gradient in samples incubated overnight with MVs. Acute addition of MVs (AA-MVs) does not cause statistically significant changes in Aβ 1–42 distribution (the Kruskal–Wallis ANOVA, $P<0.001$; Tukey's test for comparison among groups, $^*P<0.05$). (**i**) ThT fluorescence emission spectra of aggregated Aβ 1–42 (blue lines) or Aβ 1–42 fibrils (red lines), untreated (solid lines) or pretreated (dashed lines) with shed MVs. Spectra of aggregated Aβ 1–42 or Aβ 1–42 fibrils exposed to MVs lipids (dotted lines) are also shown. (**j**) Basal $[Ca^{2+}]_i$ of neurons exposed for 1 h to Aβ 1–42 pretreated with intact MVs, small unilamellar vesicles of MV lipids (MV lipids) or artificial liposomes. Note that vesicles made by lipids extracted from shed MVs but not artificial liposomes significantly enhance basal $[Ca^{2+}]_i$

supernatant (Supplementary Figure S1B). Detection of globular species in the soluble fraction from Aβ 1–42 and MVs mixture prompted us to investigate by an array of techniques whether shed MVs change the equilibrium between soluble and insoluble Aβ 1–42.

Possible alterations in the content of aggregated Aβ 1–42 were first monitored using a thioflavin-T (ThT) dye-binding assay. By this approach, we found that overnight pretreatment with shed MVs caused a 21.26 ± 0.56% reduction in fibrillar Aβ 1–42 (Figure 2d, red lines; $n=3$) and a 38 ± 6.3% reduction of aggregated Aβ 1–42, dissolved in DMSO and incubated overnight at 37 °C in neuronal medium (Figure 2d, blue lines; $n=4$). No changes in ThT spectra were detected upon acute MV addition, thus excluding possible interference of MV lipids with the ThT-binding site of Aβ1–42 (Supplementary Figure S2). Time course analysis of aggregated Aβ 1–42 (Figure 2f) confirmed that shed MVs induce aggregate solubilization (Figure 2e). Consistent with these data, confocal microscopy using fluorescently labeled Aβ 1–42 fibrils showed that MVs reduce fibril size (Figure 2g), as indicated by the shift of fluorescent fibrils toward smaller size in the cumulative distribution (Figure 2g, right $n=3$). Altogether, these observations indicate that aggregated Aβ 1–42 disassembles into soluble species upon MV exposure.

To prove the capability of shed MVs to promote formation of soluble species, soluble amyloid forms generated in Aβ 1–42/MVs mixture were separated from insoluble species by sucrose gradient centrifugation at 100 000 × *g* for 1 h[13] and quantified by ELISA. While acute addition of MVs, immediately before ultracentrifugation on sucrose gradient, partially but not significantly promoted Aβ 1–42 flotation (AA-MVs, Figure 2h), a marked redistribution of Aβ 1–42 to the top of the gradient was detected upon overnight incubation with MVs (Figure 2h; $n=3$).

MV lipids promote extracellular formation of neurotoxic Aβ 1–42 species. The next step was to investigate whether lipids were the active components of shed MVs, responsible for the dissolution of insoluble Aβ1–42 species. The ThT assay showed that the lipid fraction extracted from MVs reduced the amount of fibrillar (Figure 2f-Aβ, red lines) or aggregated (Aβ, blue lines) Aβ1–42, similar to intact MVs (Figure 2i). Furthermore, assessment of neuron viability revealed a similar percentage of dying neurons, characterized by abnormally high calcium levels, in cultures exposed to Aβ 1–42 in combination with intact MVs or their lipid component (MV lipids, Figure 2j, $n=3$). Notably, Aβ1–42 pre-incubated with synthetic liposomes, similar in size to MVs and mimicking the phospholipid composition of the plasma membrane (60% PC, 20% cholesterol, 10% SM and 10% PS) did not produce any increase in the basal calcium concentration (Figure 2j).

Binding of newly generated soluble Aβ 1–42–488 to neurons is competed by PrP^C. We next attempted to visualize soluble Aβ 1–42 forms, generated in the presence of MVs, by imaging their binding to cultured neurons. We observed that culture exposure to 488-Aβ 1–42/MVs mixture for 1 h produced a strong labeling of MAP-2-positive dendrites, which exceeded by almost fourfolds the staining produced by fluorescent Aβ 1–42 alone (Figures 3a and b). 488-Aβ 1–42 binding to dendrites was paralleled by a marked reduction of MAP-2 staining (Figure 3a), according to previous evidence.[36] No preferential association of 488-Aβ1–42 with synapses was detected (data not shown). Fractionation of 488-Aβ 1–42/MVs mixture into two phases by centrifugation showed that the fluorescent Aβ1–42 forms capable of binding to neurons were mainly recovered in the soluble fraction (Supplementary Figures S1C–E). Notably, Aβ binding was specifically competed by the high-affinity oligomer-interacting protein PrP^{c16} and virtually abolished by the anti-Aβ antibodies A_{11} and 6E10 (Figures 3a and b) Unlike the 89–230 truncated PrP^C, both full-length folded PrP^C and anti-Aβ Abs neutralized the toxicity of Aβ1–42/MVs mixture, as revealed by calcium recording (Figure 3c; $n=3$) and PI/calcein staining (Figure 3d; $n=3$).

Finally, as the soluble but not the fibrillar Aβ forms activate NMDA receptors[37] and our unpublished data), we used a bioassay to assess the capability of Aβ species generated in the presence of MVs to enhance NMDA receptor activity. FURA-2-loaded neurons, expressing functional NMDA receptors, were used as sensor cells for soluble Aβ 1–42. By this approach, we detected calcium responses in about 30% of neurons exposed to Aβ 1–42 in combination with MVs, but not Aβ 1–42 or shed MVs alone (Figure 3e; $n=3$). No calcium transients were observed upon neuron challenging with scrambled Aβ 1–42 and MVs (data not shown). Calcium responses evoked by Aβ 1–42 pretreated with MVs were inhibited by the NMDA receptor antagonist APV (100 μM) (Figures 3f and g; $n=3$). Direct HPLC measurements of glutamate content in MVs or Aβ 1–42/MVs preparations revealed concentrations lower than 1 μM, that is, the minimal concentration required to detect calcium influx in our system (mean glutamate concentration: 137 ± 70 nM, MVs alone; 196 ± 115 nM, Aβ 1–42/MVs mixtures). These data exclude possible interference of ambient glutamate in the NMDA-dependent calcium response. Therefore, soluble Aβ 1–42 species generated in the presence of shed MVs are able to activate NMDA calcium channels, triggering excitotoxicity.

MVs carry neurotoxic species generated from internalized Aβ 1–42. As amyloid plaques are surrounded by activated microglia that actively phagocyte and degrade Aβ, we investigated whether MVs may contain toxic Aβ species, generated from internalized peptides. Confocal analysis of microglia exposed to Aβ1–42 for 24–48 h, extensively washed and stained with 6E10 anti-Aβ antibody, revealed intracellular Aβ aggregates, which can reach the plasma membrane, stained by IB4 (Figure 4a). Notably, few Aβ and IB4 double-positive particles were detected extracellularly in cell proximity (Figure 4a, bottom right panel), suggesting that EMVs derived from Aβ-loaded microglia may indeed contain Aβ species. We explored this hypothesis by western blot analysis of EMVs collected from supernatant of microglia exposed to biotynilated Aβ1–42. Upon ATP stimulation for 30 min, a condition that mimics an inflammatory context and favors shedding of MVs (P2 and P3 fraction) *versus* exosome (P4 fraction) release,[38] biotin-conjugated Aβ1–42 was recovered in shed MVs, labeled by Tsg101 (Figure 4b, bottom panel). Consistently, SELDI-TOF mass spectrometry

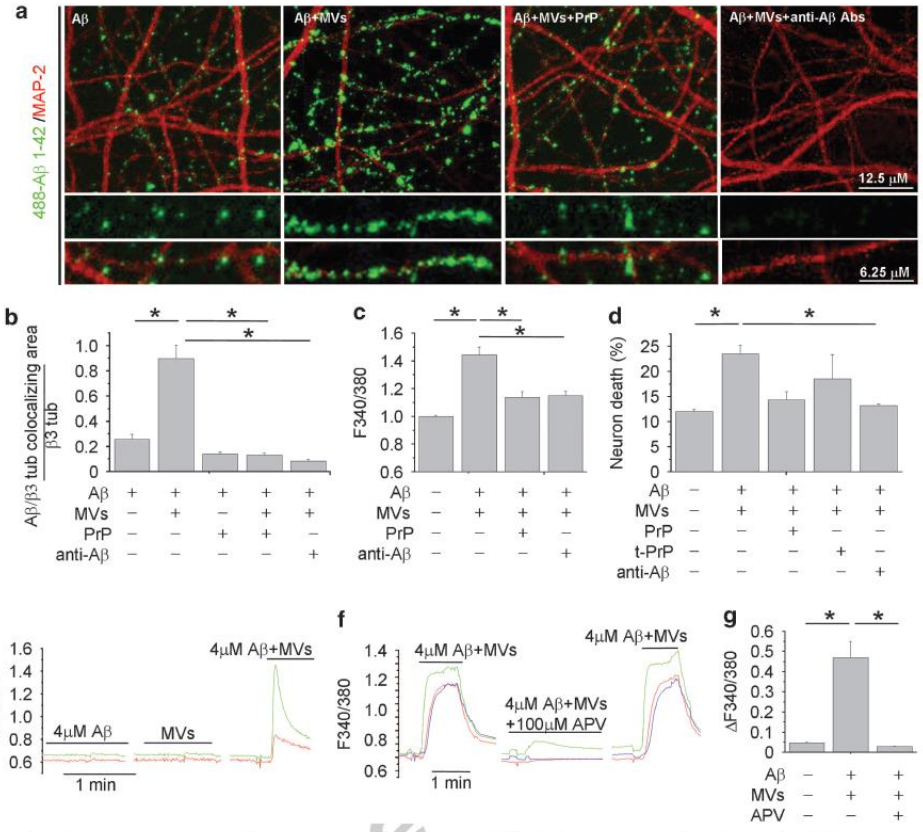

Figure 3 Binding of newly generated soluble 488-Aβ-1–42 to neurons is competed by PrP^C. (**a**) Representative confocal images of 14DIV neurons exposed to 488-Aβ 1–42 alone or in combination with MVs, with or without pretreatment with PrP or with the anti-Aβ antibodies A11 and 6E10. (**b**) Corresponding quantification of 488-Aβ 1–42 binding to cultured neurons expressed as colocalizing area between 488-Aβ and β tubulin, relative to total β tubulin (see Materials and Methods) (the Kruskal–Wallis ANOVA, $P<0.001$; Dunn's test comparison among groups, $^*P<0.05$). (**c** and **d**) Basal $[Ca^{2+}]_i$ (**c**) and percentage of calcein − /PI + neurons (**d**) in 9–14 DIV cultures exposed to different combinations of Aβ 1–42, MVs, A11 plus 6E10 antibodies, full-length or truncated ($tPrP^C$) PrP^C (the Kruskal–Wallis ANOVA, $P<0.001$; Dunn's test for comparison among groups, $^*P<0.05$). (**e**–**g**) Bio-detection of soluble Aβ 1–42 by fura-2-loaded sensor neurons, expressing functional NMDA receptors. Representative traces of $[Ca^{2+}]_i$ changes recorded in neurons upon exposure to KRH containing Aβ 1–42 alone (4 μM) or MVs alone (1 μg/100 μl) or their combination (**e**). $[Ca^{2+}]_i$ responses induced by Aβ 1–42/MVs mixture are strongly inhibited by the NMDA receptor antagonist APV (**f**), as quantified in **g**. Values represent peak $[Ca^{2+}]_i$ increases (ΔF340/380 fluorescence) from about 30 neurons/condition (the Kruskal–Wallis ANOVA, $P<0.001$; Dunn's test for comparison among groups, $^*P<0.05$)

using 6E10 and 4G8 anti-Aβ antibodies revealed the presence of preloaded Aβ1–42 and of its cleavage product Aβ1–40, along with traces of other carboxy-terminally truncated isoforms, in MVs shed from the plasma membrane (P2 + P3 fractions) (Figure 4c). Ten times less Aβ was recovered in exosomes (P4 fraction) (Figure 4c), although Aβ1–42 species were clearly detectable in exosomes constitutively accumulated for 24 h in microglia supernatant (Supplementary Figure S3). In line with the presence of Aβ species, MVs derived from microglia stimulated for 48 h with 4 μM Aβ 1–42 (Aβ-MVs) were highly neurotoxic as compared with MVs derived from resting cells (Figure 4d, $n=4$). MV neurotoxicity was significantly decreased by anti-Aβ antibodies. These data indicate that microglia internalize and generate Aβ neurotoxic species, which are delivered to neurons in association with MVs, possibly on MV external membrane.

MVs from AD patients are neurotoxic. Recent results from our laboratories indicated that microglia-derived MVs are detectable in the CSF of humans and that their amount reflects the extent of microglia activation in the course of neuroinflammation.[30] To verify whether production of MVs from microglia could be elevated in AD, we collected CSF from patients with mild cognitive impairment (MCI) or AD, as well as from age- and gender-matched healthy donors. Flow cytometry analysis showed strikingly higher levels of MVs positive for the myeloid marker IB4 (more than 10-fold) in MCI and AD patients than in control subjects (Figure 5a). IB4-positive MVs accounted for ~65% of total EMVs detectable by flow cytometry. The number of IB4-positive MVs is correlated with a known CSF marker of neurodegeneration, namely, total Tau protein (Figure 5b; $P<0.0001$).[39] We next examined the effects of MVs collected from AD patients on the equilibrium between soluble and insoluble Aβ

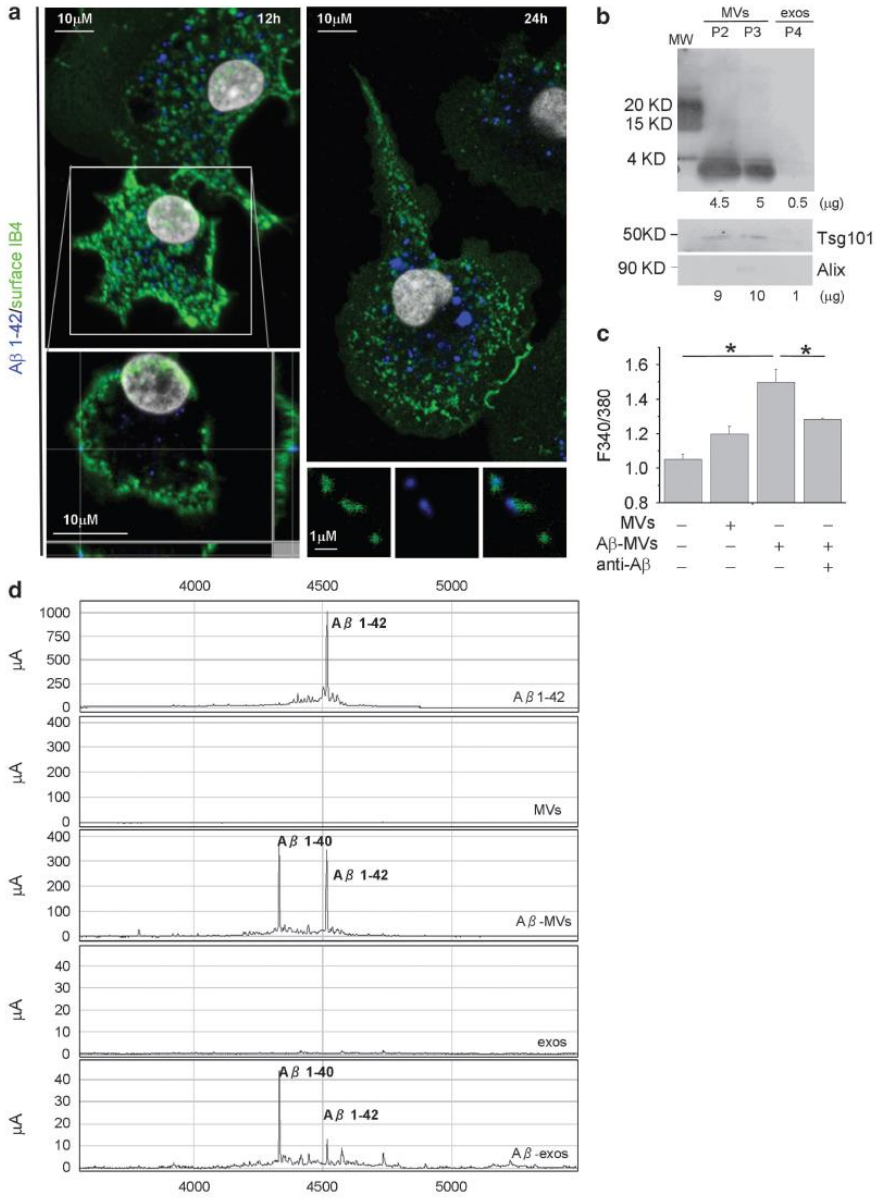

Figure 4 Soluble Aβ forms are released in association with shed MVs from microglia activated with Aβ 1–42. (**a**) Living rat microglia were exposed to human Aβ 1–42 for 12–48 h and stained with IB4-FITC to label the cell surface before being fixed and counterstained with 6E10 antibody, which recognizes human but not rat amyloids. Top left panel shows representative *xy* plane maximum projection of microglia, revealing several 6E10 immunoreactive puncta inside the cells, some of which are double positive for surface IB4-FITC. Bottom left panel showing single stack of the selected cell, shown at higher magnification, reveals a clear association of internalized Aβ 1–42 to the cell surface, further revealed by the *z* axis scan. Note, an increase in the size of internalized Aβ 1–42 after incubation for 48 h (top right panel). Examples of EMVs, double positive for 6E10 and IB4-FITC are shown in bottom right panels. (**b**) Western blot analysis of Aβ 1–42 species present in shed MVs (P2 and P3 fractions) and exosomes (P4 fraction) released upon 30 min ATP stimulation by 4×10^6 microglia pre-exposed to biotinylated Aβ 1–42 (4 μM). Blots were carried out using a 15% Tris-glycine gel and membranes were probed with streptavidin. Shed MVs and exosomes produced by 8×10^6 donor microglia were probed in parallel for the EMV markers Tsg101 and the exosomal marker Alix (lower panels). Numbers below each lane indicate the estimated amount of loaded proteins. (**c**) Shed MVs and exosomes produced by 1×10^6 rat microglia pre-exposed to human Aβ 1–42 were analyzed by a SELDI-TOF MS immunoproteomic assay employing anti-human Aβ antibodies (4G8 and 6E10) on PS20 chip array to capture Aβ 1–42 and carboxy-terminally truncated Aβ isoforms. The following representative spectra of samples in NP40 1% lysis buffer are shown (from top to bottom): 4 μM Aβ1–42 peptide incubated overnight in KRH; MVs from control microglia, not exposed to Aβ1–42; MVs from Aβ1–42 preloaded microglia (Aβ-MVs); exosomes from control microglia (exos); exosomes from Aβ1–42 preloaded microglia (Aβ-exos). (**d**) Basal $[Ca^{2+}]_i$ recorded from neurons exposed to MVs produced from microglia either resting or pretreated for 48 h with Aβ 1–42 (Aβ-MVs), in the presence or in the absence of anti-Aβ antibodies (A11 + 6E10) (the Kruskal–Wallis ANOVA, $P<0.001$; Dunn's test for comparison among groups, $^*P<0.05$). See also Supplementary Figure S1

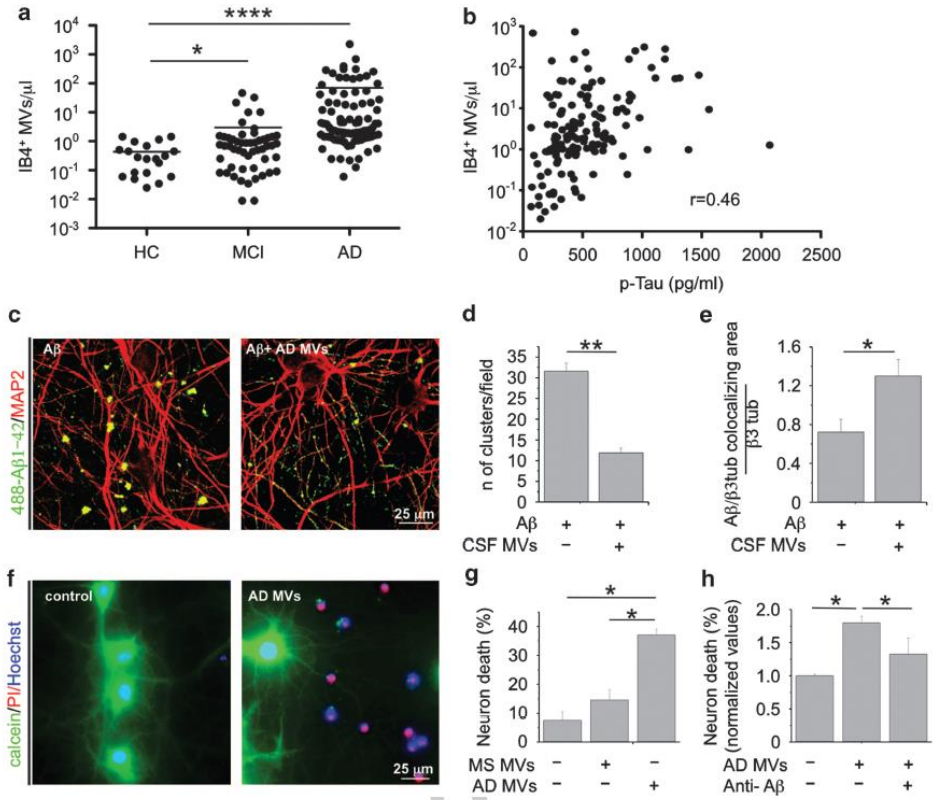

Figure 5 CSF MVs isolated from AD patients. (**a**) Quantitative flow cytometry analysis of IB4$^+$ MVs in CSF collected from MCI patients ($n=53$), AD patients ($n=89$) and age- and gender-matched controls (HC; $n=20$) (the Mann–Whitney test, $P<0.0001$ AD *versus* HC; $P<0.0329$ MCI *versus* HC). (**b**) Correlation between IB4$^+$ MVs and total tau protein in the CSF of MCI and AD patients, (rho $=0.46$, $P<0.0001$, Spearman's correlation). (**c**) Representative confocal images of cultured neurons, exposed to aggregated 488-Aβ 1–42 untreated or pretreated overnight with MVs from AD patients and stained for MAP-2 after fixation (red). Aβ species bind to MAP-2 dendrites. Note the decrease in the number of large fluorescent Aβ clusters in neurons exposed to 488-Aβ 1–42 in combination with AD MVs. (**d**) Quantification of 488-Aβ 1–42 aggregates (larger than 5 µm) per field (data follow normal distribution, Student's *t*-test, $^{**}P<0.001$). (**e**) Quantification of 488-Aβ 1–42 binding to cultured neurons, expressed as colocalizing area between 488-Aβ and β tubulin, relative to total β tubulin (see materials and Methods; data follow normal distribution, Student's *t*-test, $^{**}P<0.001$). (**f**) Representative fluorescence microscopy images of 14DIV neurons triple stained for calcein, PI and Hoechst 24 h after exposure to AD MVs or maintained in control conditions. (**g**) Quantification of the percentage of calcein −/PI + neurons (dead cells) in cultures exposed to AD MVs or MVs isolated from patients with multiple sclerosis (the Kruskal–Wallis ANOVA, $P<0.001$; Dunn's test for comparison among groups, $^{*}P<0.05$). (**h**) Percentage of dead neurons in cultures exposed to MVs isolated from the CSF of AD patients in the presence of anti-Aβ antibodies A11 and 6E10 (ANOVA, $P<0.001$, the Holm–Sidak method, $P<0.05$). See also Supplementary Figure S2 and Supplementary Table S1

1–42 species and assessed their toxic potential on cultured neurons. Confocal analysis of neurons exposed to 488-Aβ 1–42 pre-incubated overnight with AD MVs revealed a threefold decrease in the content of fluorescent Aβ aggregates (Figures 5c and d) and a parallel increase in fluorescent Aβ species bound to dendrites (Figures 5c and e).

Consistently, with *in vitro* results showing that microglial MVs carry neurotoxic species generated from internalized Aβ 1–42, MVs recovered from AD patients were highly toxic, as indicated by quantification of calcein − /PI + dead neurons, as compared with MVs isolated from patients with multiple sclerosis (Figures 5f and g, $n=3$). Neurotoxicity of AD MVs was significantly decreased by pretreatment with anti-Aβ antibodies (Figure 5h). Interestingly, Aβ 1–40, Aβ 1–42 and other truncated Aβ peptides were detected by SELDI-TOF mass spectrometry in CSF MVs of a patient affected by AD (Supplementary Figure S4).

Discussion

In the present study, we unveil a novel mechanism by which microglia contribute to neuronal damage in AD. We show that MVs, extracellularly released by cultured microglia, strongly increase Aβ neurotoxicity *in vitro*. This effect is due to the lipid components of MVs, which promote formation of small soluble neurotoxic species from Aβ 1–42 extracellular aggregates. Although Aβ species can associate with MVs, as suggested by increased Aβ flotation on sucrose gradient upon acute addition of MVs, most of neurotoxic soluble forms do not bind to MVs strongly. This is indicated by our observations that free soluble Aβ 1–42 species, not associated with MVs, bind efficiently to a subpopulation of neurons *in vitro*, increase NMDA receptor permeability and cause an excitotoxic damage. Conversely, Aβ 1–42 forms pelleted along with

MVs from Aβ/MVs mixture display low toxicity and little neuronal-binding capacity. These data identify microglial MVs as an endogenous source of lipids able to shift the equilibrium toward toxic Aβ species. This conclusion is in complete agreement with previous evidence that brain membrane lipids, including phosho- and (glycol)sphingolipids, favor formation of soluble forms, either promoting solubilization of inert fibrils,[13] or hindering their conversion to insoluble fibrils.[14] Interestingly, exosomes released by neurons have been found to promote rather than reduce Aβ fibrillogenesis,[40] thus indicating that lipid composition of different EMVs generated by distinct cell types may have opposite effects on Aβ extracellular assembly. Notably, MVs have a distinct repertoire of lipids not only compared with exosomes (our unpublished data)[41] but also to the plasma membrane of origin. Indeed, MVs are enriched in cholesterol, sphingomyelin and ceramide, and contain lipid raft elements,[28] including GM1 and GM3 gangliosides and flotillin-2.[42] Accordingly, artificial liposomes, composed of the main phospholipids of the plasma membrane, neither induce fibril solubilization nor promote Aβ neurotoxicity. Lipidomic profiling of microglial MVs will identify endogenous lipids responsible for the generation of neurotoxic Aβ species, which could themselves represent putative AD biomarkers.[9,43,44]

MV-mediated Aβ processing, leading to neurotoxic forms does not occur only extracellularly. Indeed, microglial MVs also contain toxic forms generated from internalized Aβ 1–42. It has been previously shown that a fraction of intracellular Aβ can be released through exosomes by neurons and oligodendrocytes.[32,45–47] In addition, phagocytosed Aβ has been found to be re-secreted from microglia, although through an undefined mechanism.[48] We now show that microglia release neurotoxic Aβ 1–42 and Aβ 1–40 species in association with MVs. This is the first evidence that microglia – which control extracellular plaque load[49,50] by phagocytosis and degradation of Aβ fibrils or macropinocytosis of soluble Aβ[51,52] – may seed and feed formation of neurotoxic amyloids throughout the brain. MV-mediated release of neurotoxic Aβ forms likely occurs when intracellular pathways of Aβ degradation are saturated and production of MVs becomes a way for microglia to eliminate undigested Aβ. Neurotoxic Aβ species may be processed in early to late endosomes and lysosomes[53] after disassembly of phagocytosed Aβ and sorted to the external surface of MVs through association with the GPI-anchored protein PrP^C or GM1 gangliosides, all of which are localized to raft domains[42] and bind tightly Aβ oligomers.[54] Alternatively, neurotoxic Aβ species may be generated at the cell surface,[55] where components of the γ-secretase complex, which can cleave the carboxyl terminal of Aβ 1–42 at position 40 are also localized,[53] possibly inside lipid rafts. This sorting mechanism may be consistent with the proposed role of lipid rafts in setting up platforms to concentrate into MVs proteins destined to secretion.[28,56] Finally, processing of Aβ 1–42 to Aβ 1–40 may even proceed within MVs. Indeed, previous evidence showed that neuron-derived EMVs contain some components of the γ-secretase complex,[57] whereas the insulin-degrading enzyme, which proteolyzes Aβ 1–42 and Aβ 1–40, has been detected among cargo proteins of microglial EMVs.[58] The significant decrease in neurotoxicity observed upon pretreatment with anti-Aβ antibodies strongly supports the theory that neurotoxic Aβ forms are in fact localized to the outer lipid bilayer of MVs. However, further studies are required to unequivocally define the topology of Aβ species and to clarify whether Aβ forms are actually associated to the extracellular membrane of shed MVs.

Our findings have clear clinical implications. First, production of MVs is very high in MCI and AD patients, reflecting microgliosis,[30] which typically characterizes the disease.[8] Second, MVs collected from the CSF of AD patients promote extracellular formation of neurotoxic Aβ species similar to MVs shed from cultured cells. Finally, MVs collected from AD patients are extremely toxic for cultured neurons and their neurotoxicity results, at least in part, from their Aβ cargo. However, it is still to be defined whether MVs may associate with toxic forms of Aβ present in the parenchyma/blood vessel as well as plaques during their travel to CSF. In agreement with their pathogenic role, levels of microglia-derived MVs are positively correlated with classical biomarkers of neuronal injury such as tau[39] in MCI and AD subjects, and with damage to white matter structures of the temporal lobe in MCI patients, as revealed by MRI scans (Dalla Libera *et al.*, manuscript in preparation). Correlation between microglia-derived MVs and brain damage suggests that MVs may represent a novel companion tool for AD diagnosis, and paves the way for future therapies targeting MVs to control the impact of neurotoxic Aβ species on brain function. We anticipate that analysis of Aβ content and lipidomic profiling of MVs in a large cohort of AD and healthy subjects will clarify whether changes in the conformation and/or in the amount of Aβ forms account for MV neurotoxicity. Furthermore, lipidomic profiling of human MVs will lead to the identification of new putative AD biomarkers, thereby increasing the diagnostic potential of MVs in AD.

Materials and Methods

Glial cells and MVs isolation. Primary rat microglial cells were isolated from mixed cultures of cortical and hippocampal astrocytes, established from E21 rat embryos and maintained as described previously.[27] All efforts were made to minimize animal suffering and to reduce the number of animals used in accordance with the European Communities Council Directive of September 20, 2010 (2010/63/UE). All procedures involving animals were performed according to the guidelines of the Institutional Animal Care and Use Committee of the University of Milan.

To induce MV shedding, microglia were exposed to ATP (1 mM) for 30 min in Krebs–Ringer solution (KRH). Shed MVs were pelletted from the supernatant at 10 000 × *g* for 30 min, whereas exosomes were pelleted at 100 000 × *g* for 1 h, as described previously.[38] For biochemical fractionation of shed MVs, total lipids were extracted through the method previously described[59] with 2 : 1 (by volume) of chloroform and methanol. The lipid fraction was evaporated under a nitrogen stream, dried and resuspended in PBS at 40 °C in order to obtain multilamellar vesicles. Small unilamellar vesicles were obtained by sonicating multilamellar vesicles.

Aβ 1–42 preparations. Unless otherwise stated, Aβ 1–42 (Anaspec, Fremont, CA, USA) was dissolved at a concentration of 2 mM in DMSO. The stock was kept at − 80 °C, directly diluted to 4 μM in neuronal medium and kept overnight at 37 °C. We refer to this Aβ 1–42 preparation as aggregated Aβ 1–42, to distinguish it from fibrillar Aβ 1–42 preparation, which is detailed below. To prepare soluble and fibrillar Aβ 1–42, the peptide was initially monomerized by dissolving it in 100% hexafluoroisopropanol (Sigma, St. Louis, MO, USA) to obtain a 1-mM solution and then aliquoted in sterile microcentrifuge tubes. The hexafluoroisopropanol was removed under vacuum using a SpeedVac and the peptide film was stored (desiccated) at − 80 °C. Soluble Aβ 1–42 was prepared as described by Klein *et al.*[60]. Briefly, the peptide film was freshly resuspended in 100% DMSO to 5 mM, further diluted to 100 μM in F-12 medium

(Invitrogen, Paisley PA4 9RF, UK) and incubated for 24 h at 5 °C. Following incubation it was centrifuged at 140 000 × *g* for 10 min at 4 °C and the soluble forms were collected in the supernatant. For fibrillar Aβ 1–42 preparation, Aβ 1–42 or Hylite-488-Aβ 1–42 peptide film freshly resuspended in DMSO was further diluted to 100 μM in 10 mM HCl.[61] It was vortexed for 15 s and incubated for 24 h at 37 °C. After incubation, it was diluted to 4 μM in neuronal medium.

The aggregation state of Aβ 1–42 preparation was assessed by transmission electron microscopy with a Tecnai G2 T20 Twin microscope (FEI, Eindhoven The Netherlands).

ThT assay. Aβ preparations, incubated or not with MVs, were diluted to 4 μM in KRH and incubated overnight at 37 °C. For ThT assays, ThT (Fisher Scientific, Waltham, MA, USA) was added to the Aβ preparations and monitored in a Perkin-Elmer LS50 spectrofluorometer. ThT fluorescence emission spectra were recorded between 465 and 565 nm with 5 nm slits, using an excitation wavelength of 450 nm. For the time course experiments, the samples were kept at 37 °C and aliquots of 100 μl were removed from the sample at each time point. The aliquots were mixed with ThT to obtain a final concentration of 10 μM and then their fluorescence spectra were acquired.

Neuronal cultures and *in vitro* stimulation. Primary cultures of hippocampal neurons were established from E18 rat pups as previously described,[62], plated onto poly-L-lysine-treated coverslips at 500 cells/mm^2 cell density and maintained in Neurobasal with 2% B27 supplement and 2 mM glutamine (neuronal medium). DIV hippocampal neurons (9–14) were exposed to Aβ 1–42 (4 μM), to MVs (1 μg/100 μl) or to a combination of Aβ 1–42 and MVs for 1 h. Aβ 1–42, MVs or their combination were kept overnight at 37 C° before being exposed to neurons. Neurons (1.7×10^5) were exposed to MVs produced by 1×10^6 microglia (microglia : neuron ratio, 6 : 1).

In a set of experiments, Aβ 1–42/MVs mixtures were added with anti-TNF-α plus anti-IL-1β antibodies (R&D, Minneapolis, MN, USA) or with the anti-Aβ antibodies 6E10 (Covance, Emerville, CA, USA) plus A11 (Invitrogen, Life Technologies Ltd., Paisley, UK), or with the PrP^C (4 μM) for 30 min before being exposed to cultured neurons.

Cell viability assays

PI/calcein staining: Neuron viability was analyzed by simultaneous fluorescence staining of viable and dead cells with calcein-AM (0.5 mg/ml, Invitrogen, Life Technologies Ltd.), PI (1 μg/ml, Molecular Probes, Life Technologies Ltd., Paisley, UK) and Hoechst (8.1 μM, Molecular Probes, Life Technologies Ltd.). Incubation was performed for 20 min in neuronal medium at 37 °C and 5% CO_2. Calcein-AM emits green fluorescence signal in viable cells. Conversely, PI reaches nuclei of dead cells only where it emits red fluorescence. Fluorescence images were acquired by Leica DMI 4000B microscope, equipped with DIC microscopy. The percentage of neuronal death was calculated as the ratio of PI + calcein–dead cells to the total number of Hoechst stained neurons in at least 15 fields/condition.

Annexin-V assay: Living neurons were incubated with annexin-V-FITC (1 : 100, BD Pharmingen, Franklin Lakes, NJ, USA) for 5 min, fixed with 4% paraformaldehyde and counterstained for the neuronal marker SNAP-25 (mouse anti-SNAP-25, Sternberger Monoclonals, Baltimora, MD, USA) in nonpermeabilizing condition to preserve annexin-V staining. Fluorescence images were acquired by a SPE Leica confocal microscope, equipped with an ACS APO × 40/1.15 oil objective. Area of annexin-V + apoptotic processes was quantified by Image J 1.46r software and normalized to SNAP-25 immunoreactive area as an index of neurite density.

Monitoring of cytoplasmic calcium concentration: Hippocampal neurons were loaded with 2 μM Fura-2/AM (Invitrogen, Life Technologies Ltd.) in neuronal medium for 40 min at 37 °C, washed in KRH and transferred to the recording chamber of an inverted microscope (Axiovert 100, Zeiss) equipped with a calcium imaging unit. Polychrome V (TILL Photonics) was used as the light source. Images were collected with a CCD Imago-QE camera (TILL Photonics) and analyzed with TILLvisION 4.01 software. After excitation at 340 and 380 nm wavelengths, the emitted light was acquired at 505 nm at 1 Hz. Calcium concentration was expressed as F340/380 fluorescence ratio. The ratio values in selected region of interest corresponding to neuronal somata were calculated from sequences of images to obtain temporal analysis. Basal calcium concentration was recorded from at least 100 neurons/condition in each experiment.

Immunocytochemical staining. Immunofluorescence staining of fixed neurons was performed using the following antibodies: rabbit anti-beta tubulin (Sigma) guinea pig anti-vGLUT-1 (Synaptic System, Gottingen, Germany), mouse anti-PSD-95 (UC Davis/NIH NeuroMab Facility, CA, USA) and mouse anti-MAP-2 (Synaptic System). Secondary antibodies were conjugated with Alexa-488, Alexa-555 or Alexa-633 fluorophores (Invitrogen, Life Technologies Ltd.). For quantification of V-glut-1 puncta per length unit, the length of single neuritis was measured using Image J 1.46r software, and the number of positive puncta whose dimension was greater than 0.01 μm was quantified.

Binding to neurons of Hylite-488-labeled Aβ 1–42 (Anaspec) was quantified using Image J 1.46r software. Hylite-488-Aβ 1–42 and β tubulin double-positive puncta were revealed by generating a Hylite-488-Aβ 1–42/β tubulin double-positive image using the 'and' option of 'image calculator' function. A fixed threshold was then set in the double-positive image and, having selected the pixel area parameter at 3-infinite, total colocalizing area was quantified using the 'analyze particle' function. Total β tubulin fluorescence area was directly measured in β tubulin fluorescence images, after setting a fixed threshold using the 'analyze particle' function, as described above. Finally, total Hylite-488-Aβ 1–42/β tubulin-colocalizing area was normalized to total β tubulin area in each field. β tubulin was revealed by Alexa-633 fluorophore to avoid significant interference of Hylite-488 in the red channel. Quantification of binding was normalized to β tubulin towing to the decrease in MAP-2 immunofluorescence staining upon Aβ 1–42 binding.

Maximum projection of confocal stacks in the *x*–*y* plane and *z* axis scans were generated using Image J 1.46r software.

Confocal imaging and measurements of fluorescent fibrils. Hylite-488-Aβ 1–42 fibrils (Anaspec) were prepared as described above, overnight exposed or not to MVs and incubated for 1 h with primary cultures of hippocampal neurons. Neurons were then fixed and stained for MAP-2. Fluorescence images of Aβ 1–42 fibrils were acquired with a Leica SPE confocal microscope by an operator blinded to the study and analyzed using Image J 1.46r software. A fixed threshold was set on Hylite-488-Aβ 1–42-positive images. After selecting the area parameter (μm) at 0.1-infinite, the area of single fibrils was automatically measured using the 'analyze particle' function. The percentage of fibrils with increasing area values – at intervals of 5 μm^2 – was calculated and the cumulative distribution plot was constructed using OriginPro 8 software.

Western blotting. Lysates of shed MVs and exosomes were separated by electrophoresis, blotted on nitrocellulose membrane and revealed using streptavidin (1 : 1500, Sigma), rabbit anti-alix (1 : 1000, Covalab, Billerica, MA, USA) and mouse anti-Tsg101 (1 : 1000, Abcam, Cambridge, UK). Immunoreactive bands were detected using SuperSignal West Femto Pierce ECL (Thermo Fisher Scientific Inc., Rockford, IL, USA) and ECL film (Amersham, GE Healthcare Limited, UK).

Endogenous glutamate determination. Endogenous glutamate content was measured by high-performance liquid chromatography analysis following pre-column derivatization with *o*-phthalaldehyde and discontinuous triphase gradient separation on a C18 reverse-phase chromatographic column (10 × 4.6 mm^2, 3 μm; at 30 °C; Chrompack, Middleburg, The Netherlands) coupled with fluorometric detection (excitation wavelength 350 nm; emission wavelength 450 nm). Homoserine was used as an internal standard.[63]

SELDI-TOF mass spectrometry. The immune-proteomic assay for Aβ isoforms detection was performed as previously reported.[64] Briefly, 3 μl of the specific monoclonal antibodies (6E10 + 4G8) (Covance) at total mAbs concentration of 0.125 mg/ml (concentration of each mAb 0.0625 mg/ml) were incubated in a humidity chamber for 2 h at RT to allow covalent binding to the PS20 ProteinChip Array (Bio-Rad, Hercules, CA, USA). Unreacted sites were blocked with Tris-HCl 0.5 M, pH 8 in a humid chamber at RT for 30 min. Each spot was first washed three times with PBS containing 0.5% (v/v) TritonX-100 and then twice with PBS. The spots were coated with 5 μl of sample and incubated in a humid chamber overnight. Each spot was first washed three times with PBS containing 0.1% (v/v) TritonX-100, twice with PBS and finally with deionized water. One microliter of α-cyano-4-hydroxy cinnamic acid (Bio-Rad) was added to coated spots. Mass identification was made using the ProteinChip SELDI System, Enterprise Edition (Bio-Rad).

ELISA quantification. Quantitative determination of Aβ 1–42 was performed using innotest ELISA kit (Innogenetics, Gent, Belgium) according to the manufacturer's procedures. Absorbance was detected by 1420 Multilabel Counter Victor 2 (Wallac, Finland).

Human subjects. Human CSF samples were obtained for diagnostic purposes from subjects with MCI ($n=53$), definitive AD ($n=89$) according to the Dubois criteria and from age- and sex-matched (Supplementary Table S1) cognitively preserved and neurologically healthy subjects, undergoing spinal anesthesia for orthopedic surgery, serving as controls ($n=20$). Clinical features of AD and MCI patients are described in Supplementary Table S1. This research project was approved by the ethical committee of the San Raffaele Scientific Institute, and all subjects signed written informed consent.

Quantification and isolation of MVs from human CSF. Samples of CSF collected by lumbar puncture (200–300 μl) were analyzed by flow cytometry, as described previously.[30] Briefly, human CSF was stained with the myeloid marker IB4-FITC (Sigma). Labeled MVs were quantified within a fixed time interval on a Canto II HTS flow cytometer and analyzed using FCS 3 software. Using side-scatter and forward side-scatter, a vesicle gate was determined over the instrument noise (set by running PBS filtered through a 100-nm filter). Within this gate, IB4-positive events (number of events per ml) were evaluated as a parameter of MV concentration. In a set of experiments, after flow cytometry quantification, human MVs were pelletted at 10 000 $\times$ *g* from the volume of CSF yielding 400 MVs, which is the amount produced *in vitro* by 1×10^6 microglia. MVs were then resuspended in neuronal medium and exposed to 1.7×10^5 neurons. Alternatively, MVs (10 000 $\times$ *g* pellet) were processed and analyzed using SELDI-TOF mass spectrometry.

Statistical analysis. All data are presented as mean $\pm$ S.E. from the indicated number of experiments. Statistical analysis was performed using SigmaStat 3.5 (Jandel Scientific) software. After testing data for normal distribution, the appropriate statistical test has been used; see figure legends. The differences are considered to be significant if $P<0.05$ indicated by an asterisk, and those at $P<0.01$ indicated by a double asterisk.

Q18

Q19

Conflict of Interest

The authors declare no conflict of interest.

Acknowledgements. We thank Paola Viani (University of Milan) and Elisabetta Menna (CNR Institute of Neuroscience, Milan) for discussion, Annamaria Finardi (San Raffaele Scientific Institute, Milan) for flow cytometry assistance, Maria Rosa Accomazzo (University of Milan) for spectrofluorometer assistance, Maura Francolini and Simona Rodighiero for support with negative staining electron microscopy (Fondazione Filarete, Milan), Marco Milanese (University of Genova) for HPLC measurements, Cinzia Cagnoli and Martina Gabrielli (University of Milan) for help in some experiments. This work was supported by a grant from Fondazione Veronesi to CV, PNR-CNR Aging program 2012–2014, FIRB 2011-'RBAP11FRE9_001 to GL and RF, Cariplo 2008-3184 to MM and Ricerca Corrente Italian Ministry of Health to RG.

1. Herring A, Lewejohann L, Panzer AL, Donath A, Kroll O, Sachser N *et al.* Preventive and therapeutic types of environmental enrichment counteract beta amyloid pathology by different molecular mechanisms. *Neurobiol Dis* 2011; **42**: 530–538.
2. Schilling S, Lauber T, Schaupp M, Manhart S, Scheel E, Bohm G *et al.* On the seeding and oligomerization of pGlu-amyloid peptides (*in vitro*). *Biochemistry* 2006; **45**: 12393–12399.
3. Bieschke J, Herbst M, Wiglenda T, Friedrich RP, Boeddrich A, Schiele F *et al.* Small-molecule conversion of toxic oligomers to nontoxic beta-sheet-rich amyloid fibrils. *Nat Chem Biol* 2012; **8**: 93–101.
4. Winklhofer KF, Tatzelt J, Haass C. The two faces of protein misfolding: gain- and loss-of-function in neurodegenerative diseases. *EMBO J* 2008; **27**: 336–349.
5. Benilova I, Karran E, De Strooper B. The toxic Abeta oligomer and Alzheimer's disease: an emperor in need of clothes. *Nat Neurosci* 2012; **15**: 349–357.
6. Lue LF, Brachova L, Civin WH, Rogers J. Inflammation, A beta deposition, and neurofibrillary tangle formation as correlates of Alzheimer's disease neurodegeneration. *J Neuropathol Exp Neurol* 1996; **55**: 1083–1088.
7. Haass C, Mandelkow E. Fyn-tau-amyloid: a toxic triad. *Cell* 2010; **142**: 356–358.
8. Serrano-Pozo A, Mielke ML, Gomez-Isla T, Betensky RA, Growdon JH, Frosch MP *et al.* Reactive glia not only associates with plaques but also parallels tangles in Alzheimer's disease. *Am J Pathol* 2011; **179**: 1373–1384.
9. Serrano-Pozo A, Mielke ML, Muzitansky A, Gomez-Isla T, Growdon JH, Bacskai BJ *et al.* Stable size distribution of amyloid plaques over the course of Alzheimer disease. *J Neuropathol Exp Neurol* 2012; **71**: 694–701.
10. Walsh DM, Selkoe DJ. A beta oligomers—a decade of discovery. *J Neurochem* 2007; **101**: 1172–1184.
11. McLean CA, Cherny RA, Fraser FW, Fuller SJ, Smith MJ, Beyreuther K *et al.* Soluble pool of Abeta amyloid as a determinant of severity of neurodegeneration in Alzheimer's disease. *Ann Neurol* 1999; **46**: 860–866.
12. Mielke MM, Haughey NJ, Bandaru VV, Weinberg DD, Darby E, Zaidi N *et al.* Plasma sphingomyelins are associated with cognitive progression in Alzheimer's disease. *J Alzheimers Dis* 2011; **27**: 259–269.
13. Martins IC, Kuperstein I, Wilkinson H, Maes E, Vanbrabant M, Jonckheere W *et al.* Lipids revert inert Abeta amyloid fibrils to neurotoxic protofibrils that affect learning in mice. *EMBO J* 2008; **27**: 224–233.
14. Johansson AS, Garlind A, Berglind-Dehlin F, Karlsson G, Edwards K, Gellerfors P *et al.* Docosahexaenoic acid stabilizes soluble amyloid-beta protofibrils and sustains amyloid-beta-induced neurotoxicity *in vitro*. *FEBS J* 2007; **274**: 990–1000.
15. Snyder EM, Nong Y, Almeida CG, Paul S, Moran T, Choi EY *et al.* Regulation of NMDA receptor trafficking by amyloid-beta. *Nat Neurosci* 2005; **8**: 1051–1058.
16. Lauren J, Gimbel DA, Nygaard HB, Gilbert JW, Strittmatter SM. Cellular prion protein mediates impairment of synaptic plasticity by amyloid-beta oligomers. *Nature* 2009; **457**: 1128–1132.
17. Um JW, Nygaard HB, Heiss JK, Kostylev MA, Stagi M, Vortmeyer A *et al.* Alzheimer amyloid-beta oligomer bound to postsynaptic prion protein activates Fyn to impair neurons. *Nat Neurosci* 2012; **15**: 1227–1235.
18. Verdier Y, Zarandi M, Penke B. Amyloid beta-peptide interactions with neuronal and glial cell plasma membrane: binding sites and implications for Alzheimer's disease. *J Pept Sci* 2004; **10**: 229–248.
19. Edison P, Archer HA, Gerhard A, Hinz R, Pavese N, Turkheimer FE *et al.* Microglia, amyloid, and cognition in Alzheimer's disease: An [11C](R)PK11195-PET and [11C]PIB-PET study. *Neurobiol Dis* 2008; **32**: 412–419.
20. Okello A, Edison P, Archer HA, Turkheimer FE, Kennedy J, Bullock R *et al.* Microglial activation and amyloid deposition in mild cognitive impairment: a PET study. *Neurology* 2009; **72**: 56–62.
21. Hollingworth P, Harold D, Sims R, Gerrish A, Lambert JC, Carrasquillo MM *et al.* Common variants at ABCA7, MS4A6A/MS4A4E, EPHA1, CD33 and CD2AP are associated with Alzheimer's disease. *Nat Genet* 2011; **43**: 429–435.
22. Guerreiro R, Wojtas A, Bras J, Carrasquillo M, Rogaeva E, Majounie E *et al.* TREM2 variants in Alzheimer's disease. *N Engl J Med* 2013; **368**: 117–127.
23. Giulian D, Haverkamp LJ, Yu JH, Karshin W, Tom D, Li J *et al.* Specific domains of beta-amyloid from Alzheimer plaque elicit neuron killing in human microglia. *J Neurosci* 1996; **16**: 6021–6037.
24. Fuhrmann M, Bittner T, Jung CK, Burgold S, Page RM, Mitteregger G *et al.* Microglial Cx3cr1 knockout prevents neuron loss in a mouse model of Alzheimer's disease. *Nat Neurosci* 2010; **13**: 411–413.
25. Tan B, Choi RH, Chin TJ, Kaur C, Ling EA. Manipulation of microglial activity as a therapy for Alzheimer's disease. *Front Biosci* 2012; **4**: 1402–1412.
26. Weitz TM, Town T. Microglia in Alzheimer's Disease: it's all about context. *Int J Alzheimers Dis* 2012; **2012**: 314185.
27. Bianco F, Pravettoni E, Colombo A, Schenk U, Moller T, Matteoli M *et al.* induces vesicle shedding and IL-1 beta release from microglia. *J Immunol* 2005; **174**: 7268–7277.
28. Del Conde I, Shrimpton CN, Thiagarajan P, Lopez JA. Tissue-factor-bearing microvesicles arise from lipid rafts and fuse with activated platelets to initiate coagulation. *Blood* 2005; **106**: 1604–1611.
29. Gonnord P, Delarasse C, Auger R, Benihoud K, Prigent M, Cuif MH *et al.* Palmitoylation of the P2X7 receptor, an ATP-gated channel, controls its expression and association with lipid rafts. *FASEB J* 2009; **23**: 795–805.
30. Verderio C, Muzio L, Turola E, Bergami A, Novellino L, Ruffini F *et al.* Myeloid microvesicles are a marker and therapeutic target for neuroinflammation. *Ann Neurol* 2012; **72**: 610–624.
31. Colombo E, Borgiani B, Verderio C, Furlan R. Microvesicles: novel biomarkers for neurological disorders. *Front Physiol* 2012; **3**: 63.
32. Rajendran L, Honsho M, Zahn TR, Keller P, Geiger KD, Verkade P *et al.* Alzheimer's disease beta-amyloid peptides are released in association with exosomes. *Proc Natl Acad Sci USA* 2006; **103**: 11172–11177.
33. Perry VH, Nicoll JA, Holmes C. Microglia in neurodegenerative disease. *Nat Rev Neurol* 2010; **6**: 193–201.
34. Fukunaga S, Ueno H, Yamaguchi T, Yano Y, Hoshino M, Matsuzaki K. GM1 cluster mediates formation of toxic Abeta fibrils by providing hydrophobic environments. *Biochemistry* 2012; **51**: 8125–8131.
35. Turola E, Furlan R, Bianco F, Matteoli M, Verderio C. Microglial microvesicle secretion and intercellular signaling. *Front Physiol* 2012; **3**: 149.
36. Jana A, Pahan K. Fibrillar amyloid-beta-activated human astroglia kill primary human neurons via neutral sphingomyelinase: implications for Alzheimer's disease. *J Neurosci* 2010; **30**: 12676–12689.
37. Alberdi E, Sanchez-Gomez MV, Cavaliere F, Perez-Samartin A, Zugaza JL, Trullas R *et al.* Amyloid beta oligomers induce Ca2+ dysregulation and neuronal death through activation of ionotropic glutamate receptors. *Cell Calcium* 2010; **47**: 264–272.

38. Bianco F, Perrotta C, Novellino L, Francolini M, Riganti L, Menna E *et al.* Acid sphingomyelinase activity triggers microparticle release from glial cells. *EMBO J* 2009; **28**: 1043–1054.
39. Holtzman DM. CSF biomarkers for Alzheimer's disease: current utility and potential future use. *Neurobiol Aging* 2011; **32**(Suppl 1): S4–S9.
40. Yuyama K, Sun H, Mitsutake S, Igarashi Y. Sphingolipid-modulated exosome secretion promotes clearance of amyloid-beta by microglia. *J Biol Chem* 2012; **287**: 10977–10989.
41. Thery C, Ostrowski M, Segura E. Membrane vesicles as conveyors of immune responses. *Nat Rev Immunol* 2009; **9**: 581–593.
42. Mattei V, Barenco MG, Tasciotti V, Garofalo T, Longo A, Boller K *et al.* Paracrine diffusion of PrP(C) and propagation of prion infectivity by plasma membrane-derived microvesicles. *PLoS One* 2009; **4**: e5057.
43. Han X, Fagan AM, Cheng H, Morris JC, Xiong C, Holtzman DM. Cerebrospinal fluid sulfatide is decreased in subjects with incipient dementia. *Ann Neurol* 2003; **54**: 115–119.
44. Malnar M, Kosicek M, Bene R, Tarnik IP, Pavelin S, Babic I *et al.* Use of cerebrospinal fluid biomarker analysis for improving Alzheimer's disease diagnosis in a non-specialized setting. *Acta Neurobiol Exp* 2012; **72**: 264–271.
45. Ghidoni R, Paterlini A, Albertini V, Glionna M, Monti E, Schiaffonati L *et al.* Cystatin C is released in association with exosomes: a new tool of neuronal communication which is unbalanced in Alzheimer's disease. *Neurobiol Aging* 2011; **32**: 1435–1442.
46. Vella LJ, Sharples RA, Nisbet RM, Cappai R, Hill AF. The role of exosomes in the processing of proteins associated with neurodegenerative diseases. *Eur Biophys J* 2008; **37**: 323–332.
47. Vingtdeux V, Hamdane M, Begard S, Loyens A, Delacourte A, Beauvillain JC *et al.* Intracellular pH regulates amyloid precursor protein intracellular domain accumulation. *Neurobiol Dis* 2007; **25**: 686–696.
48. Yamamoto M, Kiyota T, Walsh SM, Liu J, Kipnis J, Ikezu T. Cytokine-mediated inhibition of fibrillar amyloid-beta peptide degradation by human mononuclear phagocytes. *J Immunol* 2008; **181**: 3877–3886.
49. Aguzzi A, Barres BA, Bennett ML. Microglia: scapegoat, saboteur, or something else? *Science* 2013; **339**: 156–161.
50. Prinz M, Priller J, Sisodia SS, Ransohoff RM. Heterogeneity of CNS myeloid cells and their roles in neurodegeneration. *Nat Neurosci* 2011; **14**: 1227–1235.
51. Paresce DM, Chung H, Maxfield FR. Slow degradation of aggregates of the Alzheimer's disease amyloid beta-protein by microglial cells. *J Biol Chem* 1997; **272**: 29390–29397.
52. Lee CY, Landreth GE. The role of microglia in amyloid clearance from the AD brain. *J Neural Transm* 2010; **117**: 949–960.
53. Rajendran L, Annaert W. Membrane trafficking pathways in Alzheimer's disease. *Traffic* 2012; **13**: 759–770.
54. Ariga T, Kobayashi K, Hasegawa A, Kiso M, Ishida H, Miyatake T. Characterization of high-affinity binding between gangliosides and amyloid beta-protein. *Arch Biochem Biophys* 2001; **388**: 225–230.
55. Kiyota T, Yamamoto M, Xiong H, Lambert MP, Klein WL, Gendelman HE *et al.* CCL2 accelerates microglia-mediated Abeta oligomer formation and progression of neurocognitive dysfunction. *PLoS One* 2009; **4**: e6197.
56. Shen B, Wu N, Yang JM, Gould SJ. Protein targeting to exosomes/microvesicles by plasma membrane anchors. *J Biol Chem* 2011; **286**: 14383–14395.
57. Sharples RA, Vella LJ, Nisbet RM, Naylor R, Perez K, Barnham KJ *et al.* Inhibition of gamma-secretase causes increased secretion of amyloid precursor protein C-terminal fragments in association with exosomes. *FASEB J* 2008; **22**: 1469–1478.
58. Tamboli IY, Barth E, Christian L, Siepmann M, Kumar S, Singh S *et al.* Statins promote the degradation of extracellular amyloid {beta}-peptide by microglia via stimulation of exosome-associated insulin-degrading enzyme (IDE) secretion. *J Biol Chem* 2010; **285**: 37405–37414.
59. Antonucci F, Turola E, Riganti L, Caleo M, Gabrielli M, Perrotta C *et al.* Microvesicles released from microglia stimulate synaptic activity via enhanced sphingolipid metabolism. *EMBO J* 2012; **31**: 1231–1240.
60. Klein WL. Abeta toxicity in Alzheimer's disease: globular oligomers (ADDLs) as new vaccine and drug targets. *Neurochem Int* 2002; **41**: 345–352.
61. De Felice FG, Wu D, Lambert MP, Fernandez SJ, Velasco PT, Lacor PN *et al.* Alzheimer's disease-type neuronal tau hyperphosphorylation induced by A beta oligomers. *Neurobiol Aging* 2008; **29**: 1334–1347.
62. Frassoni C, Inverardi F, Coco S, Ortino B, Grumelli C, Pozzi D *et al.* Analysis of SNAP-25 immunoreactivity in hippocampal inhibitory neurons during development in culture and in situ. *Neuroscience* 2005; **131**: 813–823.
63. Paluzzi S, Alloisio S, Zappettini S, Milanese M, Raiteri L, Nobile M *et al.* Adult astroglia is competent for Na+/Ca2+ exchanger-operated exocytotic glutamate release triggered by mild depolarization. *J Neurochem* 2007; **103**: 1196–1207.
64. Albertini V, Bruno A, Paterlini A, Lista S, Benussi L, Cereda C *et al.* Optimization protocol for amyloid-beta peptides detection in human cerebrospinal fluid using SELDI TOF MS. *Proteomics Clin Appl* 2010; **4**: 352–357.

Supplementary Information accompanies this paper on Cell Death and Differentiation website (http://www.nature.com/cdd)